

MODELING THE REACTIONS OF COAL LIQUIDS

Thesis by
David Thomas Allen

In Partial Fulfillment of the Requirements
for the Degree of
Doctor of Philosophy

California Institute of Technology
Pasadena, California

1983

(Submitted May 9, 1983)

This thesis is dedicated to my parents.

Climb the mountains and get their good tidings.
The winds will bring you their freshness,
and the storms their energy and peace,
and cares will fall away like autumn leaves.

- John Muir

Copyright © by
David T. Allen
1983

Acknowledgements

I wish to thank my thesis advisor, George Gavalas, for the support and guidance he provided throughout this investigation. His patience and insight, and the freedom he granted me to pursue my research interests, are deeply appreciated. The advice and experience of Leon Petrakis, Dave Grandy and Art Ferari of Gulf Research and Development Company and Mitsuo Oka of the California State Polytechnic University were also invaluable in performing this work.

I gratefully acknowledge the financial support of the Gulf Research and Development Company, the Department of Energy and the California Institute of Technology.

Finally, the encouragement and moral support of my friends and colleagues at Caltech and JPL made performing this research and living in Pasadena a pleasure. Teri, Michael, Puvion, Murray and Dinah showed me new worlds to explore and have been true friends.

ABSTRACT

This thesis begins the development of a new approach to the kinetic modeling of complex hydrocarbon mixtures. The approach is based on functional group reactions and its implementation involves three steps. The first step is to characterize complex hydrocarbon mixtures, such as coal-derived liquids, heavy oils and shale oils, in terms of their constituent functional groups. A methodology is defined for estimating functional group concentrations from elemental analysis and NMR data. Mass spectra, infrared spectra, separation yields and other analytical data may also be incorporated into the concentration estimates. The methodology is demonstrated for a heavy oil and for a wide variety of coal liquids.

The concentrations provide a starting point for kinetic modeling. The second step of the modeling procedure is to determine the rates and pathways of the reactions of the functional groups by investigating the reactions of pure compounds containing the same functionalities. The reactions of a number of these model compound systems were examined. The studies focused on the reactions of atomic hydrogen under conditions appropriate to coal liquefaction.

The final step in the modeling is the development of a mathematical model which can predict changes in functional group concentrations given initial concentrations and reaction rates. This is outside the scope of this thesis, but general guidelines and valid simplifications are discussed.

Table of Contents

Acknowledgements.....	iii
Abstract.....	iv
Chapter 1: Introduction.....	1
Part I: Structural Characterization of Complex Hydrocarbon Mixtures	
Chapter 2: Structural Characterization of Complex Hydrocarbon Mixtures - Introduction....	9
Chapter 3: Functional Group Analysis of Synthetic Fuels.....	21
Chapter 4: Functional Group Analysis of Coal Liquids.....	53
Chapter 5: Application of Functional Group Analysis to Heavy Oils.....	75
Chapter 6: Recommendations for Future Work.....	85
Appendix A: Algorithm and Computer Codes for Non-linear Minimization with Linear Inequality and Equality Constraints...	86
Part II: Model Compound Studies	
Chapter 7: Model Compound Studies - Introduction.....	109
Chapter 8: Kinetics of Dialin Thermolysis.....	114
Chapter 9: Reactions of Methylene and Ether Bridges.....	130
Chapter 10: Model Compound Studies: Conclusions and Recommendations for Future Work...	157

Chapter 1

Introduction

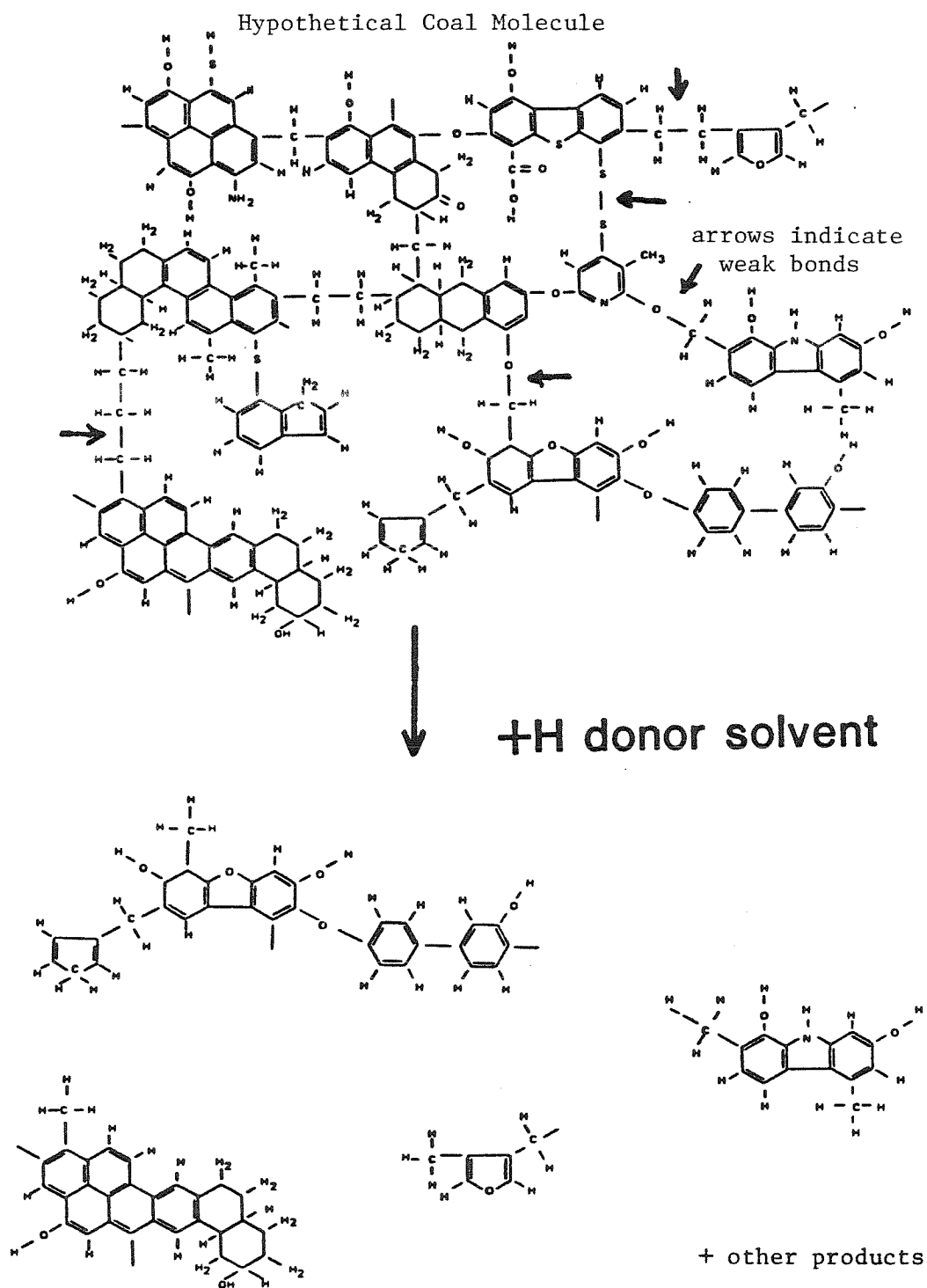
In the past decade, the development of processes designed to utilize coal as a substitute for petroleum has seen a renewed interest. Coal liquefaction has been viewed as one of the principal means of converting coal from a soot and SO_x producing fuel to a clean burning petroleum substitute. In coal liquefaction processes, weak bonds in large coal molecules are thermally cracked in the presence of a hydrogen donating solvent to form lighter products. The cracking reactions produce free radicals which are capped by the hydrogen donor solvent (1). The process is shown schematically in Figure 1. The lighter products can be treated further to produce clean burning fuels and chemical feedstocks.

A major goal of many research efforts directed towards coal has been the development of a kinetic model of coal liquefaction processes. The chemistry and transport phenomena associated with coal liquefaction are too complex to allow a complete chemical and physical model of molecular reactions to be developed, so recourse was necessarily made to approximate approaches (2). Models of coal liquefaction reactions that have appeared in the literature have generally utilized solubility fractions in a kinetic lumping procedure (3,4). A typical model is shown in Figure 2. Extensive experimental and modeling efforts have gone into determining the topology and rates of this type of reaction network. There are two problems associated with this approach, however. The first is that the results are specific to one coal and are valid only over the

2.

Figure 1

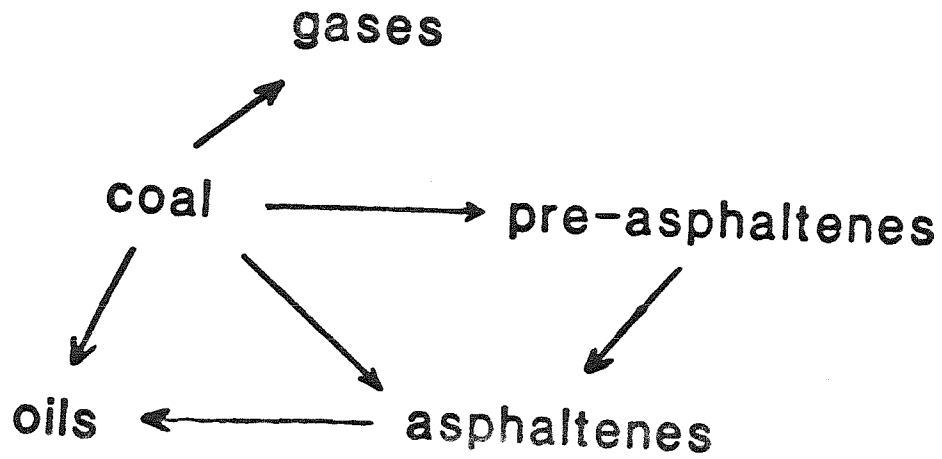
Simplified Coal Liquefaction Mechanism



3.

Figure 2

A Typical Kinetic Model of Coal Liquefaction Reactions



reaction conditions that were experimentally examined. Thus, the models may be useful in qualitatively explaining observed phenomena, but since the reactants and reaction pathways are not well defined chemically, it is difficult to derive any fundamental chemical or rate information from the results. A second major problem with this type of model is that the structures of the solubility fractions are functions of the extent of reaction. Defining a reaction network based on the concentrations of solubility fractions which change in character with time is not valid.

A new approach to the modeling of this type of complex system is necessary. In order to develop a new approach, a process simpler than, but related to, coal liquefaction will be considered in this thesis. The reactions of liquids derived from coal liquefaction processes is an appropriate system.

In general, liquids derived from coal liquefaction processes must be hydrodesulfurized and hydrodenitrogenated before they can be used as fuels. The hydrogen requirements of the hydrotreatment processes are immense, so the practical motivation is great for developing a predictive kinetic model that would identify conditions which minimize hydrogen consumption. Using the reactions of coal liquids to develop a new approach to the kinetic modeling of complex mixtures has several advantages.

- [1] Since the reactions occur in a fluid of moderate viscosity, mass transfer and diffusional limitations can be neglected.
- [2] Liquid reactants and products are more easily sampled and chemically characterized than solids.

The object of this thesis is to begin the development of a kinetic model of the reactions of complex hydrocarbon mixtures such as coal liquids. A new approach will be utilized which is based on the premise that while these complex mixtures contain thousands of components, the components contain only a small number of functionalities. This premise is supported by a large body of experimental evidence, including results from nuclear magnetic resonance, infrared spectroscopy and mass spectrometry (5,6). The chemical properties of the complex mixtures are characterized by determining the concentrations of a representative set of functional groups. The kinetic behavior of the mixture can then be modeled by determining the rates of reactions of the set of functional groups. Thus, the development of a general and fundamentally based kinetic model should include the following steps.

- [1] Definition of a methodology for characterizing complex mixtures in terms of their constituent functional groups.
- [2] Identification of the principal reaction pathways of the functional groups and determination of the rate parameters.
- [3] Development of a mathematical model which can predict changes in functional group concentrations given initial concentrations and reaction pathways.

Since the reaction network topology and rates derived for a particular set of functional groups is independent of the starting concentrations, a single model of this type is applicable to a large number of different feedstocks. A successful model would represent a first step toward a more fundamental understanding of coal liquefaction and other complex reacting systems. The development

of a general model is a very large task, however, and this thesis takes only the first few steps towards its completion. The scope of the work presented here is confined to the characterization of complex mixtures in terms of their functional groups and some initial studies of reaction pathways.

The work presented in this thesis is divided into two parts. Part I, comprising Chapters 2-6, accomplishes step 1 of the modeling procedure. That is, a methodology for the characterization of complex hydrocarbon mixtures is defined and demonstrated. The advantages of a characterization of complex mixtures based on functional group concentrations are not limited to merely serving as a starting point for kinetic modeling. Some additional applications are described in Part I. Part II presents results related to step 2 of the procedure. Chapters 7-9 describe thermolysis experiments performed on pure compounds having the same types of functional groups that are present in coal liquids. Chapter 10 discusses the advantages and limitations of these model compound experiments and describes some possible methods for completing steps 2 and 3 of the modeling procedure.

References

- [1] D.D. Whitehurst, T.O. Mitchell and M. Farcasiu, *Coal Liquefaction*, Academic Press, New York, 1980, Chapter 2.
- [2] A.J. Szladow and P.H. Given, *I.&E.C. Proc. Des. Dev.*, **20**, 27 (1981).
- [3] D.C. Cronauer, Y.T. Shah and R.G. Ruberto, *I.&E.C. Proc. Des. Dev.*, **17**, 281 (1978).
- [4] Y.T. Shah, D.C. Cronauer, H.G. McIlvried and J.A. Paraskos, *I.&E.C. Proc. Des. Dev.*, **17**, 288 (1978).
- [5] J.T. Swansiger, F.E. Dickson and H.T. Best, *Anal. Chem.*, **46**, 730 (1974).
- [6] P.R. Solomon, *Prepr.-Amer. Chem. Soc., Div. Fuel Chem.*, **24** (2), 184 (1979).

8.

PART I

Structural Characterization of Complex Hydrocarbon Mixtures

Chapter 2

Structural Characterization of Complex Hydrocarbon Mixtures

Tremendous increases in the cost of crude oil over the past decade have sparked an interest in the use of coal liquids, heavy crude oils and shale oils as alternative fuels. In general, these fuels must undergo expensive hydrotreatment before they can be utilized. Optimizing the hydrotreatment process is a critical step in making alternative fuels economically attractive. However, little optimization can be done without a detailed understanding of the chemical nature of the fuels. Isolation and identification of each of the thousands of components in the fuels is an intractable problem, so recourse must be made to approximate characterization methods.

The work presented in Chapters 3-5 of this thesis defines and demonstrates a method for the structural characterization of these liquid fuels. The goals of the characterization are to provide as detailed a characterization as the analytical data allow and to define a characterization which is a reasonable basis for kinetic modeling.

In developing a structural characterization method for complex mixtures such as coal liquids, heavy crudes and shale oils, it is first necessary to critically examine the sources of data on which the characterization will be based. In the case of coal liquids and heavy crude oils, the principal sources of structural data are elemental analysis, nuclear magnetic resonance (NMR) spectra, infrared(IR) spectra, separation yields and mass spectra. The precision, accu-

racy and cost of each of these data sources, along with the type of information which they provide, are described below.

Elemental analysis

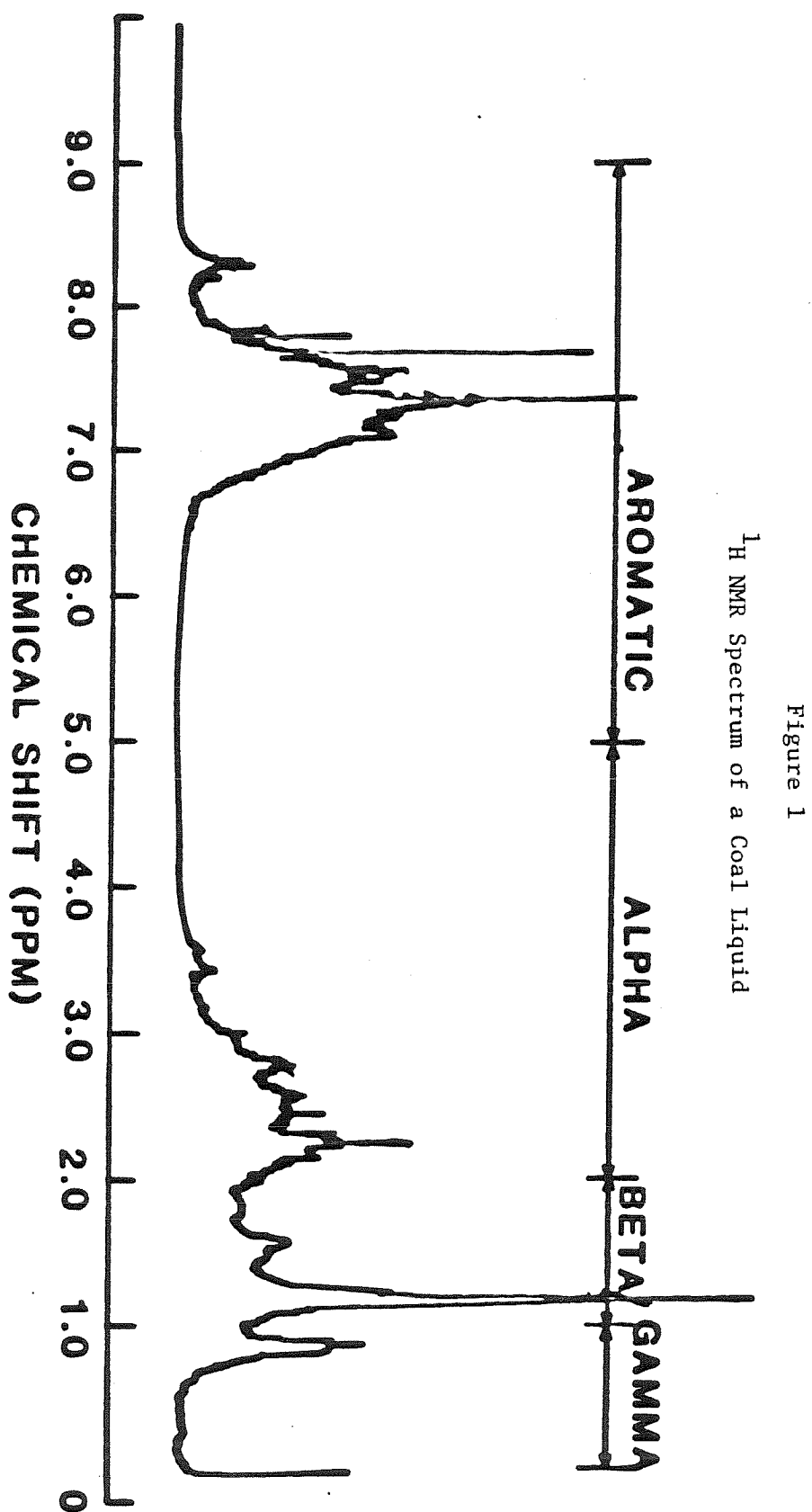
Typically, elemental analysis determines the weight percentage of C,H, N, and S with O calculated by difference. The data are relatively inexpensive to obtain and provide reproducible, quantitative information.

Proton NMR

^1H NMR distinguishes between protons in various bonding environments. A typical ^1H NMR spectrum of a coal liquid is shown in Figure 1. The spectrum is divided into four bands (1) corresponding to the four bonding environments listed in Table 1. The intensity integrated over each of the bands is proportional to the number of protons in the bonding environment assigned to the band. Despite the slight overlap of some of the bands, spectra taken on model compound mixtures indicate that these data are accurate and reproducible.

Carbon-13 NMR

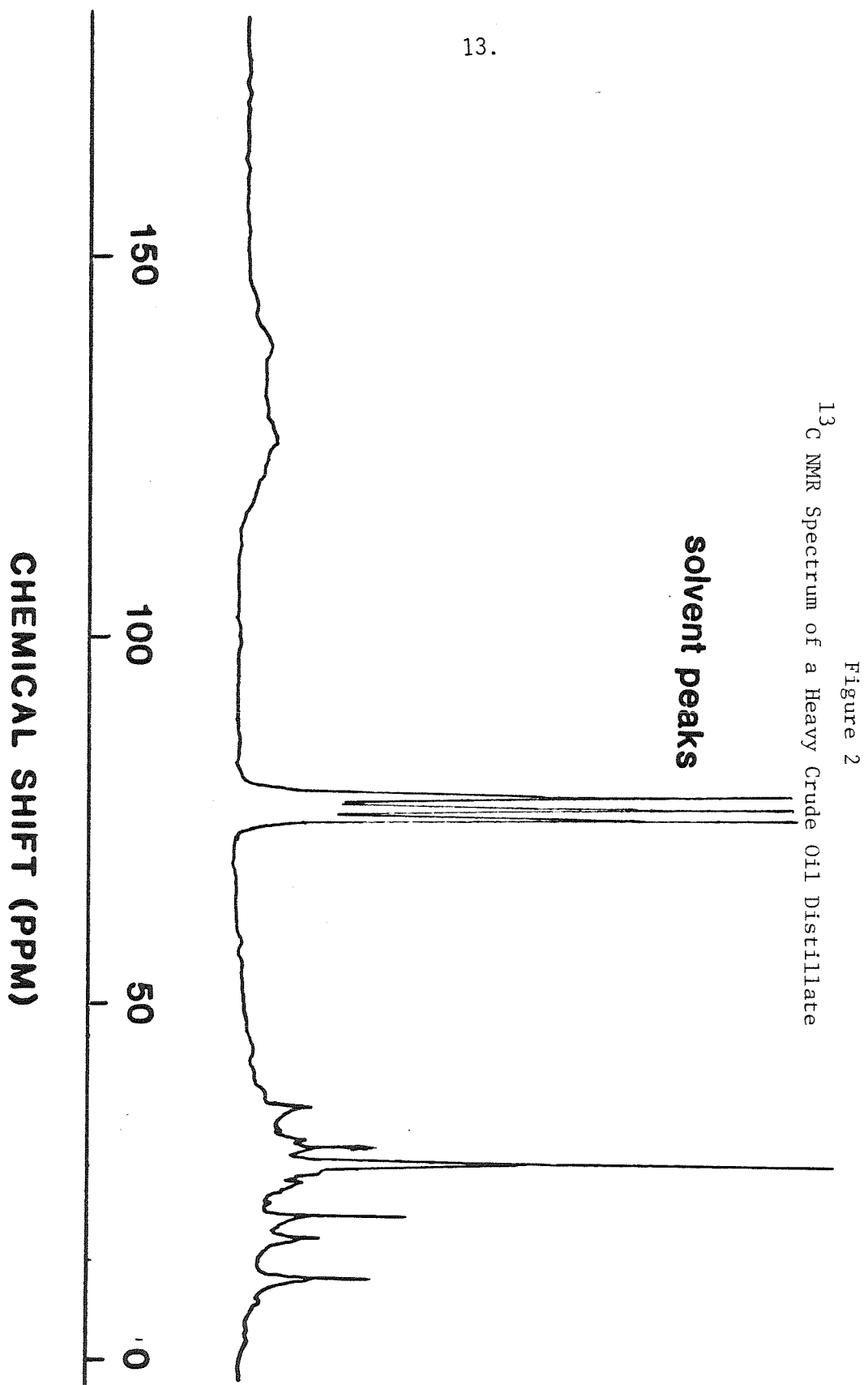
In the work on coal liquids presented here, ^{13}C NMR has been used to quantitatively distinguish between aromatic and aliphatic carbon. High relaxation times and low isotopic abundance make the acquisition of more detailed data difficult. In the case of crude oils, however, the aliphatic portion of the spectra show considerable detail and more information can be derived from the spectra. The differences between coal liquid and crude oil spectra are made particularly evident by comparing the ^{13}C spectrum of a crude oil shown in Figure 2 to the spectrum of a coal liquid, shown in Figure 3. The ^{13}C NMR band assignments (2) for both coal liquids and crude oils are listed in Table 2.



12.

Table 1

Band Assignments for ^1H NMR Spectra	
Hydrogen type	Chemical shift range (ppm from TMS)
Aromatic hydrogen	9.0-5.0
Hydrogen in CH , CH_2 and CH_3 groups alpha to an aromatic ring	5.0-1.9
Hydrogen in CH and CH_2 groups beta or farther from an aromatic ring, Hydrogen in CH_3 groups beta to an aromatic ring	1.9-1.0
Hydrogen in CH_3 groups gamma or farther from an aromatic ring	1.0-0.5



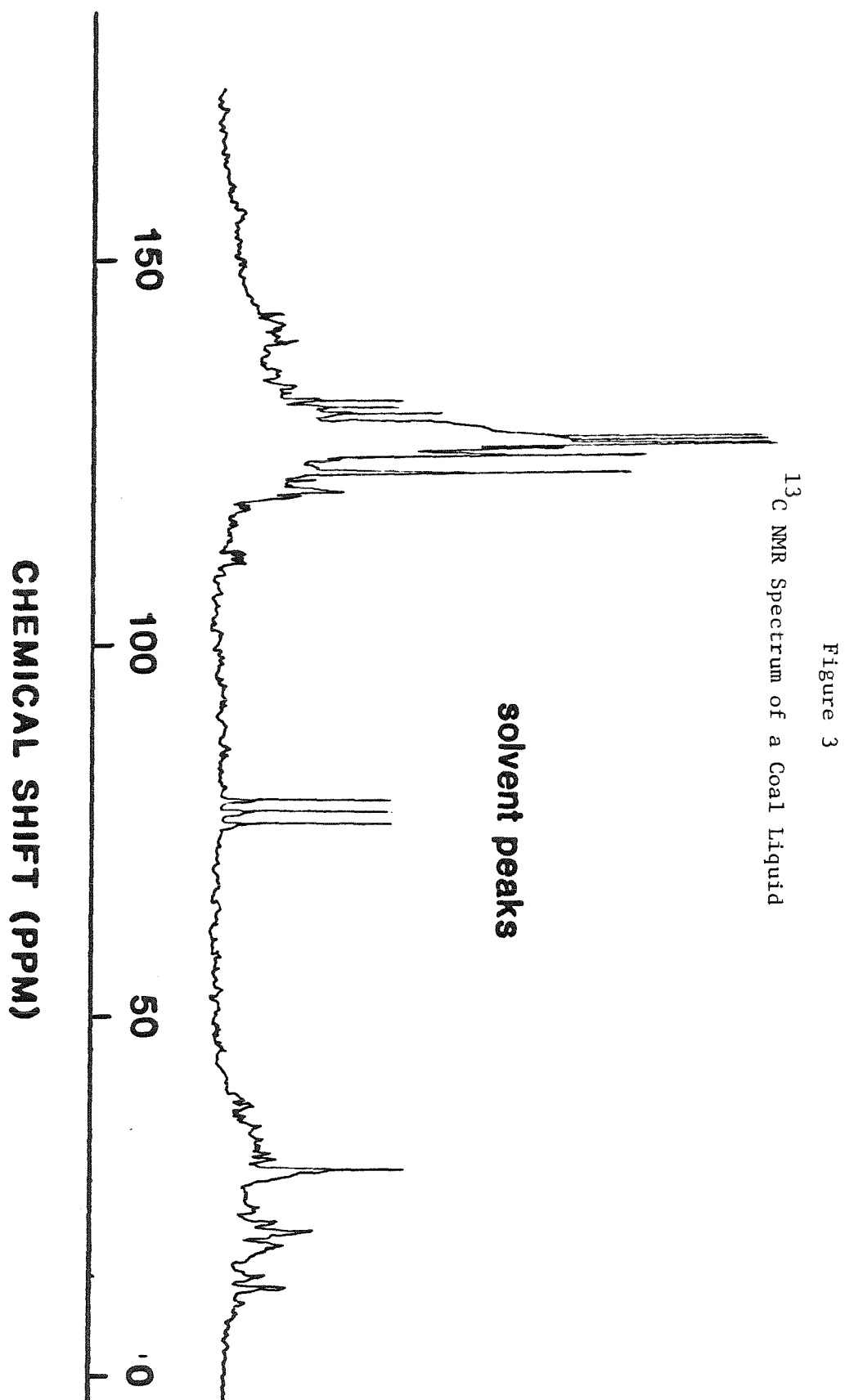


Table 2

Band Assignments for ^{13}C Spectra of Coal Liquids	
Carbon type	Chemical shift range (ppm from TMS)
Aromatic carbon	100-170
Aliphatic carbon	11-60
Band Assignments for ^{13}C Spectra of Crude Oils	
Aromatic carbon	100-170
Carbon in CH groups	37-60
Carbon in naphthenic CH_2 groups Carbon in CH_2 groups alpha and gamma or farther from an aromatic ring	27.5-37
Carbon in CH_2 groups beta to an aromatic ring	24-27.5
Carbon in CH_2 groups next to a terminal methyl; Carbon in CH_2 groups beta to an aromatic ring in tetralin structures	22.5-24
Carbon in CH_3 groups alpha to an aromatic ring	20.5-22.5
Carbon in CH_3 groups attached to hydroaromatic structures	18-20.5
Carbon in CH_3 groups beta to an aromatic ring	15-18
Carbon in CH_3 groups gamma or farther from an aromatic ring	11-15

Infrared spectra

Infrared spectra provide inexpensive, qualitative information concerning the types of functionalities which may be present in a sample. Quantitative interpretation is difficult, however, since peaks are generally broad and converting peak intensities to concentrations is not straightforward. Thus, the interpretation of IR spectra in this work was confined to use as supporting evidence for the choice of functional groups used in the structural characterizations.

Separation Procedures

Preparative chromatography can be used to separate various types of heteroatomic functionalities into distinct fractions (3,4). The yields of the fractions provide information concerning the relative abundance of certain heteroatomic functional groups. This information is useful but it is very time consuming to obtain.

Mass spectra

Both high and low resolution mass spectra were used in the structural characterizations presented here. The interpretation of these data involves several assumptions which limit the accuracy of the data. These assumptions and the format of the data are discussed at length in chapter 3. Even with the uncertainties involved in the data interpretation, mass spectral data provide extremely detailed information on the structures present in complex mixtures. Unfortunately, the data are relatively expensive to obtain for mixtures with molecular weights approaching 1000 (such as heavy oils and coal liquids).

In summary, the sources of data available for structural characterizations which are quantitative, inexpensive and readily available are elemental analysis and various types of NMR spectra. In developing a methodology for the structural characterization of complex mixtures, we should rely predominantly on these sources of data, but we should also be able to utilize powerful sources of data, such as mass spectra, if they are available. With this goal in mind, we will review the principal method of characterization used in the current literature and our new approach to the structural analysis of complex mixtures.

The most common method used to characterize the structure of complex hydrocarbon mixtures is to calculate the values of a set of structural parameters (5-12). The values of the parameters are based on elemental analysis and NMR data. The advantages and disadvantages of the method are best demonstrated by an example. In Table 3, the average parameters for a coal liquid are shown (7). Examination of the values gives a rough indication of the types of structures that are present in the liquid. The form of the characterization allows quantitative comparisons between samples to be made. There are two distinct disadvantages to the characterization, however. First, it is difficult to incorporate any data other than elemental analysis and NMR into the characterization. As more analytical methods are applied to complex mixtures, this inflexibility becomes more important. A second disadvantage is that this type of characterization is not a reasonable starting point for kinetic modeling of the reactions of complex mixtures. Any kinetic model representing the changes in values of these parameters as reactions proceed would merely be an empirical curve fit. No extrapolation would be possible and insight into the chemical processes occurring would be limited.

Table 3

Structural Parameters for a Coal Liquid

Number of carbon atoms per substituent	1.34
C/H weight ratio in alkyl groups	6.03
C/H weight ratio in aromatic groups	18.5
Fraction of carbons that are aromatic	0.889
Average number of aromatic carbons per molecule	15.9
Number of nonbridge aromatic carbons per molecule	11.8
Number of saturate carbons per molecule	2.0
Percent substitution of nonbridge aromatic carbon	12.6
Number of fused aromatic rings per molecule	3.1
Number of saturate rings per molecule	0.8

An alternative method for the structural characterization of complex mixtures is developed and demonstrated in the following chapters. The method, termed functional group analysis, relies on the premise that while complex hydrocarbon mixtures contain thousands of components, the number of different functionalities present is small. The goal of the characterization is to calculate the concentrations of a small number of representative functionalities. This type of characterization and the methodology used to implement it solve some of the problems of the parameters approach yet retain the advantages. The functional group analysis method allows quantitative comparisons to be made between samples, it is flexible in the types of data that it utilizes and it can serve as a logical starting point for kinetic modeling.

The algorithm for calculating functional group concentrations is defined and demonstrated in Chapter 3. Appendix A details the mathematical techniques and computer codes used in the algorithm. Chapter 4 describes the application of the method to several samples of coal liquids and Chapter 5 extends the method to the characterization of heavy crudes. Recommendations for future structural characterization work are given in Chapter 6.

References

- [1] C.E. Snape, W.R. Ladner, and K.D. Bartle, *Coal Liquefaction; NMR Spectroscopic Characterization and Production Processes*, in press, chapter 5.
- [2] K.D. Bartle, W.R. Ladner, T.G. Martin, C.E. Snape and D.F. Williams, *Fuel*, **58**, 413 (1978).
- [3] D.M. Jewell, E.W. Albaugh, B.E. Davis and R.G. Ruberto, *I.&E.C. Fund.*, **13** (3), 278 (1974).
- [4] D.M. Jewell, J.H. Weber, J.W. Bunger, H. Plancher, D.R. Latham, *Anal. Chem.*, **44**, 1391 (1972).
- [5] J.K. Brown and W.R. Ladner, *Fuel*, **39**, 87 (1960).
- [6] K.D. Bartle, T.G. Martin, D.F. Williams, *Fuel*, **54**, 226 (1975).
- [7] D.M. Cantor, *Anal. Chem.*, **50**, 1185 (1978).
- [8] J.M. Charlesworth, *Fuel*, **59**, 865 (1980).
- [9] D.R. Clutter, L. Petrakis, R.L. Stenger and R.K. Jensen, *Anal. Chem.*, **44**, 1395 (1972).
- [10] E.M. Dickinson, *Fuel*, **59**, 290 (1980).
- [11] S. Gillet, P. Rubini, J. Delpuech, J. Escalier and P. Valentin, *Fuel*, **60**, 254 (1981).
- [12] G.A. Haley, *Anal. Chem.*, **44**, 580 (1972).

Chapter 3

FUNCTIONAL GROUP ANALYSIS OF SYNTHETIC FUELS

David T. Allen^{1,2}, Leonidas Petrakis², George R. Gavalas¹
and Bruce C. Gates³

(1) Department of Chemical Engineering, California Institute of Technology,
Pasadena, California 91125

(2) Gulf Research and Development Company, Pittsburgh, Pennsylvania 15230

(3) Department of Chemical Engineering, University of Delaware, Newark,
Delaware 19711

This chapter was submitted as a manuscript to the journal *Analytical Chemistry*

ABSTRACT

A new method for the structural characterization of complex mixtures is developed which utilizes elemental analysis , NMR and other analytical data to determine functional group concentrations. The method is tested with a mixture of known composition and is applied to a set of hydrodesulfurized coal liquids. The results are compared with mass spectroscopic data and with the results of established methods of structural analysis.

BRIEF

A new method for the structural characterization of complex mixtures utilizes elemental analysis , NMR and other analytical data to determine functional group concentrations.

INTRODUCTION

The structural characterization of complex, multicomponent fractions of coal liquids, shale oils and petroleum distillates is an important problem that has received considerable attention. Numerous separation and spectroscopic techniques have been used, either singly or in combination, in order to obtain detailed structural profiles of these fossil fuels (1-4). High resolution ^1H and ^{13}C nuclear magnetic resonance (NMR) have been particularly useful in determining the structures of the carbon skeletons of these fuels. However, neither NMR spectra, nor other spectroscopic and analytical data provide enough information to delineate fully the individual components present in the mixtures. Thus, recourse must be made to the approximate characterization methods of structural analysis. Three general approaches have been employed to obtain structural information from NMR spectra and possibly other supplemental measurements. These approaches are characterization by parameters, average molecule construction and functional group analysis.

In the first of these approaches, complex hydrocarbon mixtures, such as coal liquids and petroleum distillates, are characterized by calculating a set of average structural parameters (5-16). The parameters describe structural features, such as the fraction of carbon that is aromatic, the number and average length of alkyl substituents, the percentage of carbons that are substituted, and the number of aromatic rings per molecule. The parameters are derived from NMR and elemental analysis data using a number of assumptions. The nature of these assumptions depends on the specific parameters being calculated, but typical methods (5) assume a value for the average ratio of hydrogen to carbon in the aliphatic structures. Given sufficient data, the estimated

parameters can provide a useful characterization of a hydrocarbon mixture, however, the approach presents two difficulties. The first difficulty is assessing the validity of the assumptions made in calculating the parameters. Experimental verification of the assumptions is time consuming and is rarely done. The second difficulty is that the estimated parameters represent average values and may not provide information about the actual components of the mixture. For example, a value of 3 for the average number of carbons in an alkyl chain could indicate either a uniform distribution of chain length about 3 or a bimodal distribution with high concentrations of very short and much longer aliphatic chains.

A second approach to structural analysis utilizes NMR, elemental composition and average molecular weight data to construct average or representative molecular structures. The structural formula of an average molecule can be determined in a straightforward manner from elemental analysis and average molecular weight data. After rounding the structural formula to the nearest whole integers, the algorithm of Oka (17) can be used to find all possible structures that are consistent with the NMR data. The molecular structures generated by this method are useful in visualizing the types of structures that may be present, but must be viewed with caution. The structures represent a statistical averaging of the properties of the molecules in the mixture and may or may not actually exist in the liquids. In addition, small variations in the average empirical formula can lead to very different structures, so comparisons between similarly treated samples are difficult to make.

This work presents a third approach to the structural characterization of mixtures, termed functional group analysis. The premise of this method is

that while the number of individual molecules in a mixture may be large, all of these molecules are composed of a relatively small number of functional groups. For coal liquids, this premise is supported by a large body of experimental evidence, including results from mass spectrometry (18), IR (19), NMR and chromatography (3). Since functional groups determine chemical behavior, a useful characterization of a mixture of coal liquids consists of listing the concentrations of the constituent functional groups. This method provides a characterization that is easy to visualize and allows quantitative comparisons between similar samples. If sufficiently precise functional group concentrations can be determined, this method could be used to elucidate reaction pathways and kinetics.

The purpose of this paper is to define a method for estimating functional group concentrations. The method is illustrated by application to several samples of hydrodesulfurized coal liquids and to two simpler samples of known composition. The calculations are based on elemental analysis and NMR data. Mass spectroscopic data are used to support the results.

EXPERIMENTAL SECTION

A neutral oil derived from a hydroliquefied Powhatan #5 coal was fed to a catalytic hydrodesulfurization reactor. The neutral oil consisted primarily of molecules containing little or no acid-base characteristics and with boiling points between 290 and 440 °C. The heteroatoms in the oil were largely sulfur and oxygen in thiophene- and furan-type structures. Saturate structures with an average carbon number of 18 amounted to approximately 6 wt.% of the neutral oil. The saturates were separated from the oil and were analyzed by ^1H

NMR. Using these data and assuming that the saturates would be relatively inert to further hydrotreatment, the contribution of the saturates was subtracted from the analytical data obtained on the whole oils. The remainder of this work deals with the structures of the aromatic component of the neutral oils. An extensive description of the neutral oil is given in reference (20).

The neutral oils were hydrodesulfurized in the stirred autoclave described in reference (21). A slurry consisting of 280.9 g of the oil and 5 g of a cobalt/moly catalyst was heated to 350 °C under 34 atm of hydrogen pressure. Samples were removed at residence times of 0., 3.0, 7.5, and 25 h. Elemental composition, ^1H NMR spectra and low and high resolution mass spectra were obtained for each of the samples.

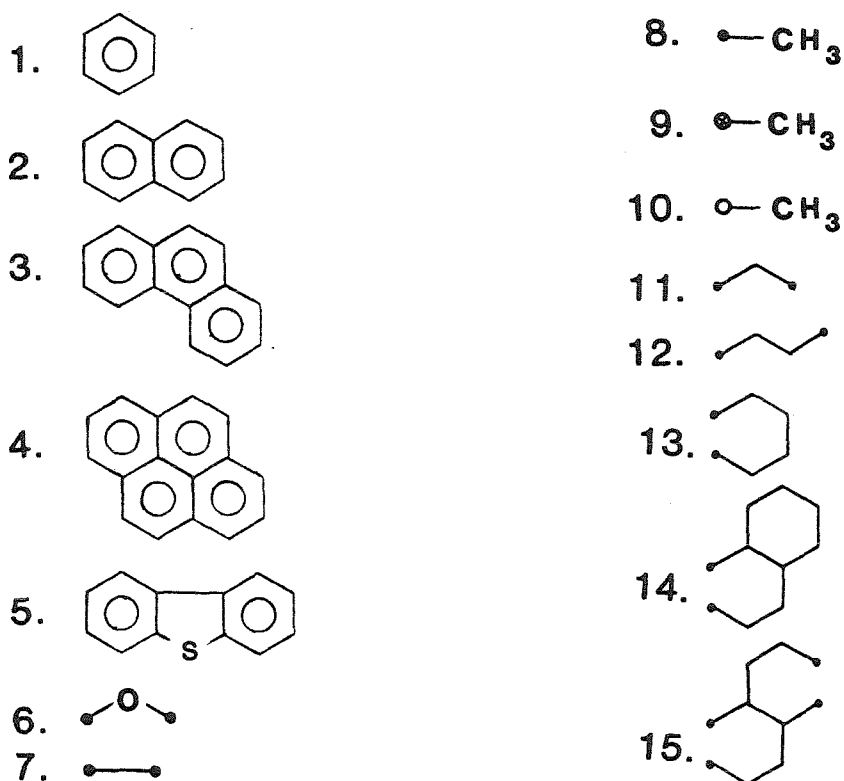
RESULTS AND DISCUSSION

Methodology


The goal of functional group analysis is to determine the concentrations of functional groups which characterize the structure of a complex mixture. The first step in the analysis is to propose a set of functional groups, such as the set in Figure 1. The set must be adequate to account for the observed data, yet it must be as concise as possible since the number of meaningful concentrations that can be determined is limited by the amount of available data.

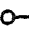
Once the functional groups have been specified, concentrations which satisfy the elemental analysis and NMR data must be found. This is done by relating the concentrations of the functional groups to the experimental data through a set of balance equations. As an example, consider the balance for alpha hydrogen. The concentration of alpha hydrogen in the sample is

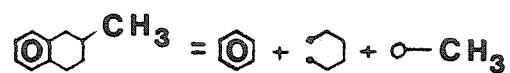
Figure 1

Coal liquid functional groups**Notation:**

 — bound directly to an aromatic ring

 — bound to a carbon alpha to an aromatic ring

 — bound to a carbon beta or further from an aromatic ring

Example:

calculated using ^1H NMR and elemental analysis data. This concentration must equal the concentration of each functional group times the number of alpha hydrogens in that group, summed over all groups. The balance equations form a set of linear equations:

$$\sum_{j=1}^n A_{ij} y_j = b_i \quad (i=1, \dots, m) \quad (1)$$

where y_j ($j=1, \dots, n$) are the unknown functional group concentrations, b_i ($i=1, \dots, m$) are quantities representing the elemental and NMR data and A_{ij} are stoichiometric coefficients. The concentrations must be non-negative.

$$y_j \geq 0 \quad (2)$$

Since the number of equations is invariably smaller than the number of unknown concentrations, equations 1 and 2 can yield either no solutions or a space of feasible solutions. If the equations have no solution, then the proposed set of functional groups is insufficient to describe the observed data and must be revised. If a space of solutions exists, then the mixture can be characterized by selecting a single solution from the feasible space.

To select a single solution from the feasible region, we adopt a procedure that is computationally straightforward. The concentrations y_1, \dots, y_n are chosen such that a function $P(y_1, \dots, y_n)$ is minimized subject to the constraints of equations 1 and 2. The form of the function P depends on what, if any, data are available in addition to elemental analysis and NMR. Data other than elemental analysis and NMR can be introduced as additional balance equations or can be incorporated into the function P . The method for handling the data is chosen on the basis of the data's accuracy and precision. Highly precise and

accurate data are used in constructing the balance equations. More qualitative data are utilized in formulating the minimization functions.

Three different minimization functions will be discussed. The first is a general function which is applied when all of the available data has been used in formulating the balance equations. The second and third functions are designed to utilize high and low resolution mass spectroscopic data, respectively. Other types of minimization functions are possible, and may be formulated to take advantage of additional data sources. For comparison, all three methods will be applied to the set of hydrodesulfurized coal liquids.

General Minimization Function

The general minimization function is used if no information is available on the relative abundance of the various functional groups. We formulate the function by assuming that all functional groups are equally probable. As a concrete example of this, consider the distribution of carbons among groups 1-5 and 8-15 of Figure 1. If these 13 groups were equally probable, each would contain 1/13 of the carbon. This statement can be implemented by minimizing:

$$P_1 = \sum_{A_{1j} \neq 0} \left(\frac{b_1}{13A_{1j}} - y_j \right)^2 \quad (3)$$

subject to equations 1 and 2, where b_1 is the concentration of carbon in the sample.

However, there is no reason to single out carbon to equidistribute among functional groups. For aromatic hydrogen the function to be minimized is:

$$P_2 = \sum_{A_{2j} \neq 0} \left(\frac{1}{5A_{2j}} (b_2 + 2y_6 + 2y_7 + y_8 + 2y_{11} + 2y_{12} + 2y_{13} + 2y_{14} + 4y_{15}) - y_j \right)^2 \quad (4)$$

where b_2 is the concentration of aromatic hydrogen in the sample. The total number of aromatic hydrogen positions to be distributed among the five functional groups is equal to the number of aromatic hydrogens plus the number of aromatic substituents. Similarly, the expressions for the distribution of the remaining experimental quantities determined from NMR and elemental analysis data, i.e., alpha, beta and gamma hydrogen, oxygen and sulfur concentrations are:

$$P_3 = \sum_{A_{3j} \neq 0} \left(\frac{1}{6A_{3j}} (b_3 + y_9) - y_j \right)^2 \quad (5)$$

$$P_4 = \sum_{A_{4j} \neq 0} \left(\frac{1}{4A_{4j}} (b_4 + y_{10}) - y_j \right)^2 \quad (6)$$

$$P_5 = \left(\frac{b_5}{3} - y_{10} \right)^2 \quad (7)$$

$$P_6 = (b_6 - y_8)^2 \quad (8)$$

$$P_7 = (b_7 - y_5)^2 \quad (9)$$

Minimizing any of the functions P_i ($i=1, \dots, 7$) would express a lack of preference among functional groups with respect to a particular concentration, e.g., aromatic hydrogen. If we minimize the sum of the individual P_i s we will get solutions that express the lack of preference among functional groups with respect to all of the concentrations. Thus, P_8 is the function that is minimized in the functional group analysis method when no data other than NMR and elemental analysis are available.

$$P_8 = \sum_{i=1}^7 P_i \quad (10)$$

Minimization Function Based on High Resolution Mass Spectral Data


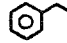

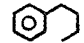
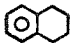

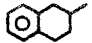

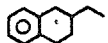



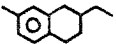
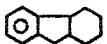




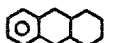
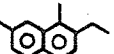






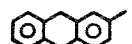
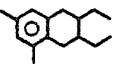
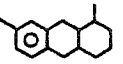
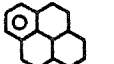
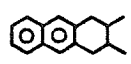
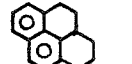
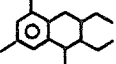
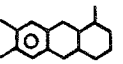
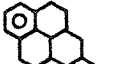
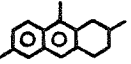

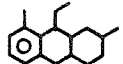
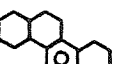
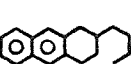
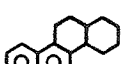
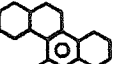
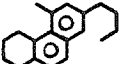
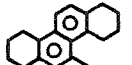
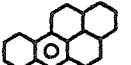
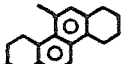
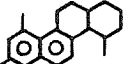
High resolution mass spectra provide a wealth of information on the structure of fossil fuel fractions. For typical coal liquids, approximately 90 separate peaks can be resolved in the spectra. Since high resolution mass spectrometry can resolve masses to one part in 150,000, heteroatoms can be resolved from the hydrocarbon background, and precise empirical formulas can be assigned to each peak in the spectra. Quantitative interpretation of the spectra is difficult, however, because the relationship between peak intensities and concentrations is not always known and peaks are often difficult to resolve. Thus, the mass spectra are less quantitative than the NMR and elemental analysis data and are more appropriately used in the minimization function than in the balance equations.

In constructing the minimization function, functional group concentrations are determined from the mass spectra. This is done by assigning a structure to each molecular formula appearing as a peak in the mass spectrum. The types of structures assigned to the peaks are given by Herod et al. (22) and are shown in Figure 2. Each of the structures is broken into its constituent functional groups, and the apparent concentrations of a set of functional groups are then calculated.

This method of interpreting the high resolution mass spectra involves several approximations. First, it is assumed that each peak in the mass spectrum can be represented by one structure. Many of the molecular formulas have more than one isomer. In some cases, this is not a concern since the

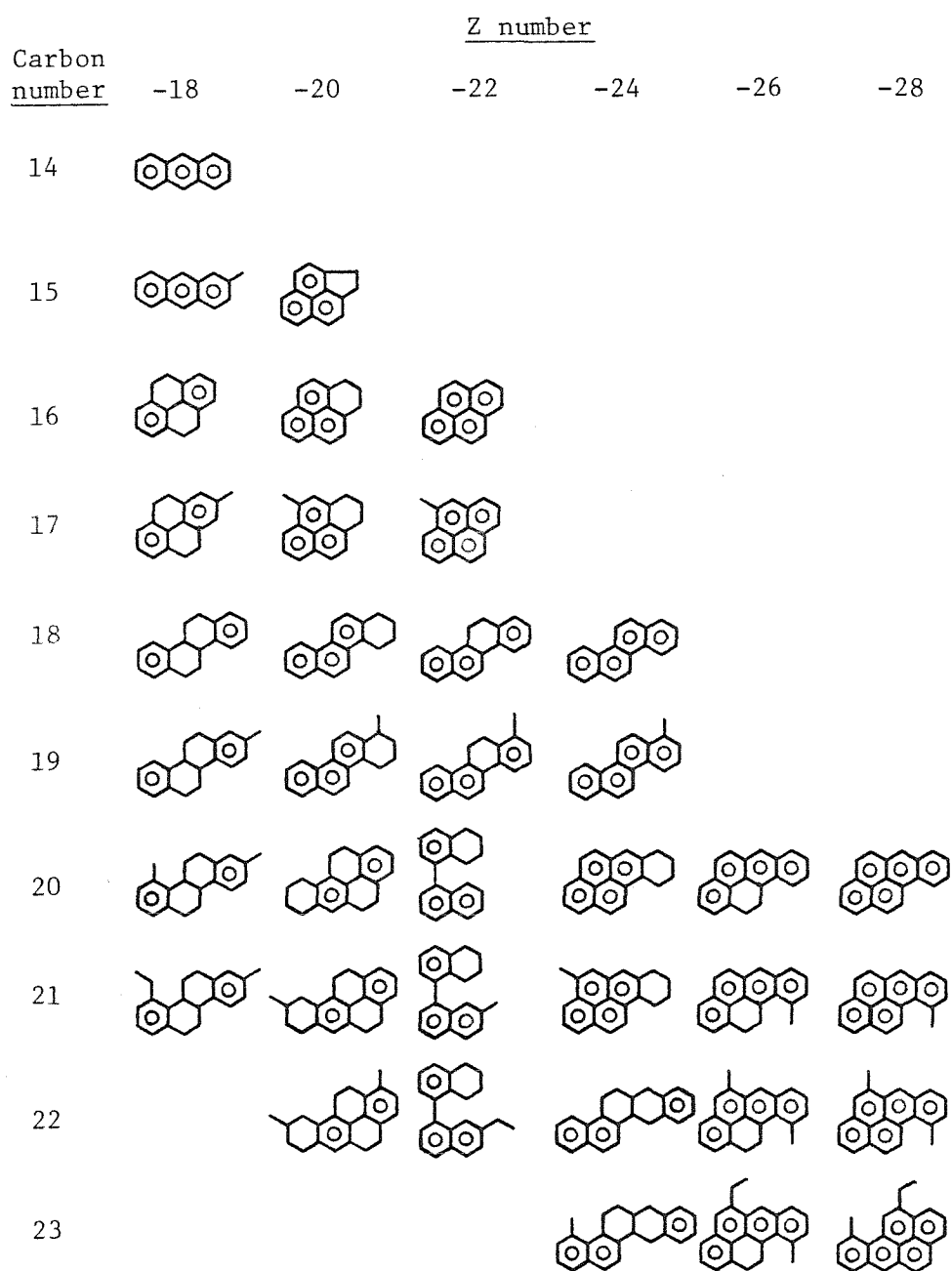
Figure 2

Structure Assignments for Hydrocarbon Peaks
in Coal Liquid Mass Spectra

Carbon number	<u>Z number</u> *					
	-6	-8	-10	-12	-14	-16
7						
8						
9						
10						
11						
12						
13						
14						
15						
16						
17						
18						
19						
20						
21						

* Peaks reported by carbon number
and Z number
Z number = H number - 2 * carbon number

Figure 2 (contd.)



different isomers can be constructed from identical functional groups. When isomers are composed of different functional groups, the structure selected to represent the peak is the structure considered most likely to be found in the liquid being considered.

A second assumption is that a concise set of functional groups can be used to represent all of the structures assigned to the peaks. The functional groups are chosen to provide as complete a description as possible of the structure of the sample, while maintaining a low number of functional groups. Groups that participate only in structures present in extremely low concentrations are generally incorporated into the concentrations of similar functional groups. This assumption does not usually present a serious problem since the vast majority of the structures can be exactly constructed from a small set of functional groups.

The set of functional group concentrations which most closely resembles the concentrations derived from the high resolution mass spectra, yet still satisfies the elemental composition and NMR data, is determined by minimizing equation 11 subject to the constraints of equations 1 and 2:

$$P = \sum_{i=1}^n (y_i - f_i)^2 \quad (11)$$

where f_i is the concentration of functional group i determined from the mass spec data. Equation 11 may be thought of as the minimum distance between the point defined by the mass spec concentrations and the space of feasible solutions defined by equations 1 and 2. The minimum value of P serves as a measure of the agreement between the concentrations determined from the high resolution mass spec data and the rest of the analytical data.

Minimization Function Based on Low Resolution Mass Spectral Data

The approximations involved in interpreting the high resolution mass spectra also apply to the low resolution spectra, so the data are treated in an analogous manner. Structures are assigned to the peaks resolved in the low resolution spectrum and estimates of the functional group concentrations are calculated.

Since any alkyl chains present in the structures are removed during the high voltage ionization used in obtaining the low resolution spectrum, alkyl chains are not detected. Thus, the low resolution spectra only give data on the relative concentrations of aromatic and hydroaromatic groups. Functional group analysis is used to find the set of concentrations which most closely resemble the concentration ratios predicted by the low resolution mass spectra. Equation 12 is the appropriate function to be minimized for this purpose. The value of the minimum serves as a measure of the agreement between the mass spec concentrations and the NMR and elemental analysis data.

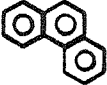




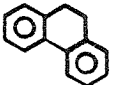

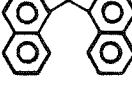
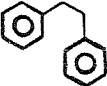


$$P = \sum_{i=2}^n \left(\frac{y_i}{y_1} - \frac{f_i}{f_1} \right)^2 \quad (12)$$

Application of Functional Group Analysis


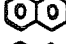
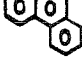
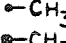
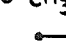




The method of functional group analysis will now be applied to mixtures of known composition and demonstrated in detail on a set of four hydrodesulfurized coal liquids. The mixtures of known composition are described in Table I. Two sets of calculations were made on the mixtures. First, functional group concentrations were estimated for both mixtures using only elemental analysis and NMR data. These concentrations indicate how well the general method

Table I

FUNCTIONAL GROUP ANALYSIS OF MODEL COMPOUND MIXTURES

Mixture Composition					
	Mixture			Mixture	
	#1 (g)	#2 (g)		#1 (g)	#2 (g)
	13.2	13.2		13.1	13.1
	3.3	3.3		31.4	14.3
	14.0	14.0		6.7	6.7
	7.4	7.4		7.8	7.8
	6.9	6.9		6.3	6.3
	7.0	7.0			

Functional Group Concentrations

	Mixture #1		Mixture #2			
	True Conc.	Result of Algorithm Eqns 1,2,10	True Conc.	Result of Algorithm Eqns 1,2,10	Concentration estimated from Mass Spectrum	Result of Algorithm Eqns 1,2,11
	.585	.463	.585	.420	.503	.516
	.309	.279	.199	.245	.211	.215
	.075	.148	.075	.112	.098	.093
	.251	.250	.141	.140	.177	.140
	.202	.240	.092	.150	.108	.098
	.129	.000	.129	.000	.113	.096
	.143	.153	.143	.135	.097	.106
	.076	.109	.076	.138	.063	.099
	.165	.137	.165	.122	.121	.162

estimates absolute concentrations and changes in concentrations between samples. Next, concentrations for one of the samples were estimated using a high resolution mass spectrum of the mixture. Concentrations were estimated directly from the mass spectrum and by using equation 12 as the minimization function in the functional group analysis algorithm. The results, shown in Table I, show that the general method, utilizing only elemental analysis and NMR data, gives fair estimates of absolute concentrations and good estimates of changes in concentrations. When additional data, particularly high resolution mass spectra, are available the estimates become more accurate. While the results for coal liquids may not be as accurate as for these simple mixtures, these results at least give an estimate of the uncertainties involved.

We now proceed to the examination of the hydrodesulfurized neutral oils. Elemental composition, ^1H NMR spectra and low and high resolution mass spectra were obtained for each of the samples. The elemental composition and ^1H NMR data are given in Table 2. The ^1H NMR spectra were divided into aromatic, alpha, beta and gamma bands, using the chemical shift assignments of Snape (23). The low resolution mass spec data are shown in Table 3 and a summary of a typical high resolution spectrum is given in Table 4.

The set of fifteen functional groups adopted for these samples is listed in Figure 1. This list is not meant to be an exhaustive compilation of all functional groups present in the neutral oils. Instead, it contains groups representative of the basic structural features of the oils, i.e., aromatic clusters, hydroaromatic groups, aliphatic chains, bridges, and oxygen containing groups. Ether- and furan-type structures were the only oxygen groups considered because the procedure used to obtain the oils removes phenolic

Table 2

Elemental Composition and NMR Data

<u>Hydrotreatment (h)</u>	<u>Elemental Composition Data</u>			
	<u>%C</u>	<u>%H</u>	<u>%O</u>	<u>%S</u>
0.0	91.4	7.3	0.29	0.62
3.0	91.6	7.6	0.45	0.36
7.5	92.6	7.8	0.19	0.35
25.0	91.4	8.2	0.18	0.18

<u>Hydrotreatment (h)</u>	<u>¹H NMR Data</u>			
	<u>%Aromatic (9.0-5.0 ppm)</u>	<u>%Alpha (5.0-1.9 ppm)</u>	<u>%Beta (1.9-1.0 ppm)</u>	<u>%Gamma (1.0-0.5 ppm)</u>
0.0	43.8	33.0	19.3	4.0
3.0	40.0	32.5	21.7	5.8
7.5	37.6	31.6	24.9	6.0
25.0	34.6	35.4	24.4	5.5

Table 3

Low Resolution Mass Spectral Data

Group Type	Weight %			
	Hydrotreatment (h)			
	<u>0.0</u>	<u>3.0</u>	<u>7.5</u>	<u>25.0</u>
Decahydrobenzochrysenes	0.6	0.4	0.3	0.1
Octahydrobenzochrysenes	0.6	0.4	0.4	0.4
Hexahydrobenzochrysenes	0.5	0.3	0.4	0.3
Tetrahydrobenzochrysenes	0.6	0.3	0.4	0.3
Benzochrysenes	0.5	0.4	0.4	0.4
Decahydrobenzopyrenes	0.8	0.9	0.9	0.9
Octahydrobenzopyrenes	0.9	0.9	0.8	0.7
Hexahydrobenzopyrenes	1.1	1.0	1.0	0.9
Tetrahydrobenzopyrene	0.9	0.7	0.7	0.6
Binaphthyls	0.7	0.5	0.5	0.5
Benzopyrenes	1.8	1.3	1.2	1.2
Dodecahydrochrysenes	1.8	1.5	1.5	1.5
Octahydrochrysenes	0.7	1.1	1.2	1.1
Hexahydrochrysenes	1.1	1.4	1.5	1.3
Chrysenes	1.7	0.9	0.9	0.8
Decahydropyrenes	2.8	3.0	2.9	2.4
Hexahydropyrenes	5.6	7.2	7.6	7.2
Tetrahydrofluoranthenes	2.8	3.4	3.3	2.9
Pyrenes	11.2	9.5	9.4	8.7
Phenylanthralenes	6.8	7.0	6.5	5.7
Octahydrophenanthrenes	1.9	4.1	5.6	7.2
Hexahydrophenanthrenes	1.7	1.5	1.1	0.7
Tetrahydrophenanthrenes	10.2	10.1	10.3	10.9
Phenanthrenes	12.1	10.4	9.5	8.1
Fluorenes	10.0	11.3	10.9	10.2
Biphenyls	10.7	10.4	10.5	11.9
Tetralins	0.0	0.3	0.6	1.3
Tetrahydroacenaphthalenes	1.0	2.6	2.9	3.3
Naphthalenes	5.7	4.5	3.9	4.1
Benzenes	3.2	2.8	3.1	4.4

Table 4

Summary of a Typical High Resolution Mass Spectrum

Sample: Neutral oil feed

<u>Hydrocarbon type</u>	<u>Avg. C #</u>	<u>Wt.%</u>	<u>Total wt.%</u>
Monoaromatics	-	-	3.76
Alkylbenzenes	7.10	0.69	-
Indans	14.88	1.16	-
Indenes	14.34	1.91	-
Diaromatics	-	-	36.14
Naphthalenes	13.93	8.36	-
Biphenyls	14.65	16.03	-
Fluorenes	15.29	11.75	-
Triaromatics	-	-	25.61
Phenanthrenes	15.31	19.16	-
Phenanthrocylo- paraffins	17.43	6.45	-
Tetraaromatics	-	-	20.54
Pyrenes	17.25	16.43	-
Chrysenes	19.29	4.11	-
Pentaaromatics	-	-	4.58
Chrysocycloparaffins	20.48	1.87	-
Benzopyrenes	21.09	2.00	-
Dibenzanthracenes	21.73	0.71	-
Polyaromatics	22.32	0.98	0.98
Sulfur Peaks	-	-	1.81
Dibenzothiophenes	13.18	1.59	-
Benzonaphthothiophenes	16.49	0.19	-
Oxygen Peaks	-	-	6.59
Phenols	0.00	0.00	-
Dibenzofurans	14.54	5.95	-
Benzonaphthofurans	17.27	0.64	-

functionalities. Additional groups, such as larger condensed aromatic structures and longer alkyl chains, may be necessary for some samples of coal liquids, but were not needed to explain the analytical data presented here.

Having specified the functional groups, the balance equations can be immediately written down. For example, the balance equation for alpha hydrogen is:

$$3y_8 - y_9 + 2y_{11} + 4y_{12} + 4y_{13} + 3y_{14} + 6y_{15} = b_3 \quad (13)$$

where b_3 is the experimentally determined concentration of alpha hydrogen, y_j is the concentration of functional group j (as defined in Figure 1) and the numerical coefficients are the stoichiometric A_{ij} .

There are seven balance equations in the fifteen unknowns y_1, \dots, y_{15} . Table 5 gives the concentrations obtained from the elemental analyses and the ^1H integrals for the four distinct hydrogen types and for total carbon, oxygen and sulfur. Table 6 gives the stoichiometric coefficients which relate each of the fifteen functional groups to the hydrogen types and the C, O, and S elemental contents.

Functional group concentrations were determined by minimizing the function defined in equation 10, subject to equations 1 and 2. This procedure requires only elemental analysis and ^1H NMR data. The algorithm of Luus and Jaakola (24) was used in the minimization. The results are listed in Table 7. Equations 11 and 12 were also minimized subject to equations 1 and 2. This procedure determined the concentrations which most closely resemble the concentrations derived from the low and high resolution mass spectra. The results are listed in Table 7. The concentrations derived from the mass

Table 5

Coefficients B_j , for the Experimental Data (Constraints)

Hydrotreatment (h)	B_1^*	B_2^*	B_3^*	B_4^*	B_5^*	B_6^*	B_7^*
0.0	7.62	3.18	2.39	1.40	0.288	0.018	0.020
3.0	7.63	3.05	2.48	1.66	0.440	0.028	0.011
7.5	7.72	2.92	2.45	1.93	0.461	0.012	0.011
25.0	7.62	2.82	2.89	1.99	0.449	0.011	0.006

42.

- *
 B_1 = Moles of carbon/ 100 g of sample
 B_2 = Moles of aromatic hydrogen/100 g of sample
 B_3 = Moles of alpha hydrogen/100 g of sample
 B_4 = Moles of beta hydrogen/100 g of sample
 B_5 = Moles of gamma hydrogen/100 g of sample
 B_6 = Moles of oxygen/100 g of sample
 B_7 = Moles of sulfur/100 g of sample

Table 6

Stoichiometric Coefficients, A_{ij} , Relating Functional Groups and the Experimental Data (Constraints)

Constraint i^{**}	Functional Group j^*														
	<u>1</u>	<u>2</u>	<u>3</u>	<u>4</u>	<u>5</u>	<u>6</u>	<u>7</u>	<u>8</u>	<u>9</u>	<u>10</u>	<u>11</u>	<u>12</u>	<u>13</u>	<u>14</u>	<u>15</u>
1. Carbon	6	10	14	16	12	0	0	1	1	1	1	2	4	8	6
2. Aromatic Hydrogen	6	8	10	10	8	-2	-2	-1	0	0	-2	-2	-2	-2	-4
3. Alpha Hydrogen	0	0	0	0	0	0	0	3	-1	0	2	4	4	3	6
4. Beta Hydrogen	0	0	0	0	0	0	0	0	3	-1	0	0	4	11	4
5. Gamma Hydrogen	0	0	0	0	0	0	0	0	0	3	0	0	0	0	0
6. Oxygen	0	0	0	0	0	1	0	0	0	0	0	0	0	0	0
7. Sulfur	0	0	0	0	1	0	0	0	0	0	0	0	0	0	0

* Functional group numbers are defined in Figure 2.

** Constraint numbers are defined in Table 5

Table 7

Functional Group Analysis Results
(Concentrations in moles/100 g of sample)



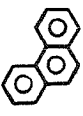


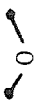

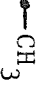
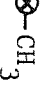
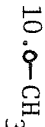



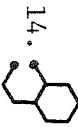
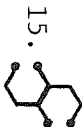
Functional Group	General Results *				Results Based on Mass Spectroscopy ***							
	Hydrotreatment (h)				High Resolution **				Low Resolution			
	0	3.0	7.5	25.0	0	3.0	7.5	25.0	0	3.0	7.5	25.0
1. 	.236	.247	.238	.305	.301	.355	.346	.389	.369	.394	.408	.418
2. 	.135	.144	.129	.122	.151	.155	.153	.179	.129	.133	.122	.130
3. 	.094	.088	.092	.074	.086	.088	.086	.074	.055	.051	.043	.039
4. 	.081	.071	.074	.061	.055	.028	.043	.002	.074	.064	.061	.052
5. 	.020	.011	.011	.006	.020	.011	.011	.006	.020	.011	.011	.006
6. 	.018	.028	.012	.011	.018	.028	.012	.011	.018	.028	.012	.011
7. 	.000	.000	.000	.000	.074	.046	.069	.020	.140	.133	.144	.125
8. 	.288	.360	.308	.533	.303	.248	.222	.318	.365	.398	.285	.584
9.  -CH ₃	.082	.139	.190	.238	.060	.053	.107	.040	.098	.198	.182	.317

Table 7

Functional Group Analysis Results
(Concentrations in moles/100 g of sample)

Functional Group	Results Based on Mass Spectroscopy											
	General Results *				High Resolution **				Low Resolution ***			
	Hydrotreatment (h)				Hydrotreatment (h)				Hydrotreatment (h)			
	0	3.0	7.5	25.0	0	3.0	7.5	25.0	0	3.0	7.5	25.0
10.  -CH ₃	.096	.147	.154	.150	.096	.147	.154	.150	.096	.147	.154	.150
11. 	.004	.001	.002	.002	.088	.092	.096	.062	.067	.067	.073	.057
12. 	.151	.116	.145	.101	.086	.088	.086	.074	.076	.090	.100	.085
13. 	.117	.160	.139	.190	.162	.203	.208	.263	.140	.171	.199	.202
14. 	.049	.052	.064	.050	.046	.065	.066	.083	.040	.027	.044	.020
15. 	.064	.047	.064	.035	.039	.042	.054	.042	.046	.036	.050	.023
P	-	-	-	-	.005	.013	.005	.022	.024	.010	.026	.003

* Equation 10 minimized
 ** Equation 11 minimized
 *** Equation 12 minimized

spectra are given in Table 8 .



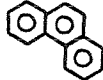

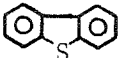
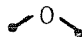

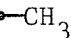
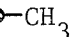
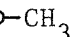



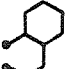
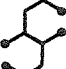
Examination of the functional group concentrations reveals the following trends. With increasing residence time, the concentration of large aromatic clusters decreases while hydroaromatics and small aromatic clusters increase. Aliphatic chains increase slightly and bridge concentrations remain roughly constant. These trends support the view that condensed aromatic units are being partially hydrogenated while short aliphatic chains remain relatively inert. Splitting of hydroaromatics may account for a small observed rise in aliphatic chain concentrations.

The results obtained by minimizing equations 10, 11 and 12 are similar in both their trends and absolute values. The only significant differences occur in functional groups 9, 11 and 12. The various results disagree on the distribution of aliphatic groups among alkyl chains and bridges. The only independent experimental evidence available on these concentrations are estimates of functional group 11 concentrations obtained from ^1H NMR. Assuming all hydrogens with chemical shifts between 3.4 and 5.0 ppm are in group 11 structures gives concentrations of .07-.10 moles/100 g. This is in reasonable agreement with the results based on the mass spectra. The model compound results of Table I also tend to support the concentrations which utilize the mass spectral data. ^{13}C NMR spectra could be used to better define the distribution between alkyl chain and bridge groups. Overall, the functional group concentrations obtained using minimization functions derived by the 3 approaches are in reasonable agreement.

The concentrations derived from the mass spectra, shown in Table 8 , very

Table 8

Functional Group Concentrations Derived from Mass Spectra

	High Resolution Data				Low Resolution Data			
	Concentrations in moles/100 g				Relative Concentrations			
	Hydrotreatment (h)				Hydrotreatment (h)			
	<u>0</u>	<u>3.0</u>	<u>7.5</u>	<u>25.0</u>	<u>0.</u>	<u>3.0</u>	<u>7.5</u>	<u>25.0</u>
1. 	.285	.323	.332	.335	1	1	1	1
2. 	.150	.147	.153	.162	.390	.356	.342	.317
3. 	.096	.082	.069	.067	.167	.132	.119	.095
4. 	.083	.078	.070	.065	.174	.126	.123	.106
5. 	.010	.007	.004	.002	-	-	-	-
6. 	.034	.031	.026	.024	-	-	-	-
7. 	.100	.092	.089	.089	.323	.297	.289	.275
8. 					-	-	-	-
9. 	.445	.424	.467	.477	-	-	-	-
10. 					-	-	-	-
11. 	.098	.112	.103	.096	.135	.140	.133	.116
12. 	.082	.081	.077	.074	.171	.209	.212	.190
13. 	.127	.146	.170	.186	.356	.422	.464	.474
14. 	.012	.016	.027	.031	.029	.030	.027	.022
15. 	.025	.027	.031	.031	.038	.031	.030	.027

nearly match those derived from the functional group analysis. Considering the approximate nature of the NMR band assignments and the assumptions involved in the interpretation of the mass spectra, the agreement is quite good. The close agreement of the concentrations based on two independent sources of data supports the utility of functional group characterization of mixtures.

Finally, the results of the functional group analysis method were compared to the results of an established method of structural analysis. The average structural parameters defined by Clutter et al. (9) were used for the comparison. The average parameters were calculated in the standard manner using ^1H NMR spectra and by direct evaluation from the functional group concentrations. The excellent agreement between the two results, shown in Table 9, is further support for the proposed algorithm of functional group analysis.

CONCLUSIONS

The proposed method of functional group analysis was applied to two test mixtures of known composition and to several samples of coal derived liquids. In the case of the test mixtures, using elemental composition and NMR data, the method gave fair estimates of absolute concentrations and good estimates of changes in concentrations. When mass spectroscopic data were used in conjunction with the NMR and elemental analysis data, the estimates of absolute concentrations improved considerably. Application to the samples of coal liquids yielded fair to good agreement between concentrations estimated from elemental composition and NMR data on the one hand, and concentrations estimated from elemental composition, NMR and mass spectroscopic data. The functional group analysis method is very flexible in accommodating a variety

Table 9

Comparison of Functional Group Analysis
Results with Average Molecule Calculation

Parameter	Value determined from functional group concentrations (general results)				¹ H NMR average molecule calculations			
	Hydrotreatment (h)				Hydrotreatment (h)			
	0	3.0	7.5	25.0	0	3.0	7.5	25.0
Aromatic carbon/total carbon	.70	.69	.67	.66	.72	.69	.67	.65
Average number of rings in an aromatic cluster	2.04	1.97	2.00	1.80	2.0	2.0	1.9	1.8
Nonbridge aromatic carbons/total carbons	.56	.55	.53	.54	.58	.56	.55	.54
Naphthenic carbon/ total carbon	.17	.18	.19	.18	.18	.19	.25	.24
% of nonbridge aromatic carbons which are substituted	29.	30.	32.	34.	29.	31.	33.	36.

50.

analytical data in a systematic fashion.

References

- [1] K.S. Seshadri and D.C. Cronauer, *Prepr. Am. Chem. Soc. Div. Fuel Chem.*, **27** (2), 64 (1982).
- [2] D.W. Kuehn, A. Davis, R.W. Snyder, M. Starsinic and P.C. Painter, *Prepr. Am. Chem. Soc. Div. Fuel Chem.*, **27** (2), 55 (1982).
- [3] R.G. Ruberto, D.M. Jewell, R.K. Jensen and D.C. Cronauer, *Advances in Chemistry Series, No. 151*, American Chemical Society, New York, 1976, Chapter 3.
- [4] D.A. Netzel, D.R. McKay, R.A. Heppner, F.D. Guffey, S.D. Cooke, D.L. Varie and D.E. Linn, *Fuel*, **60**, 307 (1981).
- [5] J.K. Brown and W.R. Ladner, *Fuel*, **39**, 87 (1960).
- [6] K.D. Bartle, T.G. Martin, D.F. Williams, *Fuel*, **54**, 226 (1975).
- [7] D.M. Cantor, *Anal. Chem.*, **50**, 1185 (1978).
- [8] J.M. Charlesworth, *Fuel*, **59**, 865 (1980).
- [9] D.R. Clutter, L. Petrakis, R.L. Stenger and R.K. Jensen, *Anal. Chem.*, **44**, 1395 (1972).
- [10] E.M. Dickinson, *Fuel*, **59**, 290 (1980).
- [11] S. Gillet, P. Rubini, J. Delpuech, J. Escalier and P. Valentin, *Fuel*, **60**, 254 (1981).
- [12] G.A. Haley, *Anal. Chem.*, **44**, 580 (1972).
- [13] T. Suzuki, M. Itoh, T. Yoshinobu and Y. Watanabe, *Fuel*, **61**, 402 (1982).

- [14] K.C. Tewari, T. Hara, N.C. Li and U.C. Fu, *Fuel*, **60** , 1137 (1981).
- [15] S. Yokoyama, H. Uchino, T. Katoh, Y. Sanada and T. Yoshida, *Fuel*, **60** , 254 (1981).
- [16] H.I. Retcofsky, F.K. Schweighardt and M. Hough, *Anal Chem.*, **49** , 585 (1977).
- [17] M. Oka, H. Chang and G.R. Gavalas, *Fuel*, **56** , 3 (1977).
- [18] J.T. Swansiger, F.E. Dickson and H.T. Best, *Anal. Chem.*, **46** , 730 (1974).
- [19] P.R. Solomon, *Prepr. Am. Chem. Soc. Div. Fuel Chem.*, **24** (2), 184 (1979).
- [20] L. Petrakis, R.G. Ruberto, D.C. Young, S. Katti and B.C. Gates, *I.&E.C. Fund.*, , in press.
- [21] S.S. Shih, J.R. Katzer, H. Kwart and A.B. Stiles, *Prepr. Am. Chem. Soc. Div. Pet. Chem.*, **22** , 919 (1977).
- [22] A.A. Herod, W.R. Ladner and C.E. Snape, *Phil. Trans. R. Soc. Lond.*, **A 300** , 3 (1981).
- [23] C.E. Snape, W.R. Ladner, and K.D. Bartle, *Coal Liquefaction; NMR Spectroscopic Characterization and Production Processes*, in press, chapter 5.
- [24] R.. Luus and T.H.I. Jaakola, *AIChE J.*, **19** , 760 (1973).

Chapter 4

**FUNCTIONAL GROUP ANALYSIS
OF COAL LIQUIDS**

by

David T. Allen¹, Leonidas Petrakis², David W. Grandy² and
George R. Gavalas¹

¹Department of Chemical Engineering
California Institute of Technology
Pasadena, California 91125

²Gulf Research and Development Company
Pittsburgh, Pennsylvania 15230

This chapter was submitted as a manuscript to the journal *Fuel*

ABSTRACT

A new method of structural analysis is applied to a group of hydroliquefied coal samples. The method uses elemental analysis and NMR data to estimate the concentrations of functional groups in the samples. The samples include oil and asphaltene fractions obtained in a series of hydroliquefaction experiments, and a set of 10 fractions separated from a coal-derived oil. The structural characterization of these samples demonstrates that estimates of functional group concentrations can be used to provide detailed structural profiles of complex mixtures and to obtain limited information about reaction pathways.

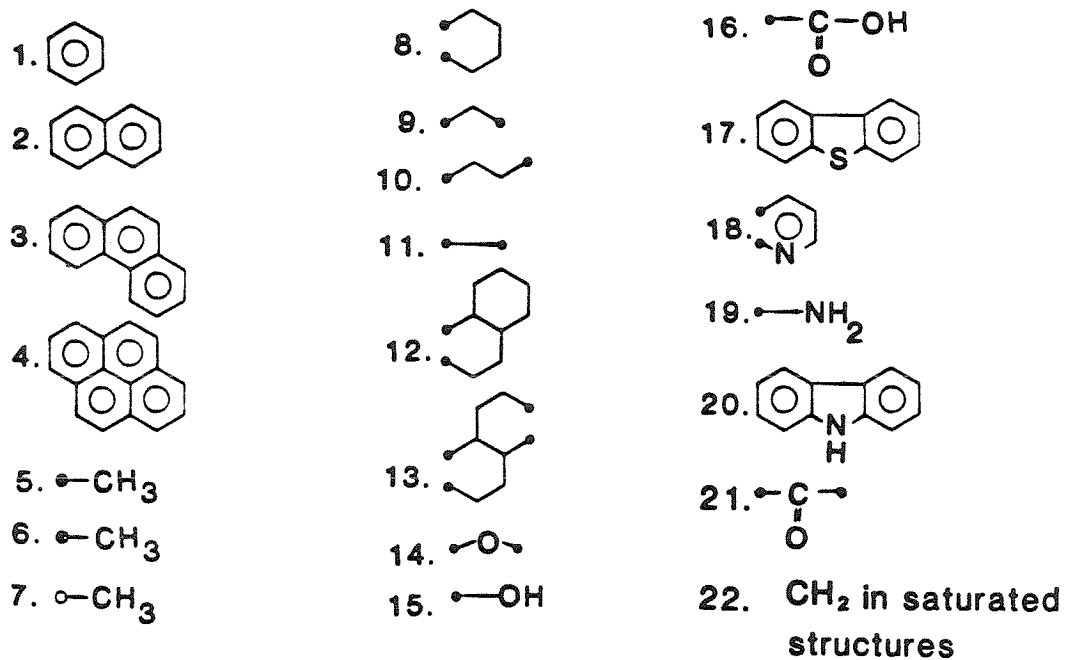
INTRODUCTION

Characterizing the structures of fuels derived from coal is an important step in developing an understanding of the chemistry of coal reactions. The determination of exact chemical structures of coal liquids from elemental composition, Nuclear Magnetic Resonance (NMR) and possibly other analytical data is an underdetermined problem, however, because of the complexity and variety of the molecules in the liquids. Since the molecular structures cannot be fully delineated, recourse must be made to approximate characterization methods. The data on which such characterizations are most commonly based are elemental analysis, ^1H nmr spectra, and less routinely, ^{13}C nmr spectra.

Structural characterization most frequently takes the form of a representative molecular structure, or a set of average parameters, such as carbon aromaticity, average length of alkyl chains, and the degree of aromatic substitution¹⁻⁵. In this work, we apply an alternative method of structural characterization, termed functional group analysis. The goal of functional group analysis is to calculate the concentrations of the functional groups present in the sample. The method is based on the premise that although the number of individual molecular species in a coal liquid is large, most of these species are composed of a limited number of functional groups. The relative concentrations of the functional groups determine the chemical behavior of the liquids. Thus, calculating the concentrations of the major functional groups is a useful structural characterization.

A set of functional groups appropriate for the characterization of hydro-treated coal liquids is given in Figure 1. This set is not a complete listing of all

Figure 1

Coal liquid functional groups**Notation:**

 bound directly to an aromatic ring

 bound to a carbon alpha to an aromatic ring

 bound to a carbon beta or further from an aromatic ring

Example:

structures known to be present in coal liquids. Rather, it is a concise representation of the major structural features of hydrotreated coal liquids, i.e., aromatic clusters, hydroaromatic groups, alkyl chains, bridges and heteroatomic groups. The method of functional group analysis seeks to calculate the concentrations of these groups utilizing elemental composition, NMR, and possibly other supplemental data. An extensive description of the methodology has been given⁶. Briefly, the NMR and elemental analysis data are used to construct linear balance equations. In these balance equations, the concentration of each atomic species is expressed as a sum of the contribution from the functional groups, each with a suitable stoichiometric coefficient. For example, the concentration of aromatic carbon equals 6 times the concentration of monoaromatic groups plus ten times the concentration of diaromatic groups plus..... . The set of balance equations can be written succinctly in the matrix form:

$$\sum_{j=1}^n A_{ij} y_j = b_i \quad (i=1, \dots, m) \quad (1)$$

where y_j ($j=1, \dots, n$) are the unknown functional group concentrations, b_i ($i=1, \dots, m$) are atomic species concentrations and A_{ij} are stoichiometric coefficients. The number of equations is smaller than the number of unknowns, $m < n$.

In addition to the constraints imposed by the balance equations, there are the constraints of non-negative concentrations:

$$y_j \geq 0 \quad (2)$$

Equations 1 and 2 define a space of feasible solutions. The structure of the coal liquid is characterized by selecting a single solution from the feasible

space. To select a solution, we adopt a procedure that is computationally straightforward. The set of concentrations y_1, \dots, y_n is selected such that a function $P(y_1, \dots, y_n)$ is minimized. The form of the function depends on what, if any, data are available in addition to elemental analysis and NMR. For example, if no data are available other than the constraints of equations 1 and 2, equation 3 is minimized:

$$P = \sum_{i=1}^m \sum_{j=1}^n \left(\frac{b_i}{A_{ij}N_i} - y_j \right)^2 \quad (3)$$

where N_i is the number of functional groups containing species i . Equation 3 was constructed by assuming that the distribution of atomic species among the functional groups was random⁶. Concentrations obtained by minimizing this equation subject to the constraints of equations 1 and 2 were found to be in good agreement with functional group concentrations based on high resolution mass spectral data and with the results of other methods of structural analysis⁶. The function to be minimized can be modified to incorporate qualitative information based on data other than NMR and elemental analysis. For example, the function to be minimized if high resolution mass spectra are available is equation 4:

$$P = \sum_{i=1}^n (y_i - f_i)^2 \quad (4)$$

where f_i is the concentration of functional group i predicted by the mass spec data⁶.

In this work, functional group concentrations will be estimated for two sets of synthetic fuel samples utilizing elemental analysis, ^1H NMR and ^{13}C NMR data. The first set of samples is a group of 10 fractions of a solvent refined

coal. Analysis of these samples will demonstrate how the functional group method can be used to provide detailed descriptions of complex mixtures. The second set of samples is a group of asphaltene and oil fractions obtained in a series of coal hydroliquefaction experiments. The functional group concentrations obtained for these samples will help to identify liquefaction pathways.

EXPERIMENTAL

In an extensive series of experiments, Powhatan #5 coal was hydroprocessed under a variety of conditions. Experimental procedures are given below and the coal liquids obtained are listed in Table 1.

Solvent Refined Coal Fractions

A heavy distillate obtained from a 50 ton/day SRC-II demonstration plant operating with Powhatan #5 coal was fractionated using a SARA chromatographic procedure⁷. The goal of the separation was to isolate heteroatomic functionalities. The ten primary fractions obtained were neutral oils (72.5 wt. %), asphaltenes (8.9%), very weak bases (2.7%), weak bases (1.9%), strong bases (6.0%), very weak acids (1.1%), weak acids (1.2%), strong acids (0.2%), neutral resins (1.2%) and saturates (4.5%). Elemental composition, ¹H NMR and ¹³C NMR data were obtained for the fractions. The data are given in Table 2.

Hydroliquefied Coal Samples

A group of pentane soluble and toluene soluble/pentane insoluble extracts were obtained from the products of a series of autoclave experiments. The samples were prepared by shaking a reactor containing 5 g of a Powhatan #5 coal and 5 g of a liquefaction solvent in a heated fluidized sand bath. The reactor consisted of a 22 ml stainless steel bomb with a .64 cm (1/4-in.) stainless

Table 1
Coal Liquid Samples

I Fractionated SRC-II Heavy Distillate

Fractions

Neutral oils
 Asphaltenes
 Very weak bases
 Weak bases
 Strong bases
 Very weak acids
 Weak acids
 Strong acids
 Neutral resins

II Hydroliquefied coal fractions-pentane soluble and toluene soluble/
 pentane insoluble fractions obtained for each experiment

Experimental Conditions

<u>Sample No.</u>	<u>Solvent</u>	<u>Reaction Temperature</u>	<u>Reaction Time (min)</u>
400T40	Tetralin	400°C	40
460T03	Tetralin	460°C	3
460T10	Tetralin	460°C	10
460T40	Tetralin	460°C	40
400S40	SRC-II heavy distillate	400°C	40
460S03	SRC-II heavy distillate	460°C	3
460S10	SRC-II heavy distillate	460°C	10
460S40	SRC-II heavy distillate	460°C	40

Table 2

Elemental Analysis and NMR Data for SRC-II Heavy Distillate Fractions

<u>Fraction</u>	<u>Yield (wt% of Heavy Distillate)</u>	<u>Elemental Analysis Data</u>					<u>NMR Data</u>				<u>Carbon Aromaticity</u>
		<u>%C</u>	<u>%H</u>	<u>%N</u>	<u>%O</u>	<u>%S</u>	<u>%Aromatic</u>	<u>¹H NMR *</u>	<u>%Beta</u>	<u>%Gamma</u>	
Neutral oils	76.86	91.4	7.2	0	.72	.66					
Aromatic fraction of neutral oils	72.49						49	28	17	6	.77
Asphaltenes	8.88	85.4	6.4	3.2	4.5	.47	59	28	10	3	.81
Very weak bases	2.69	84.3	6.8	1.3	7.1	.52	56	25	14	5	.81
Weak bases	1.87	78.8	6.7	3.9	8.3	2.2	44	23	23	10	.74
Strong bases	5.99	85.9	6.8	4.8	1.8	0.60	44	31	19	7	.74
Very weak acids	1.08	82.2	8.0	.21	8.9	.16	48	32	16	4	.74
Weak acids	1.24	82.3	7.7	0	9.8	.16	58	25	11	4	.79
Strong acids	.21	76.0	5.6	0	17.8	.60	53	32	11	3	.79
Neutral resins	1.19	84.6	7.2	.85	7.2	.15	29	20	35	16	.67
Saturates	4.52						0	0	74	26	.00

* Chemical shift assignments from Snape et al. [11].

steel gas inlet tube. In each run, the reactor was pressurized to 11.0 MPa (109 atm) with hydrogen and was shaken in the sand bath for the specified time. Not included in the nominal reaction time was the reactor heating time, i.e., the time required for the reactor's internal temperature to reach within 1 °C of the sand bath temperature. Heating time was found to be 4 minutes at both 400 and 460°C.

After the necessary time had elapsed, the reactor was removed from the sand bath and cooled with an air jet. About 2 minutes were required to cool the sample to 300 °C. After 7 to 10 minutes of cooling, the reactor was immersed in crushed dry ice. The reaction products were removed from the reactor with a methylene chloride wash. The methylene chloride was then driven off at room temperature by a nitrogen purge. Pentane and toluene extracts were obtained by successive Soxhlet extractions. The pentane and toluene were driven off, along with the liquefaction solvent, by heating the extracts at 60 °C under a nitrogen stream.

The reaction conditions were varied to determine the effect of solvent, temperature and residence time on product structure. Tetralin and the SRC-II heavy distillate (SHD) described above were chosen as solvents to represent different hydrogen donating capabilities. Experiments were done at two temperatures and three residence times.

Proton NMR, ^{13}C NMR and elemental analysis data were obtained for each of the samples. The results of the elemental analysis and the yields of the extractions are listed in Table 3. The NMR data are given in Table 4. Sharp peaks at 6.8 and 2.2 ppm were noted in the ^1H spectra of some of the toluene extracts.

Table 3

Extraction Yields and Elemental Analysis Data for Hydroliquefied Samples

<u>Sample</u>	<u>Pentane Fraction</u>				<u>Toluene Fraction</u>			
	<u>Yield[*]</u>	<u>%C</u>	<u>%H</u>	<u>%O</u>	<u>Yield^{**}</u>	<u>%C</u>	<u>%H</u>	<u>%O</u>
400S40	.117	89.5	7.4	2.2	.197	84.1	6.3	5.3
460S03	.106	88.2	7.2	2.4	.136	84.6	5.7	6.5
460S10	.154	89.0	7.0	2.2	.141	86.0	5.3	5.5
460S40	.103	90.3	6.6	2.0	.101	88.2	5.0	4.4
400T40								
460T03	.322	82.2	7.4	5.4	.176	83.9	6.4	6.4
460T10	.423	85.0	7.2	4.5	.183	86.0	6.2	6.0
460T40	.491	87.8	7.0	3.6	.213	87.9	6.0	5.4

* $\text{Pentane Yield} = 1 - \frac{\text{Wt Pentane Insolubles}}{\text{Wt Ash-Free Coal}}$

** $\text{Toluene Yield} = 1 - \frac{\text{Wt Toluene Insolubles}}{\text{Wt Ash-Free Coal}} - \text{Pentane Yield}$

Table 4
NMR Data for Hydroliquefied Samples

^1H NMR and ^{13}C Data for Pentane Fractions

<u>Sample</u> [†]	<u>Aromatic H</u> <u>(9.0-5.0ppm) *</u>	<u>αH</u> <u>(5.0-1.9 ppm) *</u>	<u>βH</u> <u>(1.9-1.0 ppm) *</u>	<u>γH</u> <u>(1.0-.5 ppm) *</u>	<u>Carbon</u> <u>Aromaticity</u>
400S40	45.6	25.9	21.2	7.2	.74
460S03	44.6	28.6	20.1	6.6	.72
460S10	48.4	29.5	17.3	4.8	.76
460S40	56.3	31.5	10.2	1.9	.81
400T40	23.1	38.1	29.5	9.3	.51
460T03	28.4	34.3	27.8	9.5	.54
460T10	29.4	33.9	28.3	8.5	.60
460T40	30.0	36.3	25.7	8.0	.69

^1H NMR and ^{13}C Data for Toluene Fractions

400S40	39.8	33.6	21.4	5.2	.79
460S03	48.7	32.4	14.9	4.1	.82
460S10	52.4	32.3	11.9	3.5	.84
460S40	66.7	24.2	7.5	1.7	.90
400T40	32.8	36.0	24.9	6.4	.67
460T03	33.9	38.0	23.7	4.4	.70
460T10	43.5	36.2	16.4	3.9	.75
460T40	53.6	29.7	13.3	3.4	.80

* Chemical shift assignments from Snape et al. [11].

† The sample number consists of the reaction temperature, solvent and reaction time, consecutively.

The peaks were believed to be the result of residual toluene from the extraction, and were subtracted from the spectra. In all cases, the toluene present represented less than 9% of the sample.

RESULTS AND DISCUSSION

For each liquid sample, the concentrations of the functional groups listed in Figure 1 were calculated. In some cases, functional groups were assigned concentrations of zero. For example, when separation procedures were specifically designed to exclude certain functionalities, e.g., phenolics in the neutral oil fraction of the SRC heavy distillate, the concentrations of those functionalities were set equal to zero. IR spectra were particularly helpful in determining the presence or absence of some functional groups in the samples.

The results of the functional group analysis for both sets of samples are discussed below. For the hydroliquefied samples, the functional group concentrations were obtained by minimizing equation 3 subject to the constraints of equations 1 and 2. The concentrations obtained for the SRC fractions were selected by minimizing a function which utilizes qualitative data based on ^1H NMR spectra⁸. Use of two different methods of selecting a particular solution from the feasible space emphasizes the versatility of the functional group analysis algorithm in handling new sources of data.

Solvent Refined Coal Fractions

The samples examined here are the fractions obtained from a SRC-II heavy distillate. The heavy distillate was separated into ten fractions which differ primarily in the heteroatomic functionalities which they contain. IR and NMR

spectra were used to identify the functional groups present in each fraction^{9,10}.

Functional group analysis was applied to each of the ten fractions and the resulting concentrations are given in Table 5. The concentrations were obtained by selecting the solution which had a distribution of aromatic ring sizes closest to that predicted by the method of Tominaga⁸. The distribution of ring sizes could have been included in the constraints of equation 1, however these data are more qualitative than the constraints of equation 1 and are therefore more appropriately used in the selection of a solution from the feasible space rather than in defining the feasible space. Thus, a solution was selected from the feasible space by minimizing equation 5 subject to the constraints of equations 1 and 2.

$$P=(C_1-2y_2-4y_3-6y_4)^2 \quad (5)$$

where C_1 is the concentration of internal carbon in the sample⁸.

Examination of the functional group concentrations reveals that the neutral oils and the asphaltenes have a higher hydroaromatic content than the various acids and bases. High concentrations of aliphatic chains and small aromatic rings appear to be associated with high heteroatomic concentrations. Another interesting feature of the results is the ring size distribution. The neutral oils are predicted to contain mostly diaromatic rings, while the remainder of the fractions are predominantly monoaromatic. The causes and significance of this result are not yet clear.

The functional group concentrations of the whole heavy distillate were determined from the concentrations and yields of each of the fractions. The 22 concentrations, which are given in Table 5, provide a detailed structural

Table 5
SRC-II Heavy Distillate Functional Group Concentrations
(Concentrations in Moles/100g)

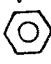

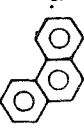





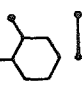
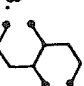
Functional Group	Neutral Oils (Aromatics)	Asphaltenes	Fraction							Whole Heavy Distillate
			Very Weak Bases	Weak Bases	Strong Bases	Very Weak Acids	Weak Acids	Strong Acids	Neutral Resins	
1. 	.035	.874	.249	.320	.301	.796	.788	.139	.150	.154
2. 	.364	.006	.104	.003	.089	.002	.016	.045	.001	.273
3. 	.080	.014	.188	.079	.072	.008	.016	.209	.192	.073
4. 	.042	.005	.021	.009	.052	.006	.015	.020	.054	.036
5. --CH_3	.073	.005	.339	.480	.218	.555	.671	.604	.680	.108
6. --CH_3	.054	.001	.001	.266	.001	.159	.199	.117	.801	.058
7. --CH_3	.136	.064	.113	.223	.160	.106	.103	.057	.383	.128
8. 	.142	.001	.001	.035	.001	.055	.001	.001	.001	.104
9. 	.063	.001	.001	.001	.001	.099	.001	.001	.001	.047
10. 	.190	.143	.050	.001	.048	.076	.001	.001	.001	.155
11. 	.018	.001	.001	.001	.001	.029	.001	.001	.001	.014
12. 	.041	.007	.096	.075	.093	.052	.031	.029	.045	.041
13. 	.025	.157	.002	.001	.107	.012	.002	.001	.001	.039

Table 5 (cont.)

(Concentrations in Moles/100 g)

Functional Group	Neutral Oils (Aromatics)	Asphaltenes	Very Weak Bases	Weak Bases	Strong Bases	Fraction			Neutral Resins	Saturates	Whole Heavy Distillate
						Very Weak Acids	Weak Acids	Strong Acids			
14.	.048	-	-	-	-	-	-	-	-	-	.035
15.	-	.281	.443	.519	.112	.556	.204	-	-	-	.062
16.	-	-	-	-	-	-	.204	.555	.150	-	.005
17.	.020	.015	.016	.069	.019	.005	.005	.019	.005	-	.019
18.	-	-	-	.279	.172	-	-	-	-	-	.016
19.	-	-	.093	-	.172	-	-	-	-	-	.013
20.	-	.230	-	-	-	.015	-	-	.061	-	.021
21.	-	-	-	-	-	-	-	-	.150	-	.002
22. CH ₂ in saturated structures	-	-	-	-	-	-	-	-	-	7.14	.309

profile of the heavy distillate and provide a reasonable starting point for the kinetic modeling of this coal liquid.

Hydroliquefied Samples

The pentane and toluene extracts examined here contain liquefaction products of moderate molecular weight. Low molecular weight products (carbon number < 10) are removed with the liquefaction solvent and very high molecular weight products tend to be insoluble in pentane and toluene. The purpose of the hydroliquefaction experiments was to help define the structures and obtain clues about the reaction pathways of these moderate molecular weight products.

We start by examining the data of Tables 3 and 4. The samples liquefied in tetralin and SRC-II heavy distillate (SHD) exhibit some straightforward trends. As the residence time increases, aromatic carbon increases, aliphatic carbon and hydrogen decrease. The samples are also deoxygenated. The changes in the content of aliphatic carbon and various types of aliphatic hydrogen are more pronounced in the samples generated in the solvent SHD relative to the samples generated in tetralin. They are also more pronounced in the toluene fractions compared to the pentane fractions.

The functional group concentrations of Tables 6 and 7 suggest the following interpretation of these data. Partially hydrogenated aromatic structures are partially or completely dehydrogenated and the hydroaromatic portion of some of these structures is being cleaved. Multiple ring hydroaromatic groups (functional groups 12 and 13) appear to be more labile than single ring hydroaromatics (group 8). An indication of the relative rates of the different

Table 6
Functional Group Concentrations for
Pentane Soluble Fraction of Hydroliquefied Samples
(Concentrations in Moles/100g)



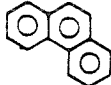
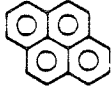

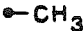





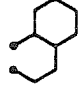
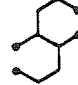



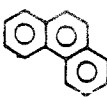
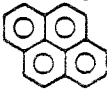

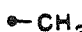
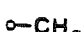



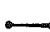
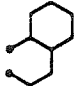
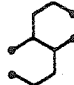

Functional Group	<u>Liquefied in Tetralin</u>				<u>Liquefied in SHD</u>			
	<u>400° 40 min</u>	<u>460° 3 min</u>	<u>460° 10 min</u>	<u>460° 40 min</u>	<u>400° 40 min</u>	<u>460° 3 min</u>	<u>460° 10 min</u>	<u>460° 40 min</u>
	.343	.320	.188	.188	.235	.270	.230	.247
	.096	.102	.112	.126	.142	.139	.141	.156
	.040	.052	.079	.093	.099	.088	.100	.112
	.002	.014	.067	.085	.083	.066	.086	.099
	.413	.283	.263	.427	.356	.302	.315	.323
	.102	.062	.245	.406	.300	.140	.150	.074
	.229	.234	.204	.187	.177	.158	.112	.042
	.199	.162	.148	.157	.144	.132	.114	.092
	.001	.000	.023	.204	.000	.000	.015	.075
	.074	.062	.137	.105	.083	.106	.124	.125
	.000	.000	.000	.159	.000	.000	.000	.000
	.158	.149	.074	.000	.020	.063	.028	.002
	.044	.069	.081	.035	.031	.040	.048	.033
	.338	.338	.281	.225	.138	.150	.138	.125

Table 7

Functional Group Concentrations for
Toluene Soluble Fraction of Hydroliquefied Samples
 (Concentrations in Moles/100g)

Functional Group	<u>Liquefied in Tetralin</u>				<u>Liquefied in SHD</u>			
	400° 40 min	460° 3 min	460° 10 min	460° 40 min	400° 40 min	460° 3 min	460° 10 min	460° 40 min
	.176	.182	.200	.218	.151	.215	.223	.246
	.114	.122	.134	.146	.116	.144	.150	.165
	.083	.091	.100	.109	.145	.108	.111	.123
	.075	.083	.091	.099	.090	.098	.102	.112
	.129	.276	.195	.128	.856	.410	.247	.212
	.123	.235	.095	.051	.478	.199	.111	.072
	.136	.094	.081	.068	.109	.078	.062	.028
	.101	.119	.083	.061	.006	.082	.069	.044
	.182	.237	.244	.201	.001	.128	.171	.116
	.133	.118	.123	.099	.001	.059	.084	.056
	.000	.063	.046	.105	.406	.384	.453	.568
	.077	.026	.032	.033	.000	.000	.000	.000
	.084	.056	.057	.050	.000	.000	.021	.002
	.400	.400	.375	.338	.331	.406	.344	.275

modes of hydroaromatic group decomposition is given by calculating the percentage of hydroaromatic carbons that are converted to alkyl and aromatic carbon. Alkyl groups will result from splitting of hydroaromatics; aromatic groups will result from dehydrogenation. Comparison of samples 460T03 and 460T40 shows a decrease in hydroaromatics (groups 8, 12 and 13) amounting to 1.63 moles of carbon per 100g of sample. Alkyl carbon increases by .44 moles/100g and aromatic carbon increases by 1.05 moles/100g, so dehydrogenation reactions appear to dominate in tetralin at 460 °C. In the pentane soluble fractions generated in tetralin and in both SHD fractions, alkyl chains decrease and aromatic rings increase in concentration with reaction time. For these fractions, dehydrogenation is also the dominant mode of hydroaromatic decomposition.

As the hydroaromatic groups dehydrogenate, the hydrogen donating ability of the fractions decreases. This decrease is less pronounced when liquefaction solvents with good hydrogen donor properties are used. This observation indicates that the oils and asphaltenes can both accept hydrogen from the liquefaction solvent and donate hydrogen to other product fractions. The donation reactions appear to be more extensive than the hydrogen accepting reactions, as evidenced by the overall loss of hydrogen in the fractions with increasing reaction time.

CONCLUSIONS

Application of the proposed method of functional group analysis to two sets of coal-derived liquids has provided the following conclusions. The method can be applied in conjunction with separation procedures to provide detailed

profiles of complex, multi-component mixtures. The method can also be used to obtain qualitative information about reaction pathways.

In general, functional group analysis is best suited for the structural analysis of complex liquids on which a large amount of data from a variety of sources is available. When applied, the method has several distinct advantages over other methods of structural characterization. It allows data from diverse sources such as NMR, IR and separation procedures to be incorporated into a single characterization; changes in structure are easily quantified; the types of structures present are easily visualized and the results could provide a starting point for kinetic modeling.

REFERENCES

- [1] J.K. Brown and W.R. Ladner, *Fuel*, **39**, 87 (1960).
- [2] J.M. Charlesworth, *Fuel*, **59**, 865 (1980).
- [3] D.R. Clutter, L. Petrakis, R.L. Stenger and R.K. Jensen, *Anal. Chem.*, **44**, 1395 (1972).
- [4] E.M. Dickinson, *Fuel*, **59**, 290 (1980).
- [5] M. Oka, H. Chang and G.R. Gavalas, *Fuel*, **56**, 3 (1977).
- [6] D.T. Allen, L. Petrakis, G.R. Gavalas and B.C. Gates, submitted to *Anal. Chem.*.
- [7] D.M. Jewell, E.W. Allbaugh, B.E. Davis and R.G. Ruberto, *Ind. Eng. Chem. Fund.*, **13** (3), 278 (1974).
- [8] H. Tominaga, I. Seiji and M. Yashiro, *Bull. Jap. Petrol. Inst.*, **19**, 50 (1977).
- [9] L. Petrakis, R.G. Ruberto, D.C. Young and B.C. Gates, *Ind. Eng. Chem. Fund.*, in press.
- [10] L. Petrakis, D.C. Young, R.G. Ruberto and B.C. Gates, *Ind. Eng. Chem. Fund.*, in press.
- [11] C.E. Snape, W.R. Ladner and K.D. Bartle, *Coal Liquefaction; NMR Spectroscopic Characterization and Production Processes*, in press, chapter 5.

Chapter 5

Application of Functional Group Analysis to Heavy Oils

In chapter 3, a new method for the characterization of complex hydrocarbon mixtures was developed. In chapter 4, this characterization, termed functional group analysis, was applied to samples of coal liquids. In this chapter, we seek to demonstrate the flexibility of the functional group analysis methodology by applying it to a sample derived from heavy crude oil.

The sample to be characterized is the atmospheric tower bottoms (ATB) from a refinery fed by a Mayan heavy crude oil. The analytical data available on the ATB sample are given in Tables 1, 2 and 3. Table 1 contains elemental analysis and ^1H NMR data. Table 2 gives the ^{13}C NMR data and Table 3 is a summary of a high resolution mass spectrum of the ATB. The procedure for estimating functional group concentrations for the ATB sample follows the general methodology defined in Chapter 3, but the utility and precision of the data are different and thus the details of the functional group calculations are slightly different.

As in the case of coal liquids, we begin by defining a set of functional groups. The functional groups proposed for the ATB are shown in Figure 1. They are different than those proposed for coal liquids, reflecting the greater abundance and variety of aliphatic structures in the oil. Separation yields and mass spectra were used in determining the concentrations and types of heteroatomic functionalities present. Mass spectra indicated that thiophene and carbazole type structures were the primary sulfur and nitrogen components. Separation

Table 1

Elemental Analysis Data				
%C	%H	%O	%N	%S
84.1	10.1	1.06	0.5	4.0

¹ H NMR Data for Mayan ATB		
Hydrogen type	Chemical shift range (ppm from TMS)	% of Hydrogen
Aromatic hydrogen	9.0-5.0	7.7
Hydrogen in CH, CH ₂ and CH ₃ groups alpha to an aromatic ring	5.0-1.9	8.3
Hydrogen in CH and CH ₂ groups beta or farther from an aromatic ring, Hydrogen in CH ₃ groups beta to an aromatic ring	1.9-1.0	62.4
Hydrogen in CH ₃ groups gamma or farther from an aromatic ring	1.0-0.5	21.6

Table 2

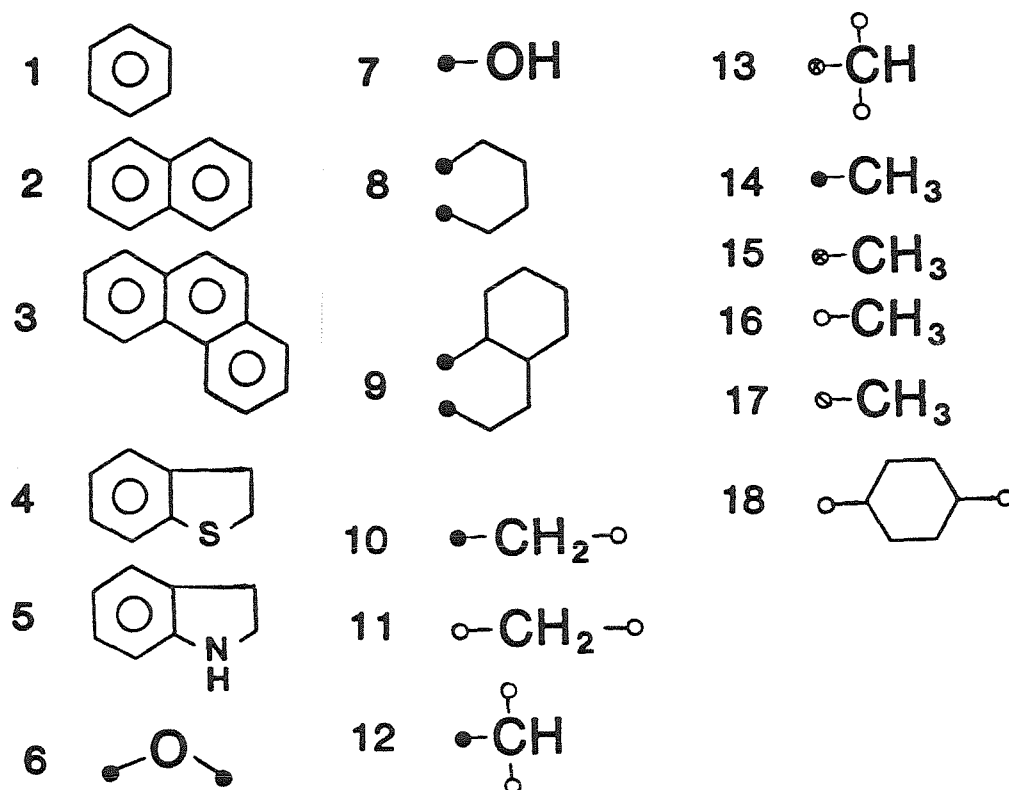
¹³ C NMR Data for Mayan ATB	
Carbon type	% of Carbon
Aromatic carbon	29.6
Carbon in CH groups	14.6
Carbon in naphthenic CH ₂ groups Carbon in CH ₂ groups alpha and gamma or farther from an aromatic ring	32.4
Carbon in CH ₂ groups beta to an aromatic ring	5.2
Carbon in CH ₂ groups next to a terminal methyl; Carbon in CH ₂ groups beta to an aromatic ring in tetralin structures	3.5
Carbon in CH ₃ groups alpha to an aromatic ring	2.7
Carbon in CH ₃ groups attached to hydroaromatic structures	4.4
Carbon in CH ₃ groups beta to an aromatic ring	2.4
Carbon in CH ₃ groups gamma or farther from an aromatic ring	5.1

Table 3
Summary of Mass Spectrum of Mayan ATB

<u>Hydrocarbon type</u>	<u>Average carbon number</u>	<u>Weight %</u>
Mono-aromatics	46	25.5
Di-aromatics	46	17.7
Tri-aromatics	48	6.6
Poly-aromatics	47	19.0
Thiophenes	44	31.2

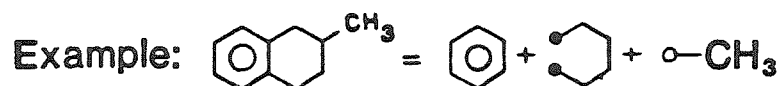
Figure 1

Heavy Oil Functional Groups



Notation:

- bound to an aromatic ring
- ◉— bound to a carbon alpha to an aromatic ring
- bound to a carbon beta to an aromatic ring
- ◉— bound to a carbon in a hydroaromatic ring



yields indicated that the ATB consisted primarily of solubility fractions that are classified as neutral oils and asphaltenes. Yields for acid and base solubility fractions were very low. Since the heteroatomic groups in neutral oils and asphaltenes are thiophenes, carbazoles, ethers and phenols, this confirmed the mass spec predictions of thiophene and carbazole type structures and indicated that most of the oxygen would be present in etheric and phenolic groups.

The next step in the functional group analysis methodology is to define the balance equations and the minimization function, as described in Chapter 3. The ^1H NMR and elemental analysis data are used to construct balance equations, exactly as before, however, the interpretation and use of the mass spectra and the ^{13}C NMR data are different.

Mass Spectra

The peaks observed in the mass spectra define the empirical formula of the structures present in the sample. The empirical formula does not provide any information about the structure of long chain hydrocarbons, however. Since the ATB consists mostly of long, branched aliphatic chains with occasional aromatic rings and heteroatoms attached, the mass spectra provide far less structural information about the ATB than they do for coal liquids. For the ATB, the mass spectrum was used in the balance equations to define the weight ratio of mono-/di-/tri-aromatics.

^{13}C NMR Spectra

As illustrated in Chapter 2, the aliphatic portion of the ^{13}C spectra of oils shows considerably more detail than the corresponding coal liquid spectrum. The spectra for the oils are divided into 9 bands, as opposed to 2 bands for

coal liquids. Since not all of the bands contain well defined peaks, such detailed interpretation of the spectra make the results somewhat more qualitative. Thus, the analytical data provided by the ^{13}C spectra are used in the minimization function. The data are used in selecting a representative solution from the feasible space defined by the elemental analysis, ^1H NMR, and mass spectral data. Specifically, a minimization algorithm finds the set of concentrations in the feasible space defined by the balance equation which minimizes the distance between the space and the point defined by the ^{13}C data. The distance is defined by equation 1:

$$D = \sum (f_i - y_i)^2 \quad (1)$$

where the y_i are the fractions of carbon in various bonding environments derived from the functional group concentrations, and the f_i are the fractions of carbon derived from the ^{13}C data of Table 2.

Using this method of estimating functional group concentrations yielded the concentration estimates of Table 4. The dominant features of the concentration estimates are the large amounts of long chain aliphatics and the high extent of branching in the chains. Hydroaromatic and alicyclic groups appear to be present in low concentration. A comparison of the ^{13}C data and the carbon distribution derived from the functional group concentrations is given in Table 5.

The characterization of this ATB sample is intended to demonstrate the utility of functional group analysis for oil samples. Although the details of the methodology and the use of analytical data are not precisely the same as for coal liquids, the general procedure is the same. Future work on the character-

Table 4

Mayan ATB Functional Group Concentrations
Estimated by Functional Group Analysis


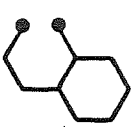


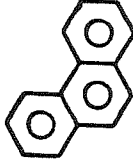


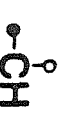
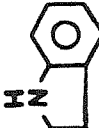








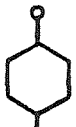
Functional Group	Concentration (moles/ 100g)	Functional Group	Concentration (moles/ 100g)
1 	benzene .077	9 	2-ring hydroaromatic .001
2 	naphthalene .033	10 	alpha CH ₂ .020
3 	phenanthrene .009	11 	beta CH ₂ 2.03
4 	benzothiophene .125	12 	alpha CH .293
5 	benzopyrrole .036	13 	beta CH .712
6 	ether bridge .051	14 	alpha terminal CH ₃ group .074
7 	phenolic substituent .015	15 	beta terminal CH ₃ .366
8 	hydroaromatic .018	16 	gamma terminal CH ₃ .431
		17 	terminal CH ₃ bound to a hydroaromatic .395
		18 	alicyclic group .013

Table 5

Comparison of Carbon Distribution from Functional Group Concentrations and NMR		
Carbon type	% of Carbon calculated from NMR spectrum	% of Carbon calculated from functional group Concentrations
Aromatic carbon	29.6	26.9
Carbon in CH groups	14.6	14.3
Carbon in naphthenic CH ₂ groups Carbon in CH ₂ groups alpha and gamma or farther from an aromatic ring	32.4	32.6
Carbon in CH ₂ groups beta to an aromatic ring	5.2	5.2
Carbon in CH ₂ groups next to a terminal methyl; Carbon in CH ₂ groups beta to an aromatic ring in tetralin structures	3.5	2.8
Carbon in CH ₃ groups alpha to an aromatic ring	2.7	1.1
Carbon in CH ₃ groups attached to hydroaromatic structures	4.4	5.6
Carbon in CH ₃ groups beta to an aromatic ring	2.4	5.2
Carbon in CH ₃ groups gamma or farther from an aromatic ring	5.1	6.1

ization of heavy oils will focus on identifying structural differences between distillation fractions and between the same fractions obtained from different crude oils.

Chapter 6

Recommendations for Future Work

Continued work on the structural characterization of coal liquids will focus on interpreting new or improved analytical methods and incorporating them into the functional group characterization. With sufficiently detailed structural characterizations available, estimation of thermodynamic and physical properties may become possible. Some proposed projects along these lines are listed below.

- [1] ^{17}O spectra and spin echo ^{13}C spectra have recently become available. Incorporating the results of these experiments into the functional group analysis algorithm is straightforward. By utilizing these data, functional group concentration estimates should become more detailed and accurate.
- [2] The functional group analysis algorithm should be applied to samples of shale oils and bitumens.
- [3] Group additivity methods for predicting thermodynamic properties are well established. If functional group concentrations are sufficiently accurate, thermodynamic properties could be estimated using group additivity. The accuracy of the estimates could be experimentally tested. It may also be possible to extend the estimation methods to physical properties.

Appendix A

Algorithm and Computer Codes for Non-linear Minimization with

Linear Inequality and Equality Constraints

As described in Chapter 3, estimates of functional group concentrations are made by minimizing a function P subject to linear equality and non-negativity constraints. The form of the function P depends on the type of data available for the structural characterization. If P is linearly dependent on the functional group concentrations y_i , then the mathematical problem of determining functional group concentrations is merely a case of linear programming and can be readily solved with the Simplex algorithm (1). The function P is usually not linear for two reasons, however. First, a linear function P makes the functional group concentrations very sensitive to small perturbations in the equality constraints. This is because the minimum of a linear function over a space defined by linear equality and inequality constraints must be on one of the corners of the space. Since small perturbations in the parameters of the constraints will change the location of some of the corners, the concentrations generated by a linear function P can exhibit large changes when the constraints are slightly perturbed. A non-linear function P , with its minimum located away from the corners of the space, is generally more desirable. A second reason why the P functions are often not linear is that a linear function is easily incorporated into the constraints.

Thus, the function P is usually a non-linear function of the functional group

concentrations y_i . The function is minimized subject to equality and inequality constraints using the direct search with area reduction algorithm of Luus and Jaakola (2). The algorithm proceeds through the following steps.

- [1] A solution within the feasible space (space 1) is located using linear programming.
- [2] A space (space 2), encompassing the entire feasible region and centered about the solution generated by linear programming, is defined.
- [3] A large number of points (> 200) are selected at random in space 2. The function P is evaluated for those points that fall within the feasible region (space 1).
- [4] The minimum value of P and the point associated with it are retained. A new space 2 is defined, centered about this point. The new space 2 has dimensions that are 95% of the dimensions of the previous space 2.
- [5] If the number of loops is less than 100, loop to step 3.

This minimization algorithm was chosen for its simplicity and its low computation costs. Additionally, the minimum that is located has been found to be independent of the starting point defined by linear programming.

An interactive computer code which can be used to estimate functional group concentrations for coal liquids is listed on the following pages. A main routine handles all data input and the minimization calculations. A subroutine, SIMPLX, uses the Simplex algorithm to find a starting point for the minimization and the data files coal5 and coal6 (called by SIMPLX) define the functional groups to be used. A detailed users' manual is not included here but is

available from the author.

References

- [1] G.B. Dantzig, *Linear Programming and Extensions*, Princeton University Press, Princeton, 1963.
- [2] R. Luus and T.H.I. Jaakola, *AIChE J.*, **19**, 760 (1973).

```

c   The method of functional group analysis characterizes complex
c   mixtures by calculating the concentrations of the functional
c   groups that make up the mixture. This program applies
c   the functional group analysis method to coal liquid
c   mixtures, utilizing a variety of data types.
c   The cases outlined below are the combinations of available
c   data that can be treated by the program.
c
c   Case 1 Proton NMR and Elemental analysis
c   Case 2 Proton NMR, carbon NMR and elemental analysis
c   Case 3 Proton NMR, elemental analysis and SARA separation yields
c   Case 4 Proton NMR, carbon NMR, elemental analysis and SARA yields
c   Case 5 Proton NMR, elemental analysis and low or high resolution MS
c   Case 6 Proton NMR, carbon NMR, elemental analysis, and low or high
c           resolution MS
c
c   For each case, different sets of functional groups are proposed.
c   As of 5/9/83 cases 1,2,5 and 6 have been completed
c
c   real b(5),x(5),f(8),bound(8),mid(8),min,hnmr(4),ea(5),sara(10)
c   2    ,c13fa(10),gmax(12),nitro,conc(17),ratio(16)
c
c   The nomenclature used is defined as follows:
c
c   f(i),x(i)=functional group concentrations
c   b(i)=concentration of atomic species i
c   mid(i)=vector used to define the center of the feasible space in
c           the direct search minimization
c   bound(i)=defines the bounds of the feasible space considered
c           in the direct search
c   min=minimum value of the function to be minimized
c   hnmr,ea=NMR and elemental analysis data
c   sara=sara separation yields
c   conc,ratio=high and low resolution mass spec data
c   gmax(i)=vector containing the concentrations yielding the minimum
c           of the function to be minimized
c
c   device numbers
c   iout=6
c   iin=4
c
c   data input section
c
c   begin by defining what data are available
c
c   write(iout,6000)
c   accept 4000,isara
c   6000 format(' data input section',/, ' Are SARA separation yields ',
c   2    'available? (1=yes 0=no)')
c   4000 format(i2)
c   write(iout,6010)
c   accept 4000, ic13
c   6010 format(' are carbon-13 NMR spectra available? (1=yes 0=no)')
c   write(iout,6020)
c   accept 4000, ihrms
c   6020 format(' Are high resolution MS data available? (1=yes 0=no)')
c   write(iout,6030)
c   accept 4000,ilrms
c   6030 format(' Are low resolution MS data available? (1=yes 0=no)')
c
c   data types have been input - determine case number (defined above)

```

```

c      if (isara .eq. 0) goto 32
      if (ic13 .eq. 0) goto 31
      icense=4
      goto 39
31  icense=3
      goto 39
32  int=ilrms+ihrms
      if(int .eq. 0) goto 35
      if(ic13 .eq. 0) goto 33
      icense=6
      goto 39
33  icense=5
      goto 39
35  if(ic13 .eq. 0) goto 37
      icense=2
      goto 39
37  icense=1
39  continue
      write(iout,6311)icense
6311 format(' case=',i2)
c
c      data input section
c
c      if (isara .eq. 0) goto 55
c
c      SARA data available; input yields
c
      write(iout,6040)
6040 format(' The functional group analysis algorithm uses the yields'
2      ,/, ' from 10 SARA fractions to calculate functional group'
3      ,/, ' concentrations. These fractions are (1) neutral oils,'
4      ,/, ' (2) asphaltenes, (3) neutral resins, (4) very weak bases'
5      ,/, ' (5) weak bases, (6) strong bases, (7) very weak acids,'
6      ,/, ' (8) weak acids, (9) strong acids, and (10) saturates.')
      write(iout,6050)
      read(iin,4050)sara(1)
6050 format(' input wt% neutral oils')
4050 format(f6.2)
      write(iout,6060)
      read(iin,4050)sara(2)
6060 format(' input wt% asphaltenes')
      write(iout,6070)
      read(iin,4050)sara(3)
6070 format(' input wt% neutral resins')
      write(iout,6080)
      read(iin,4050)sara(4)
6080 format(' input wt% very weak bases')
      write(iout,6090)
      read(iin,4050)sara(5)
6090 format(' input wt% weak bases')
      write(iout,6100)
      read(iin,4050)sara(6)
6100 format(' input wt% strong bases')
      write(iout,6110)
      read(iin,4050)sara(7)
6110 format(' input wt% very weak acids')
      write(iout,6120)
      read(iin,4050)sara(8)
6120 format(' input wt% weak acids')
      write(iout,6130)

```

```

      read(iin,4050)sara(9)
6130 format(' input wt% strong acids')
      write(iout,6140)
      read(iin,4050)sara(10)
6140 format(' input wt% saturates')
c
c      determine whether c-13 data are available
c
      if(ic13 .eq. 0) goto 55
      write(iout,6150)
      read (iin,4150)c13fa(1)
      write(iout,6160)
      read (iin,4150)c13fa(2)
      write(iout,6170)
      read (iin,4150)c13fa(3)
      write(iout,6180)
      read (iin,4150)c13fa(4)
      write(iout,6190)
      read (iin,4150)c13fa(5)
      write(iout,6200)
      read (iin,4150)c13fa(6)
      write(iout,6210)
      read (iin,4150)c13fa(7)
      write(iout,6220)
      read (iin,4150)c13fa(8)
      write(iout,6230)
      read (iin,4150)c13fa(9)
      write(iout,6240)
      read (iin,4150)c13fa(10)
6150 format(' enter C-13 aromaticity in % for each fraction')
6160 format(' input % aromaticity of neutral oils')
6170 format(' input % aromaticity of asphaltenes')
6180 format(' input % aromaticity of neutral resins')
6190 format(' input % aromaticity of very weak bases')
6200 format(' input % aromaticity of weak bases')
6210 format(' input % aromaticity of strong bases')
6220 format(' input % aromaticity of very weak acids')
6230 format(' input % aromaticity of weak acids')
6240 format(' input % aromaticity of strong acids')
      stop
      55 continue
c      input elemental analysis and proton NMR data
c
      write(iout, 6300)
6300 format(' input elemental analysis and proton NMR data')
      write(iout, 6310)
      accept 4300,ea(1)
      write(iout, 6320)
      accept 4300,ea(2)
      write(iout, 6330)
      accept 4300,ea(3)
      write(iout, 6340)
      accept 4300,ea(4)
      write(iout, 6350)
      accept 4300,ea(5)
4300 format(f6.2)
6310 format(' %C=')
6320 format(' %H=')
6330 format(' %O=')
6340 format(' %N=')
6350 format(' %S=')

```



```

      s=ea(1)+ea(2)+ea(3)+ea(4)+ea(5)
      write(iout,6352)s
6352 format(' Elemental analysis sums to ',f7.2,/,
2      ' This will be normalized to 100')
      do 73 i=1,5
73  ea(i)=ea(i)*100./s
      write(iout,6500)
      accept 4300,hnmr(1)
      write(iout,6510)
      accept 4300,hnmr(2)
      write(iout,6520)
      accept 4300,hnmr(3)
      write(iout,6530)
      accept 4300,hnmr(4)
c
c      aromatic hydrogens have chemical shifts between 5.0 and 9.0 ppm
c      alpha hydrogens have chemical shifts between 1.9 and 5.0 ppm
c      beta hydrogens have chemical shifts between 1.0 and 1.9 ppm
c      gamma hydrogens have chemical shifts between 0.5 and 1.0 ppm
c
6500 format(' % aromatic hydrogen=')
6510 format(' % alpha hydrogen=')
6520 format(' % beta hydrogen=')
6530 format(' % gamma hydrogen=')
      write(iout,6360)
6360 format(' input fraction (0<f<1)of oxygen that is phenolic',/,
2      ' (remainder assumed etheric)')
      accept 4300, fphen
      if(icas .eq. 1 .or. icas .eq. 3 .or. icas .eq. 5)goto 71
      write(iout,6370)
6370 format(' input carbon aromaticity (%)')
      accept 4300, c13ar
      write(iout,6380)c13ar
6380 format(' carbon aromaticity (%)=',f6.2)
71 continue
      if(icas .lt. 5) goto 75
      if(irlms .eq. 1) goto 74
      write (iout,6381)
6381 format(' input high resolution mass spec data as concentrations',/
2      ' (moles/100g)')
      write(iout,6382)
      accept 4301, conc(1)
4301 format(f7.3)
      write(iout,6383)
      accept 4301, conc(2)
      write(iout,6384)
      accept 4301, conc(3)
      write(iout,63841)
      accept 4301, conc(4)
      write(iout,6385)
      accept 4301, conc(5)
      write(iout,6386)
      accept 4301, conc(6)
      write(iout,6387)
      accept 4301, conc(9)
      write(iout,6390)
      accept 4301, conc(10)
      write(iout,6391)
      accept 4301, conc(11)
      write(iout,6392)
      accept 4301, conc(12)

```

```

write(iout,6393)
accept 4301, conc(13)
write(iout,6394)
accept 4301, conc(14)
write(iout,6395)
accept 4301, conc(15)
write(iout,6396)
accept 4301, conc(16)
write(iout,6397)
accept 4301, conc(17)
6382 format(' input concentration of benzene')
6383 format(' input concentration of naphthalene')
6384 format(' input concentration of phenanthrene')
63841 format(' input concentration of pyrene')
6385 format(' input concentration of biphenyl bridge')
6386 format(' input concentration of alkyl chains')
6387 format(' input concentration of methylene bridge')
6390 format(' input concentration of ethylene bridge')
6391 format(' input concentration of hydroaromatic')
6392 format(' input concentration of double hydroaromatic bridge')
6393 format(' input concentration of double hydroaromatic')
6394 format(' input concentration of phenol')
6395 format(' input concentration of furan')
6396 format(' input concentration of carbazole')
6397 format(' input concentration of dibenzothiophene')
write(iout,1001)conc
goto 75
74 continue
c low resolution data available
c
write(iout,6401)
6401 format(' input low resolution mass spec data as ',/,
2 ' concentration ratios (moles of group i/moles benzene)')
write(iout,6402)
accept 4301, ratio(1)
write(iout,6403)
accept 4301, ratio(2)
write(iout,6404)
accept 4301, ratio(3)
write(iout,6405)
accept 4301, ratio(4)
write(iout,6409)
accept 4301, ratio(8)
write(iout,6410)
accept 4301, ratio(9)
write(iout,6411)
accept 4301, ratio(10)
write(iout,6412)
accept 4301, ratio(11)
write(iout,6413)
accept 4301, ratio(12)
6402 format(' input ratio of naphthalene to benzene')
6403 format(' input ratio of phenanthrene to benzene')
6404 format(' input ratio of pyrene to benzene')
6405 format(' input ratio of biphenyl to benzene')
6407 format(' input ratio of methylene bridge to benzene')
6410 format(' input ratio of ethylene bridge to benzene')
6411 format(' input ratio of hydroaromatic to benzene')
6412 format(' input ratio of double hydroaromatic bridge to benzene')
6413 format(' input ratio of double hydroaromatic to benzene')
dummy=1.

```

```

      write(iout,6420)
6420 format(' low resolution mass spec data')
      write(iout,1003)(ratio(i),i=1,4),(ratio(j),j=8,12)
1003 format(' ratio of naphthalene to benzene=', f8.3,/,
      2      ' ratio of phenanthrene to benzene=', f8.3,/,
      2      ' ratio of pyrene to benzene=', f8.3,/,
      2      ' ratio of biphenyl bridge to benzene=', f8.3,/,
      2      ' ratio of methylene bridge to benzene=', f8.3,/,
      2      ' ratio of ethylene bridge to benzene=', f8.3,/,
      2      ' ratio of hydroaromatic to benzene=', f8.3,/,
      2      ' ratio of double hydroaromatic br. to benzene=', f8.3,/,
      2      ' ratio of double hydroaromatic to benzene=', f8.3,/)
75 continue
      write(iout,58)
      write(iout,61)ea
      write(iout,59)
      write(iout,61)hnmr
58 format(8x,'%C',11x,'%H',11x,'%O',11x,'%N',11x,'%S')
59 format(6x,'%aromatic',4x,'%alpha',7x,'%beta',8x,'%gamma')
61 format(1x,5e13.3)
      write(iout,66)fphen
66 format(' fraction of oxygen that is phenolic=',f7.3)
      min=1.0E10
      il=0
      ival=0
      do 68 in=1,6
68 mid(in)=0.
c
c      the simplex routine determines whether a feasible space exists.
c      If a feasible space exists, the routine finds a starting vector for
c      the minimization.
c
      call simplx(mid,ea,hnmr,c13ar,icase)
      write(iout,62)mid
62 format(1x,'mid vector',/,1x,6e13.3)
      do 63 i=1,8
63 gmax(i)=mid(i)
      carbon=ea(1)/12.
      aromh=hnmr(1)*ea(2)/100.
      alphah=hnmr(2)*ea(2)/100.
      betah=hnmr(3)*ea(2)/100.
      gammah=hnmr(4)*ea(2)/100.
      phenol=ea(3)*fphen/16.
      furan=ea(3)/16.-phenol
      nitro=ea(4)/14.
      sulfr=ea(5)/32.
c      f(1)=benzene ring
c      f(2)=alpha methyl
c      f(3)=hydroaromatic
c      f(4)=double hydroaromatic
c      f(5)=naphthalene
c      f(6)=methylene bridge
c      f(7)=pyrene
c      f(8)=ethylene bridge
      bound(1)=carbon/6.
      bound(2)=carbon
      bound(3)=carbon/4.
      bound(4)=carbon/8.
      bound(5)=carbon/10.
      bound(6)=carbon
      bound(7)=carbon/16.

```

```

bound(B)=carbon/2.
dum=gammah/3.
c
c to improve computing time, each of the cases 1-6 is considered
c separately from this point on
c
if(icase .eq. 2)goto 210
if(icase .eq. 6)goto 210
c
c Case 1 and Case 5 calculations
c
do 380 i=1,150
do 381 j=1,200
do 301 i=1,8
call randu(ij,ik,r)
f(i)=mid(i)+(r-.5)*bound(i)*2.
301 if(f(i) .lt. 0.) goto 381
c
c Case 1 and Case 5 iterations to find concentrations
c
b(1)=carbon-6.*f(1)-f(2)-4.*f(3)-8.*f(4)-10.*f(5)-f(6)
2 -12.*sulfr-12.*nitro-gammah/3.-16.*f(7)-2.*f(8)
b(2)=aromh-6.*f(1)+f(2)+2*f(3)+2.*f(4)-8.*f(5)+2.*f(6)
2 -8.*sulfr-8.*nitro+2.*furan-10.*f(7)+2.*f(8)
b(3)=alfah-3.*f(2)-4.*f(3)-3.*f(4)-2.*f(6)-nitro-4.*f(8)
b(4)=betah-4.*f(3)-11.*f(4)+gammah/3.
x(4)=(b(4)-2./3.*b(3))/(3.+2./3.)
x(3)=(b(3)+x(4))/6.
x(2)=(b(2)-5./7.*b(1)+5./7.*x(4)+(4+60./14.)*x(3))/(-2)
x(1)=(b(1)-x(4)-6.*x(3))/14.
do 340 i=1,4
340 if (x(i) .lt. 0.) goto 381
il=il+1
c
x(1)=phenanthrene ring
c
x(2)=biphenyl bridge
c
x(3)=double hydroaromatic bridge
c
x(4)=beta methyl
if(ilrms .eq. 1) goto 343
if(icase .eq. 1) goto 30
fun=(f(1)-conc(1))**2+(f(5)-conc(2))**2+(x(1)-conc(3))**2
2 +(f(7)-conc(4))**2+(x(2)-conc(5))**2
2 +(x(4)+f(2)+dum-conc(6))**2+(f(6)-conc(9))**2
2 +(f(8)-conc(10))**2+(f(3)-conc(11))**2
2 +(x(3)-conc(12))**2
2 +(f(4)-conc(13))**2+(phenol-conc(14))**2+(furan-conc(15))**2
2 +(nitro-conc(16))**2+(sulfr-conc(17))**2
goto 344
343 fun=(x(1)/f(1)-ratio(2))**2
2 +(x(2)/f(1)-ratio(4))**2+(x(3)/f(1)-ratio(11))**2
2 +(f(3)/f(1)-ratio(10))**2+(f(4)/f(1)-ratio(12))**2
2 +(f(5)/f(1)-ratio(1))**2+(f(6)/f(1)-ratio(8))**2
2 +(f(7)/f(1)-ratio(3))**2+(f(8)/f(1)-ratio(9))**2
goto 344
30 continue
sum1=aromh+f(2)+2.*f(3)+2.*f(4)+2.*f(6)+2.*x(2)+4.*x(3)
sum2=alfah+x(4)
sum3=betah+gammah/3.
fun=(carbon/84.-f(1))**2+(carbon/14.-f(2))**2
2 +(carbon/56.-f(3))**2+(carbon/112.-f(4))**2+(carbon/140.-f(5))**2
2 +(carbon/14.-f(6))**2+(carbon/196.-x(1))**2+(carbon/84.-x(3))**2
2 +(carbon/14.-x(4))**2+(carbon/224.-f(7))**2+(carbon/28.-f(8))**2

```

```

2 +(sum1/36.-f(1))**2+(sum1/48.-f(5))**2+(sum1/60.-x(1))**2
2 +(sum2/21.-f(2))**2+(sum2/28.-f(3))**2+(sum2/21.-f(4))**2
2 +(sum2/14.-f(6))**2+(sum2/42.-x(3))**2+(sum3/16.-f(3))**2
2 +(sum1/60.-f(7))**2+(sum2/28.-f(8))**2
2 +(sum3/44.-f(4))**2+(sum3/16.-x(3))**2+(sum3/12.-x(4))**2
344 if(fun .gt. min) goto 381
    min=fun
    do 349 i=9,12
349     gmax(i)=x(i-8)
    do 350 i=1,8
350     gmax(i)=f(i)
381 continue
    do 351 i=1,8
351 mid(i)=gmax(i)
    ieval=ieval+1
    il=0
    do 305 i=1,8
305     bound(i)=.95*bound(i)
380 continue
    if(ieval .eq. 0) write(iout,6600)
    dum=gammah/3.
    write(iout,1001)gmax(1),gmax(5),gmax(9),gmax(7),gmax(10),
2 gmax(2),gmax(12),dum,gmax(6),gmax(8),gmax(3),gmax(11),gmax(4),
3 phenol,furan,nitro,sulfr
1001 format(' benzene ring=',e12.5,/, ' naphthalene ring=',e12.5, /
2 ' phenanthrene ring=',e12.5,/, ' pyrene ring=',e12.5, /
2 ' biphenyl br.=',e12.5,/, ' alpha methyl=',e12.5, /
2 ' beta methyl=',e12.5,/, ' gamma methyl=',e12.5, /
3 ' methylene br.=',e12.5,/, ' ethylene br.=',e12.5, /
3 ' hydroaromatic=',e12.5, /
2 ' double hydroaromatic br.=',e12.5, /
2 ' double hydroaromatic=',e12.5,/, ' phenol=',e12.5, /
2 ' furan=',e12.5,/, ' carbazole=',e12.5, /
2 ' dibenzothiophene=',e12.5)
    stop
6600 format(' ERROR-no function evaluations')
c
c Case 2 and Case 6 calculations
c
210 arcar=ea(1)/12.*c13ar/100.
    alcar=ea(1)/12.*(1.-c13ar/100.)
    bound(6)=carbon/16.
    bound(7)=carbon/2.
    mid(6)=mid(7)
    mid(7)=mid(8)
    do 260 l=1,150
    do 250 j=1,200
    do 212 i=1,7
        call randu(ij,ik,r)
        f(i)=mid(i)+(r-.5)*bound(i)*2.
212     if(f(i) .lt. 0) goto 250
        b(1)=arcac-6.*f(1)-10.*f(5)-12.*(nitro+sulfr)-16.*f(6)
        b(2)=aromh-6.*f(1)+f(2)+2.*f(3)+2.*f(4)-8.*f(5)-8.*(nitro+sulfr)
        +2.*furan-10.*f(6)+2.*f(7)
        b(3)=alcar-f(2)-4.*f(3)-8.*f(4)-gammah/3.-2.*f(7)
        b(4)=alfah-3.*f(2)-4.*f(3)-nitro-4.*f(7)
        b(5)=betah-4.*f(3)-11.*f(4)+gammah/3.
c     x(5)=methylene bridge
        x(5)=(b(5)-2./3.*b(3)+7./6.*(b(4)-b(3)))/.5
        x(4)=(b(4)-b(3)-x(5))/(-2.)
        x(3)=(b(3)-x(5)-x(4))/6.

```

```

x(2)=(b(2)-10./14.*b(1)+2.*x(5)+4.*x(3))/(-2.)
x(1)=b(1)/14.
do 211 i=1,5
211   if(x(i).lt. 0.) goto 250
      il=il+1
      if(ilrms .eq. 1) goto 243
      if(icase .eq. 2) goto 20
      fun=(f(1)-conc(1))**2+(f(5)-conc(2))**2+(x(1)-conc(3))**2
2      +(f(6)-conc(4))**2+(x(2)-conc(5))**2
2      +(x(4)+f(2)+dum-conc(6))**2+(x(5)-conc(9))**2
2      +(f(7)-conc(10))**2+(f(3)-conc(11))**2
2      +(x(3)-conc(12))**2
2      +(f(4)-conc(13))**2+(phenol-conc(14))**2+(furan-conc(15))**2
2      +(nitro-conc(16))**2+(sulfr-conc(17))**2
      goto 244
243 fun=(f(5)/f(1)-ratio(1))**2
2      +(f(7)/f(1)-ratio(9))**2+(x(5)/f(1)-ratio(8))**2
2      +(f(6)/f(1)-ratio(3))**2+(f(3)/f(1)-ratio(10))**2
2      +(x(2)/f(1)-ratio(4))**2+(f(4)/f(1)-ratio(12))**2
2      +(x(3)/f(1)-ratio(11))**2+(x(1)/f(1)-ratio(2))**2
      goto 244
20 continue
      sum1=aromh+f(2)+2.*f(3)+2.*f(4)+2.*x(5)+2.*x(2)+4.*x(3)+2.*f(7)
      sum2=alfah+x(4)
      sum3=betah+gammah/3.
      fun=(alcar/8.-f(2))**2+(alcar/32.-f(3))**2+(alcar/64.-f(4))**2
2      +(alcar/8.-x(4))**2+(alcar/8.-x(5))**2+(arcar/36.-f(1))**2
2      +(arcar/60.-f(5))**2+(arcar/84.-x(1))**2
2      +(sum1/36.-f(1))**2+(sum1/48.-f(5))**2+(sum1/60.-x(1))**2
2      +(sum2/21.-f(2))**2+(sum2/28.-f(3))**2+(sum2/21.-f(4))**2
2      +(sum2/14.-f(6))**2+(sum2/42.-x(3))**2+(sum3/16.-f(3))**2
2      +(sum3/44.-f(4))**2+(sum3/16.-x(3))**2+(sum3/12.-x(4))**2
2      +(alcar/16.-f(7))**2+(arcar/84.-f(6))**2+(sum1/60.-f(6))**2
2      +(sum2/28.-f(7))**2
244 if(fun.gt. min) goto 250
      min=fun
      do 213 i=8,12
213       gmax(i)=x(i-7)
      do 214 i=1,7
214       gmax(i)=f(i)
250 continue
      do 215 i=1,7
215       mid(i)=gmax(i)
      ieval=ieval+il
      il=0
      do 216 i=1,7
216       bound(i)=.95*bound(i)
260 continue
      if(ieval .eq. 0) write(iout,6600)
      dum=gammah/3.
      write(iout,1001)gmax(1),gmax(5),gmax(8),gmax(6),gmax(9),
2      gmax(2),gmax(11),dum,gmax(12),gmax(7),gmax(3),gmax(10),gmax(4),
3      phenol,furan,nitro,sulfr
      stop
      end
      SUBROUTINE SIMPLX(MID,ea,hnmr,c13ar,icase)
      INTEGER  RNM1,RNM2,CLNM1,CLNM2,BLNK,NEG,POS,SYMB,CDID,RO,MA,FI,EO,LP
1      IBN1(40),IBN2(40),NBN1(40),NBN2(40)
      integer  x1,x2,x3,x4,x5,x6,carb,arom,alfa,beta,gama,phen,nitr,
2      sulf,fura,alca,arca,x7,x8
      real     pi(40),nbp(40),xpi(40),mid(8),ea(5),hnmr(4)

```

REAL	PIVOT, LST, XNBP, FN, CJBAR, X, VALUE, BP(40), RG(40), B(40, 40)	LP	6
DIMENSION TITLE(20)			
DATA	POS, FIN, FI, RO, MA, NEG // '+', 'fin', 'rh', 'ro', 'ma', '-' //		
data	eo, blink, alca, arca // 'eo', ' ', 'alca', 'arca' //		
data	carb, arom, alfa, beta, gama // 'carb', 'arom', 'alfa', 'beta', 'gama' //		
data	phen, fura, nitr, sulf // 'phen', 'fura', 'nitr', 'sulf' //		
data	x1, x2, x3, x4, x5, x6, x7, x8 // 'x1', 'x2', 'x3', 'x4', 'x5', 'x6', 'x7',		
2	'x8' //		
C	COMPARING WITH LP CARD CODES	LP	12
	if (icase .eq. 1) open(unit=5, name='coal5.dat', form='formatted',		
1	type='old', disp='save')		
	if (icase .eq. 2) open(unit=5, name='coal6.dat', form='formatted',		
1	type='old', disp='save')		
	if (icase .eq. 5) open(unit=5, name='coal5.dat', form='formatted',		
1	type='old', disp='save')		
	if (icase .eq. 6) open(unit=5, name='coal6.dat', form='formatted',		
1	type='old', disp='save')		
C		LP	21
C	INPUT PROGRAM	LP	22
C		LP	23
54323	CONTINUE	LP	24
	M=0	LP	25
	N=1	LP	26
	ISW = 0	LP	27
	NROWS = 0	LP	28
	NQE = 0	LP	29
	NLE = 0	LP	30
	NEG = 0	LP	31
	NEL = 0	LP	32
	NRHS = 0	LP	33
	NCOLS = 0	LP	34
C		LP	35
C	CLEAR MATRIX TO ZERO	LP	36
C		LP	37
	DO 12 I=1, 40	LP	38
	DO 12 J=1, 40	LP	39
12	B(I, J) = 0.	LP	40
C	READ PROBLEM TITLE	LP	41
	READ(5, 800) TITLE		42
800	format(20a4)		
	IF(TITLE(1) .EQ. FIN) RETURN		43
C		LP	50
C	READ FIRST CARD - SHOULD BE ROWID	LP	51
C		LP	52
	READ (5, 2) CDID		53
2	FORMAT (A2)		54
	IF (CDID-RO) 3, 680, 3	LP	55
3	continue		56
3334	STOP 1	LP	58
C		LP	59
C	READ AND STORE ROWID CARDS	LP	60
C	GENERATE POS AND NEG SLACKS AS REQUIRED	LP	61
C		LP	62
680	CONTINUE		63
681	FORMAT (80X)	LP	64
101	READ(5, 102) CDID, LGE, RNM1, RNM2		
102	FORMAT(A2, 8X, A1, 1X, A4, A1)		66
	IF (CDID-MA) 103, 504, 103		67
504	CONTINUE	LP	68
	GO TO 104	LP	69
103	M=M+1		70

NROWS = NROWS+1	LP	71
IF (LGE-POS) 105, 106, 105		72
105 IF (LGE-NEG) 107, 108, 107		73
106 IBN1(M)=RNM1	LP	74
IBN2(M)=RNM2	LP	75
NLE = NLE+1	LP	76
BP(M)= 0.		77
GO TO 101	LP	78
108 IBN1(M) = RNM1	LP	79
IBN2(M) = RNM2	LP	80
NGE = NGE+1	LP	81
BP(M) = -1.0	LP	82
B(M,N) = -1.0	LP	83
401 NBN1(N) = RNM1	LP	84
NBN2(N) = RNM2	LP	85
NBP(N) = 0.	LP	86
N = N+1	LP	87
GO TO 101	LP	88
107 IBN1(M) = RNM1	LP	89
IBN2(M) = RNM2	LP	90
NEG = NEG+1	LP	91
BP(M) = -2.0	LP	92
GO TO 101	LP	93
C	LP	94
C READ AND STORE FIRST MATRIX ELEMENT	LP	95
C	LP	96
104 READ(5,195)CDID,CLNM1,CLNM2,RNM1,RNM2,SYMB,VALUE		97
195 FORMAT(A2,8X,A4,A1,5X,A4,A1,4X,A1,F10.0)		98
GO TO 119	LP	99
109 IF(NBN1(N) - CLNM1) 111, 600, 111	LP	100
600 IF(NBN2(N)-CLNM2) 111, 601, 111	LP	101
601 CONTINUE	LP	102
112 DO 113 I=1,M	LP	103
IF(IBN1(I)-RNM1) 113, 602, 113	LP	104
602 IF(IBN2(I)-RNM2) 113, 603, 113	LP	105
113 CONTINUE	LP	106
STOP 2	LP	111
603 CONTINUE	LP	112
114 IF (SYMB-NEG) 116, 115, 116		113
115 B(I,N) = -VALUE	LP	114
GO TO 117	LP	115
116 B(I,N) = VALUE	LP	116
C	LP	117
C READ AND STORE MATRIX ELEMENTS	LP	118
C	LP	119
117 READ(5,195)CDID,CLNM1,CLNM2,RNM1,RNM2,SYMB,VALUE		120
NEL = NEL+1	LP	121
GO TO 109	LP	122
111 N = N+1	LP	123
NCOLS = NCOLS+1	LP	124
IF (CDID-FI) 119, 190, 119		125
119 NBN1(N) = CLNM1	LP	126
NBN2(N) = CLNM2	LP	127
201 IF (SYMB-NEG) 202, 203, 202	LP	128
202 NBP(N) = VALUE	LP	129
GO TO 117	LP	130
203 NBP(N) = -VALUE	LP	131
GO TO 117	LP	132
C	LP	133
C READ AND STORE RHS ELEMENTS	LP	134
C	LP	135

190 DO 191 I=1,M	LP	136
191 RG(I)=0.		137
GO TO 120	LP	138
120 READ(5,121) CDID,RNM1,RNM2,VALUE		139
if(rnm1 .eq. carb) value=ea(1)/12.		
if(rnm1 .eq. arom) value=ea(2)*hnmr(1)/100.		
if(rnm1 .eq. alfa) value=ea(2)*hnmr(2)/100.		
if(rnm1 .eq. beta) value=ea(2)*hnmr(3)/100.		
if(rnm1 .eq. gama) value=ea(2)*hnmr(4)/100.		
if(rnm1 .eq. phen) value=ea(3)*fphen/16.		
if(rnm1 .eq. fura) value=ea(3)*(1.-fphen)/16.		
if(rnm1 .eq. nitr) value=ea(4)/14.		
if(rnm1 .eq. sulf) value=ea(5)/32.		
if(rnm1 .eq. alca) value=ea(1)/12.*(1.-c13ar/100.)		
if(rnm1 .eq. arca) value=ea(1)/12.*c13ar/100.		
121 FORMAT(A2, 8X, A4, A1, 5X, F10. 0)		140
IF (CDID=EO) 122,193,122		141
122 DO 124 I=1,M	LP	142
IF (IBN1(I)-RNM1)124,610,124	LP	143
610 IF (IBN2(I)-RNM2)124,611,124	LP	144
124 CONTINUE	LP	145
STOP 3	LP	148
611 CONTINUE	LP	149
125 RG(I)=VALUE		150
NRHS = NRHS+1	LP	151
GO TO 120	LP	152
193 N = N-1	LP	153
C	LP	158
C	LP	159
C	LP	160
DO 10 I=1,M	LP	161
IF (BP(I)+1. 0)19,11,10	LP	162
11 IBN1(I) = BLNK	LP	163
IBN2(I) = BLNK	LP	164
GO TO 10	LP	165
19 BP(I) = -1. 0	LP	166
IBN1(I) = BLNK	LP	167
IBN2(I) = BLNK	LP	168
10 CONTINUE	LP	169
C	LP	170
C	LP	171
C	LP	172
NINF =0	LP	173
DO 6000 I=1,M	LP	174
IF (BP(I))6001,6000,6000	LP	175
6001 NINF = NINF+1	LP	176
6000 CONTINUE	LP	177
C	LP	178
C	LP	179
C	LP	180
DO 6101 J=1,N	LP	181
XPI(J) =0.	LP	182
DO 6101 I=1,M	LP	183
IF (BP(I))6102,6101,6101	LP	184
6102 XPI(J) = XPI(J)-B(I,J)	LP	185
6101 CONTINUE	LP	186
DO 6002 I=1,M	LP	187
6002 BP(I) = 0.	LP	188
IPHASE = 1	LP	189
C	LP	190
C	LP	191
MAIN ROUTINE		

C		LP	192
9201	continue		193
	it=0		
54325	CONTINUE	LP	196
C		LP	197
C	CALCULATE SHADOW PRICES	LP	198
C		LP	199
	DO 194 J=1,N	LP	200
	PI(J) = -NBP(J)	LP	201
	DO 194 I=1,M	LP	202
194	PI(J) = PI(J) + BP(I)*B(I,J)	LP	203
C		LP	204
C	SELECT BEST NONBASIS VECTOR	LP	205
C		LP	206
9101	LST = -.0000001	LP	207
	KCOL = 0	LP	208
	GO TO (751,552), IPHASE	LP	209
751	IF(NINF)54321, 54321, 552	LP	210
552	CONTINUE	LP	211
	DO 9102 J=1,N	LP	212
C		LP	213
C	IGNORE ARTIFICIAL VARIABLES	LP	214
C		LP	215
	IF(NBN1(J)-BLNK+NBN2(J)-BLNK)651, 9102, 651	LP	216
651	CONTINUE	LP	217
	GO TO (6003,6004), IPHASE	LP	218
6003	IF(XPI(J)-LST)6005, 6006, 6006	LP	219
6005	KCOL=J	LP	220
	LST = XPI(J)	LP	221
	GO TO 9102	LP	222
6004	CONTINUE	LP	223
	IF(PI(J)-LST)9103, 9102, 9102	LP	224
9103	KCOL = J	LP	225
	LST = PI(J)	LP	226
6006	CONTINUE	LP	227
9102	CONTINUE	LP	228
	IF (KCOL)54321, 54321, 9104	LP	229
C		LP	230
C	DETERMINE KEYROW	LP	231
C		LP	232
9104	KROW = 0	LP	233
	CJBAR = LST	LP	234
	LST = 1.0E20	LP	235
	DO 9105 I=1,M	LP	236
	IF(B(I,KCOL))9105, 9105, 9106	LP	237
9106	RATIO = RQ(I)/B(I,KCOL)	LP	238
	IF (RATIO-LST)9107, 9105, 9105	LP	239
9107	LST = RATIO	LP	240
	KROW=I	LP	241
9105	CONTINUE	LP	242
	IF(KROW)9112, 9112, 9114	LP	243
9112	WRITE(6, 9113) NBN1(KCOL), NBN2(KCOL)		244
9113	FORMAT(' VARIABLE ', A4, A1, ' UNBOUNDED ')	LP	245
	GO TO 54323	LP	246
9114	CONTINUE	LP	247
C		LP	248
C	TRANSFORM	LP	249
C		LP	250
C	DIVIDE BY PIVOT	LP	251
	PIVOT = B(KROW, KCOL)	LP	252
	DO 9108 J=1,N	LP	253

9108	B(KROW, J) = B(KROW, J)/PIVOT	LP	254
	RQ(KROW) = RQ(KROW)/PIVOT	LP	255
	DO 9109 I=1, M	LP	256
	IF(I-KROW) 9110, 9109, 9110	LP	257
9110	RQ(I) = RQ(I) - RQ(KROW)*B(I, KCOL)	LP	258
	DO 9109 J=1, N	LP	259
	IF(J-KCOL) 9111, 9109, 9111	LP	260
9111	B(I, J) = B(I, J) - B(KROW, J)*B(I, KCOL)	LP	261
9109	CONTINUE	LP	262
	DO 9300 I=1, M	LP	263
9300	B(I, KCOL) = -B(I, KCOL)/PIVOT	LP	264
	B(KROW, KCOL) = 1.0/PIVOT	LP	265
C		LP	266
C	INTERCHANGE BASIS AND NONBASIS VARIABLES	LP	267
C		LP	268
	RNM1 = NBN1(KCOL)	LP	269
	RNM2 = NBN2(KCOL)	LP	270
	NBN1(KCOL) = IBN1(KROW)	LP	271
	NBN2(KCOL) = IBN2(KROW)	LP	272
	IBN1(KROW) = RNM1	LP	273
	IBN2(KROW) = RNM2	LP	274
	LST = NBP(KCOL)	LP	275
	NBP(KCOL) = BP(KROW)	LP	276
	BP(KROW) = LST	LP	277
	IT = IT + 1	LP	278
	IF(NBN1(KCOL)-BLNK+NBN2(KCOL)-BLNK) 6201, 6200, 6201	LP	279
6200	NINF = NINF-1	LP	280
6201	CONTINUE	LP	281
C		LP	282
C	COMPUTE OBJECTIVE FUNCTION	LP	283
C		LP	284
	FN = 0.	LP	285
	DO 9301 I=1, M	LP	286
9301	FN = FN + BP(I)*RQ(I)	LP	287
	GO TO (7000, 7001), IPHASE	LP	288
7000	SAVE = PI(KCOL)	LP	289
	DO 7003 J=1, N	LP	290
	PI(J) = PI(J) - SAVE*B(KROW, J)	LP	291
	XPI(J) = XPI(J) - CJBAR*B(KROW, J)	LP	292
7003	CONTINUE	LP	293
	PI(KCOL) = -SAVE/PIVOT	LP	294
	XPI(KCOL) = -CJBAR/PIVOT	LP	295
	GO TO 7004	LP	296
7001	CONTINUE	LP	297
	DO 9302 J=1, N	LP	298
9302	PI(J) = PI(J) - CJBAR*B(KROW, J)	LP	299
	PI(KCOL) = -CJBAR/PIVOT	LP	300
7004	CONTINUE	LP	301
C	CHECK FOR ESSENTIAL ZERO	LP	302
	DO 6111 I=1, M	LP	303
	DO 6111 J=1, N	LP	304
	X=B(I, J)	LP	305
	IF(ABS(X)-.0000001) 6112, 6112, 6111	LP	306
6112	B(I, J) = 0.	LP	307
6111	CONTINUE	LP	308
C		LP	309
C		LP	310
C	LOG ITERATION	LP	311
C		LP	312
	GO TO 9101	LP	315
C		LP	316

C		LP	317
54321	CONTINUE	LP	318
	IF(IPHASE-1)8000,8000,54322	LP	319
8000	IPHASE = 2	LP	320
	IF(NINF)8003,8003,8004	LP	321
8004	WRITE(6,8005)		322
8005	FORMAT('O SOLUTION INFEASIBLE',/)	LP	323
	GO TO 54322	LP	324
8003	CONTINUE	LP	325
	GO TO 54325	LP	328
54322	CONTINUE	LP	329
C		LP	330
C	OUTPUT ROUTINE	LP	331
C		LP	332
	DO 3033 I=1,M	LP	338
C		LP	339
C	COST RANGING	LP	340
C		LP	341
	VALUE = 1.0E20	LP	342
	LST = 1.0E20	LP	343
	DO 12300 J=1,N	LP	344
	IF(NBN1(J)-BLNK+NBN2(J)-BLNK)12305,12300,12305	LP	345
12305	CONTINUE	LP	346
	IF(B(I,J))12301,12300,12302	LP	347
12302	X=PI(J)/B(I,J)	LP	348
	IF(X-LST)12303,12300,12300	LP	349
12303	LST=X	LP	350
	GO TO 12300	LP	351
12301	X=-PI(J)/B(I,J)	LP	352
	IF(X-VALUE)12304,12300,12300	LP	353
12304	VALUE = X	LP	354
12300	CONTINUE	LP	355
	LST = BP(I) - LST	LP	356
	VALUE = BP(I) + VALUE	LP	357
	if(ibn1(i) .eq. x1) mid(1)=rq(i)		
	if(ibn1(i) .eq. x2) mid(2)=rq(i)		
	if(ibn1(i) .eq. x3) mid(3)=rq(i)		
	if(ibn1(i) .eq. x4) mid(4)=rq(i)		
	if(ibn1(i) .eq. x5) mid(5)=rq(i)		
	if(ibn1(i) .eq. x6) mid(6)=rq(i)		
	if(ibn1(i) .eq. x7) mid(7)=rq(i)		
	if(ibn1(i) .eq. x8) mid(8)=rq(i)		
3033	continue		358
C		LP	367
C	RETURN TO READ NEXT PROBLEM	LP	368
C		LP	369
	go to 54323		
	end		

Data File COAL5.DAT

rowid	0 carbn		
	0 aromh		
	0 alfah		
	0 betah		
	0 gamah		
	0 nitro		
	0 sulfr		
	0 furan		
	0 pheno		
matrix			
	x1	proft	1.
	x1	carbn	6.
	x1	aromh	6.
	x5	proft	1.
	x5	carbn	10.
	x5	aromh	8.
	x7	proft	1.
	x7	carbn	16.
	x7	aromh	10.
	x26	proft	1.
	x26	carbn	14.
	x26	aromh	10.
	x6	proft	10.
	x6	carbn	1.
	x6	aromh	-2.
	x6	alfah	2.
	x2	proft	1.
	x2	carbn	1.
	x2	aromh	-1.
	x2	alfah	3.
	x10	proft	1.
	x10	carbn	1.
	x10	alfah	-1.
	x10	betah	3.
	x3	proft	10.
	x3	carbn	4.
	x3	aromh	-2.
	x3	alfah	4.
	x3	betah	4.
	x25	proft	1.
	x25	aromh	-2.
	x8	proft	1.
	x8	carbn	2.
	x8	aromh	-2.
	x8	alfah	4.
	x4	proft	1.
	x4	carbn	8.
	x4	aromh	-2.
	x4	alfah	3.
	x4	betah	11.
	x9	proft	1.
	x9	carbn	6.
	x9	aromh	-4.
	x9	alfah	6.
	x9	betah	4.
	x11	proft	1.
	x11	carbn	1.
	x11	betah	-1.
	x11	gamah	3.

	x12	proft	1.
	x12	pheno	1.
	x13	proft	1.
	x13	aromh	-2.
	x13	fulan	1.
	x14	proft	1.
	x14	carbn	12.
	x14	aromh	8.
	x14	alfah	1.
	x14	nitro	1.
	x15	proft	1.
	x15	carbn	12.
	x15	aromh	8.
	x15	sulfr	1.
rhs			
	carbn	7.62	
	aromh	3.18	
	alfah	2.39	
	betah	1.40	
	gamah	.288	
	nitro	.000	
	sulfr	.020	
	pheno	.000	
	fulan	.018	
eof			
fin			

Data File COAL6.DAT

rowid

0 arcar
 0 alcar
 0 aromh
 0 alfah
 0 betah
 0 gamah
 0 nitro
 0 sulfr
 0 furan
 0 pheno

matrix

x1	proft	1.
x1	arcar	6.
x1	aromh	6.
x5	proft	1.
x5	arcar	10.
x5	aromh	8.
x7	proft	1.
x7	arcar	16.
x7	aromh	10.
x26	proft	1.
x26	arcar	14.
x26	aromh	10.
x6	proft	1.
x6	alcar	1.
x6	aromh	-2.
x6	alfah	2.
x2	proft	1.
x2	alcar	1.
x2	aromh	-1.
x2	alfah	3.
x10	proft	1.
x10	alcar	1.
x10	alfah	-1.
x10	betah	3.
x3	proft	1.
x3	alcar	4.
x3	aromh	-2.
x3	alfah	4.
x3	betah	4.
x25	proft	1.
x25	aromh	-2.
x8	proft	1.
x8	alcar	2.
x8	aromh	-2.
x8	alfah	4.
x4	proft	1.
x4	alcar	8.
x4	aromh	-2.
x4	alfah	3.
x4	betah	11.
x9	proft	1.
x9	alcar	6.
x9	aromh	-4.
x9	alfah	6.
x9	betah	4.
x11	proft	1.
x11	alcar	1.
x11	betah	-1.

	x11	gamah	3.
	x12	proft	1.
	x12	pheno	1.
	x13	proft	1.
	x13	aromh	-2.
	x13	fulan	1.
	x14	proft	1.
	x14	alcar	12.
	x14	aromh	8.
	x14	alfah	1.
	x14	nitro	1.
	x15	proft	1.
	x15	alcar	12.
	x15	aromh	8.
	x15	sulfr	1.
rhs			
	arcar	7.62	
	alcar	7.62	
	aromh	3.18	
	alfah	2.39	
	betah	1.40	
	gamah	.288	
	nitro	.000	
	sulfr	.020	
	pheno	.000	
	fulan	.018	
eof			
fin			

PART II

Model Compound Studies

Chapter 7

Introduction

The thermal and catalytic reactions of pure compounds containing the same types of functionalities as coal-related materials have been reported extensively in the literature (1-8). The goal of these model compound experiments is to isolate and examine classes of reactions important in coal processing. The results can readily provide qualitative and quantitative information on product distributions, reaction mechanisms and the relative rates of dissociation for various types of bonds. It is more difficult, however, to utilize results of experiments using one or several model compounds to predict how complex mixtures of compounds will react. It is precisely this information which is necessary for making the step from model compound results to the reactions of coal-related materials.

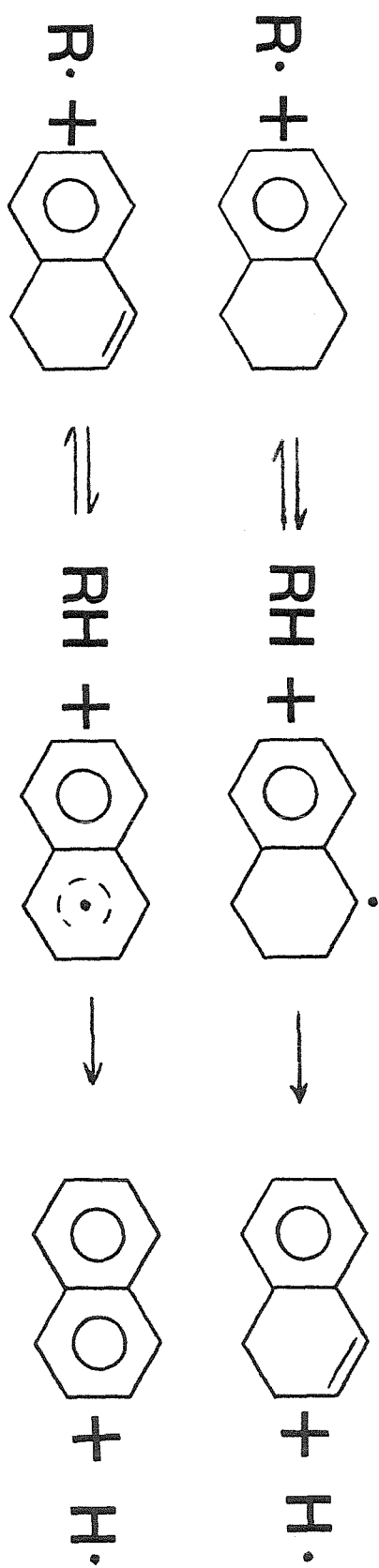
Examining the interactions between the reactions of model compounds can be approached in a number of ways. One approach is to examine experimentally all of the significant combinations of model compounds, estimating global rates of reactions. Determining which of the thousands of possible permutations of appropriate model compounds are significant makes this approach unreliable and the large number of potentially important mixtures makes it tedious. A second approach is to attempt to develop mechanistic models of the reactions of model compounds and then combine mechanisms to predict the reactions of mixtures. This is the approach that will be used in this work.

Developing mechanistic models to serve as building blocks for the kinetic analysis of complex mixtures has both advantages and disadvantages. The principal advantage is that the mechanisms provide real insight into the nature of the chemical processes that are occurring. Rate limiting steps can be identified and the extent of interaction between groups of functionalities present in mixtures can be estimated by combining mechanisms. The major drawback of a mechanistic approach is the large number of reactions necessary to model even the simplest system. The large number of reactions necessitates estimating a large number of rate parameters, but this is generally not a significant problem for coal-related systems since in each mechanism only a few reactions are rate limiting and the model is insensitive to perturbations in the values of most of the rate parameters (9). The real difficulty is that the mechanisms predicted for mixtures become overwhelming if more than just a few components are present. In predicting the kinetic behavior of complex mixtures from the mechanisms of pure compounds, some simplifications would have to be made. An additional problem associated with using mechanistic models is that factors such as homogeneous catalysis of the reactions of one compound by another cannot be predicted by merely combining mechanisms.

Overall, however, the insight provided by mechanistic models outweighs the drawbacks, so this approach was used in our work. Experimental results and proposed mechanisms for several model compound systems related to coal liquefaction are discussed in Chapters 8 and 9. The goal of studying the model compound systems of Chapters 8 and 9 was to determine the role of atomic hydrogen released from hydrogen donors in coal-related systems. 1,2,3,4

Tetrahydronaphthalene (tetralin) and related compounds are common components of coal-derived liquids. This class of compounds is generally dehydrogenated in steps during coal liquefaction, donating hydrogen to cap free radicals and releasing atomic hydrogen (10). These reactions are shown in Figure 1. The atomic hydrogen is extremely reactive and can cause dissociation of bonds that are otherwise stable. In order to study these reactions under conditions pertinent to coal liquefaction, 1,2 dihydronaphthalene (structure * in Figure 1) was used as a model hydrogen donor. 1,2 Dihydronaphthalene (dialin) rapidly dehydrogenates through the free radical scheme shown in Figure 1, releasing atomic hydrogen. Chapter 8 describes experimental data and a proposed mechanism for the thermolysis of dialin under conditions appropriate to coal liquefaction. Chapter 9 examines the reactions of the atomic hydrogen released by dialin. Mixtures of dialin and compounds containing methylene and ether bridges were thermolyzed and mechanisms are proposed. Chapter 10 summarizes the results of the experiments and the potential for using model compound results to predict the reactions of complex mixtures.

Figure 1
Dehydrogenation Mechanism



References

- [1] B.M. Benjamin, V.F. Raaen, P.H. Maupin, L.L. Brown and C.J. Collins, *Fuel*, **57**, 269 (1978).
- [2] D.C. Cronauer, D.M. Jewell, Y.T. Shah and K.A. Kueser, *Ind. Eng. Chem. Fund.*, **17**, 291 (1978).
- [3] D.C. Cronauer, D.M. Jewell, Y.T. Shah and R.J. Modi, *Ind. Eng. Chem. Fund.*, **18**, 153 (1979).
- [4] D.C. Cronauer, D.M. Jewell, R.J. Modi and K.S. Seshadri, *Ind. Eng. Chem. Fund.*, **18**, 368 (1979).
- [5] T. Yao and Y. Kamiya, *Bull. Chem. Soc. Jpn.*, **52**, 492 (1979).
- [6] R.E. Miller and S.E. Stein, *J. Phys. Chem.*, **85**, 580 (1981).
- [7] S. Krishnamurthy, S. Panvelker and Y.T. Shah, *AIChE J.*, **27**, 994 (1981).
- [8] M. Houalla, N.K. Nag, A.V. Sapre, D.H. Broderick and B.C. Gates, *AIChE J.*, **24**, 1015 (1978).
- [9] D.T. Allen and G.R. Gavalas, *Int. J. Chem. Kinet.*, **15**, 219 (1983).
- [10] D.D. Whitehurst, T.O. Mitchell and M. Farcasiu, *Coal Liquefaction*, Academic Press, New York, 1980.

Chapter 8

The Kinetics of Dialin Thermolysis

This chapter appeared in the *International Journal of Chemical Kinetics*
in March, 1983.

Kinetics of Dialin Thermolysis

D. T. ALLEN and G. R. GAVALAS

*Division of Chemistry and Chemical Engineering, California Institute of Technology,
Pasadena, California 91125*

Abstract

The liquid-phase thermolysis of 1,2-dihydronaphthalene was studied in a batch reactor in the range of 350–400°C. The measured product distributions were in good agreement with calculations based on a free-radical scheme with rate constants estimated by thermochemical methods. The kinetic calculations were carried out by numerical integration and by the long-chain approximation (LCA), which yielded a closed-form solution.

Introduction

Recent studies of coal and coal extracts have indicated that aromatic and hydroaromatic functional groups are important components of coal structures. This has sparked an increased interest in the thermal reactions of aromatic and hydroaromatic compounds [1–6]. The emphasis in most investigations of these reactions has been on measuring product distributions and elucidating reaction mechanisms. Few attempts have been made at analyzing the reaction systems quantitatively.

The purpose of this work is to provide a quantitative kinetic analysis of the pyrolysis of 1,2-dihydronaphthalene (1,2-dialin). Dialin was chosen because of the relative simplicity of its reaction mechanism and because it has been identified as an intermediate in the dehydrogenation of 1,2,3,4-tetrahydronaphthalene (tetralin), a commonly used solvent in coal liquefaction studies [7]. A quantitative description of dialin thermolysis will serve as a building block for the kinetic analysis of more complex hydroaromatic compounds and mixtures of compounds.

The experimental data base on 1,2-dialin thermolysis is limited. King and Stock [8] pyrolyzed 1,2-dialin at 300 and 400°C; Bredael and Vinh [7] examined high-temperature low-contact-time thermolysis, and Virk et al. [9] studied the reactions of dialin with phenanthrene, anthracene, and coal. This work will expand on the limited data available on 1,2-dialin reactions. With sufficient data accumulated, a standard free-radical mechanism, with parameters estimated by thermochemical methods [10], will be used to quantitatively describe product distributions. Thermochemical methods have only recently been applied to estimate the rates of liquid-phase re-

actions. Miller and Stein [6] were the first to make this application when they studied the pyrolysis of 1,2-diphenylethane.

The analysis of the complex dialin reaction mechanism will be considerably simplified by the use of the long-chain approximation (LCA). The mathematical theory of the LCA and criteria for its validity have been examined by Côme [11]. When applicable, this approximation drastically simplifies the numerical solution of the kinetic equations and allows the separate analysis of the propagation reactions on the one hand, and the initiation-termination reactions on the other. This separation allows a simpler and more direct evaluation of reaction mechanisms and estimation of rate parameters. The situation becomes particularly transparent when, as in the present problem, the LCA leads to closed-form solutions.

Experimental

Dialin was obtained from K and K Chemicals and was used without additional purification. The purity, as determined by gas chromatography, was better than 97%. The principal impurities were 1,4-dialin, tetralin, and naphthalene.

The pyrolysis of dialin was carried out in a $\frac{1}{4}$ -in.-outside-diameter stainless-steel tube reactor. One gram of reactants was charged to the reactor for each run. The reactants were degassed under vacuum, then placed under a nitrogen atmosphere. The reactor was then inserted in a molten lead bath. The bath temperature was controlled within 2°C of the set point in all runs. The time required for the reactants to be heated to within 2°C of reaction temperature was measured by a thermocouple sealed inside a second tubing bomb reactor. Heat-up time in all runs was under 45 s. The reactors were kept in the lead bath for the specified reaction time, then were cooled with an air jet and immersion in a water bath. The reactors cooled down 100°C within 30 s of removal from the lead bath.

After cooling, product gases were metered and analyzed by gas chromatography. Hydrogen was the only gas product detected. Liquid and solid products were washed from the reactor with methylene chloride and analyzed with an HP 5880A gas chromatograph equipped with a 30-m Carbowax capillary column. In selected runs, ^1H nuclear magnetic resonance was used for product identification. Product peaks were identified and calibrated by comparison with pure compounds.

Pyrolysis experiments were performed at three temperatures and at several reaction times for each temperature. Experiments were also performed with dialin diluted with tetralin or biphenyl. Reaction conditions and product concentrations are summarized in Table I.

DIALIN THERMOLYSIS

TABLE I. 1,2-Dialin thermolysis data.

		REACTANTS				PRODUCTS			
Reaction Temp. (°C)	Reaction Time (Min.)	1,2 Dialin (g)	Tetralin (g)	Biphenyl (g)	1,2 Dialin (g)	1,4 Dialin (g)	Tetralin (g)	Naphthalene (g)	H ₂ (ml at STP)
350	5	1.00	0	0	0.617	0.012	0.173	0.198	5.0
350	15	1.00	0	0	0.376	0.008	0.287	0.328	7.0
350	30	1.00	0	0	0.229	0.005	0.363	0.402	6.5
350	60	1.00	0	0	0.113	0.003	0.423	0.461	6.5
350	5	0.50	0.50	0	0.362	0.001	0.563	0.074	1.5
350	15	0.50	0.50	0	0.310	0.006	0.584	0.100	2.5
350	5	0.10	0	0.90	0.087	0	0.0061	0.0072	
375	5	1.00	0	0	0.503	0.013	0.228	0.256	5.0
375	15	1.00	0	0	0.216	0.006	0.373	0.404	5.0
375	30	1.00	0	0	0.098	0.003	0.429	0.469	7.0
400	5	1.00	0	0	0.232	0.007	0.364	0.396	6.0
400	15	1.00	0	0	0.103	0.003	0.424	0.468	7.5

ALLEN AND GAVALAS

TABLE II. Dialin thermolysis mechanism.

No.	REACTION	$\log_{10} A^a$	E^b	SOURCE
1	INITIATION: $1,2\text{-C}_{10}\text{H}_{10} + 1,2\text{-C}_{10}\text{H}_{10} \rightarrow \text{C}_{10}\text{H}_9\cdot + 1\text{-C}_{10}\text{H}_{11}\cdot$	8.0	38.	Benson & Shaw ¹⁷
2	PROPAGATION MAJOR REACTIONS: $\text{C}_{10}\text{H}_9\cdot + \text{C}_{10}\text{H}_8 + \text{H}\cdot$	14.5	27.	Group Additivity ¹⁰
3	$\text{C}_{10}\text{H}_8 + \text{H}\cdot \rightarrow \text{C}_{10}\text{H}_9\cdot$	11.0	3.	"
4	$\text{H}\cdot + 1,2\text{-C}_{10}\text{H}_{10} \rightarrow \text{C}_{10}\text{H}_9\cdot + \text{H}_2$	10.0	3.	Group Additivity ¹⁰
5	$\text{H}\cdot + \text{C}_{10}\text{H}_{12} + 1\text{-C}_{10}\text{H}_{11}\cdot \rightarrow \text{H}_2$	10.0	3.	"
6	$\text{H}\cdot + \text{C}_{10}\text{H}_{12} + 2\text{-C}_{10}\text{H}_{11}\cdot \rightarrow \text{H}_2$	10.3	10.	"
7	$\text{H}\cdot + 1,2\text{-C}_{10}\text{H}_{10} \rightarrow 1\text{-C}_{10}\text{H}_{11}\cdot$	11.0	3.	"
8	$1,2\text{-C}_{10}\text{H}_{10} + 1\text{-C}_{10}\text{H}_{11}\cdot \rightarrow \text{C}_{10}\text{H}_9\cdot + \text{C}_{10}\text{H}_{12}$	7.0	9.	"
9	$\text{C}_{10}\text{H}_9\cdot + \text{C}_{10}\text{H}_{12} + 1,2\text{-C}_{10}\text{H}_{10} + 1\text{-C}_{10}\text{H}_{11}\cdot$	7.0	11.	"
10	$2\text{-C}_{10}\text{H}_{11}\cdot + \text{C}_{10}\text{H}_{12} + 1\text{-C}_{10}\text{H}_{11}\cdot + \text{C}_{10}\text{H}_{12}$	7.0	9.	"
11	$1,2\text{-C}_{10}\text{H}_{10} + 2\text{-C}_{10}\text{H}_{11}\cdot \rightarrow \text{C}_{10}\text{H}_9\cdot + \text{C}_{10}\text{H}_{12}$	7.0	9.	"
12	MINOR REACTIONS: $\text{C}_{10}\text{H}_9\cdot + 1,2\text{-C}_{10}\text{H}_{10} + 1,4\text{-C}_{10}\text{H}_{10} + \text{C}_{10}\text{H}_9\cdot$	7.0	12.	Cox & Pilcher ²⁰
13	$\text{C}_{10}\text{H}_9\cdot + 1,4\text{-C}_{10}\text{H}_{10} + 1,2\text{-C}_{10}\text{H}_{10} + \text{C}_{10}\text{H}_9\cdot$	7.0	9.	Group Additivity ¹⁰
14	$\text{C}_{10}\text{H}_9\cdot + \text{C}_{10}\text{H}_{12} + 1\text{-C}_{10}\text{H}_{11}\cdot + 1,4\text{-C}_{10}\text{H}_{10}$	7.0	14.	Cox & Pilcher ²⁰
15	$1\text{-C}_{10}\text{H}_{11}\cdot + 1,4\text{-C}_{10}\text{H}_{10} + \text{C}_{10}\text{H}_9\cdot + \text{C}_{10}\text{H}_{12}$	7.0	9.	Group Additivity ¹⁰
16	$\text{H}\cdot + 1,4\text{-C}_{10}\text{H}_{10} + \text{C}_{10}\text{H}_9\cdot + \text{H}_2$	10.0	3.	"
17	$\text{H}\cdot + 1,4\text{-C}_{10}\text{H}_{10} + 2\text{-C}_{10}\text{H}_{11}\cdot$	11.0	10.	"
18	$1,4\text{-C}_{10}\text{H}_{10} + \text{C}_{10}\text{H}_8 + \text{H}_2$	12.0	45.	Benson & Shaw ²²
19	TERMINATION: $\text{R}\cdot + \text{R}\cdot \rightarrow \text{PRODUCTS}$	10.0	0.	Diffusion Limited

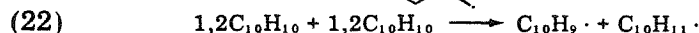
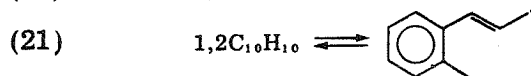
^a Units of s^{-1} for unimolecular reactions, $\text{L/mol} \cdot \text{s}$ for bimolecular reactions.^b Activation energy in kcal/mol.

Reaction Mechanism

The adopted dialin thermolysis mechanism and the rate parameters for each reaction are listed in Table II. Rate constants were estimated using the group additivity methods of Benson [10] and by analogies with rate constants available in the literature. The calculations and rationale involved in selecting the rates for each reaction are discussed in Appendix A.

DIALIN THERMOLYSIS

The proposed initiation step deserves some comment. Three plausible initiation steps are given below:



Reactions (20) and (21) have high activation energies, but should also have large frequency factors. Group additivity methods give activation energies of 82 and 56 kcal/mol, respectively. The A factors for the unimolecular reactions (20) and (21) can be estimated from transition state theory to be approximately $\log A = 13.8$ and 13. The rate parameters for reaction (22) are given in Table I. Using these rate parameters, the rate of reaction (22) is several orders of magnitude higher than that of reaction (20) and is roughly equivalent to that of reaction (21). The net rate of initiation by reaction (21) will be limited by the high rate of the reverse intramolecular recombination reaction. Thus the net rate of reaction (21) will be lower than that of reaction (22) by several orders of magnitude. Reverse disproportionation is then by far the dominant initiation step.

Two types of reactions were omitted from the mechanism given in Table II. The addition of hydrogen atoms to tetralin to form *n*-butyl-benzene was neglected since no butyl benzene was detected in the reaction products and because a rough estimate of the rate, $\log A = 8$, $E = 3$ kcal, was very low. In addition, the formation of beta radicals via hydrogen abstraction by alpha radicals [the reverse of reaction (11)] was neglected as energetically unfavorable.

No specific products are listed for the termination steps. Termination may proceed by either disproportionation or recombination, but in either case it occurs at a rate that is slow relative to product formation by propagation steps. Termination rates were assumed to be diffusion limited. Rates of diffusion-limited reactions were estimated from the viscosity of the liquid using the Stokes-Einstein equation [12]. For the case of dialin, the viscosity at reaction temperatures was estimated as 0.10 ± 0.02 cP using the correlations of Letsou and Stiel as described in [13], giving $\log k = 10$.

The differential equations for radical and stable species concentration were integrated numerically using the Gear algorithm for stiff systems. A Gear integration routine, similar to the one used in this work, is described in [14]. The dialin concentration used in these calculations was estimated using the method of Gunn and Yamada as described in [15]. All but two of the rate parameters used in the calculations were estimated by thermochemical methods or by analogy with reactions having known parameters. Two parameters were estimated directly from the data. These were the A factor for the addition of hydrogen atoms to dialin and the activation

ALLEN AND GAVALAS

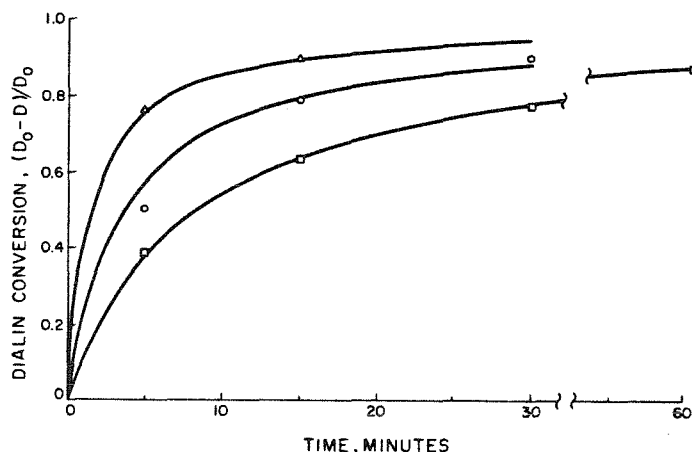


Figure 1. Dialin conversion predicted by full numerical integration. \square —623 K; \circ —648 K; Δ —673 K; D_0 —initial dialin concentration.

energy of the initiation reaction. The value of the first parameter is comparable to the experimental value reported by Benson and Shaw [16] for 1,3-cyclohexadiene pyrolysis. The estimated ratio of hydrogen addition to hydrogen abstraction was 10 compared to 5 for 1,3-cyclohexadiene. The value of 38 kcal/mol for the second parameter was in good agreement with a group additivity estimate of 35 kcal/mol.

Calculated and experimental concentrations of dialin, naphthalene, and tetralin are shown in Figures 1 and 2. The calculated concentrations of 1,4-dialin are slightly lower than the measured concentrations, but 1,4-dialin impurities in the reactants account for most of the difference. Otherwise the agreement between calculated and experimental values is very good, considering that all but two of the rate parameters were estimated a priori by thermochemical techniques or by analogy with similar reactions. Along with the work of Miller and Stein [6], these results lend support to the use of thermochemical methods in estimating the rates of reactions in liquids. Such thermochemical estimates may not be valid for reactions in either very viscous liquids or liquids which impart stability to transition states, but they should be useful for mixtures of aromatic and hydroaromatic compounds of modest molecular weight.

In order to determine the sensitivity of calculated concentrations to the estimated rate parameters, each of the major rate constants was varied individually, and the kinetic differential equations were integrated as before. The results of the integrations are shown in Table III. The effect of each parameter on dialin conversion and product distribution was expressed by comparing the perturbed reaction system to the base case. The

DIALIN THERMOLYSIS

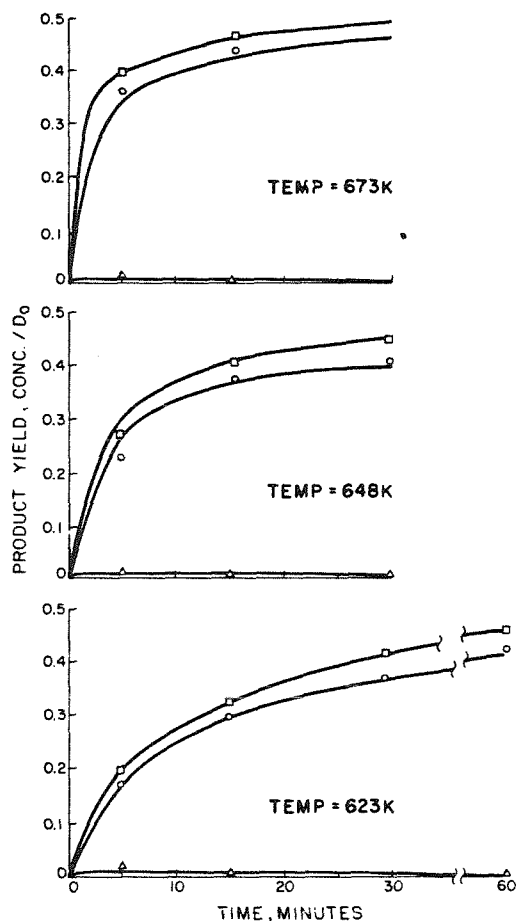


Figure 2. Product yields predicted by full numerical integration. \square — $C_{10}H_8$; \circ — $C_{10}H_{12}$; Δ — $1,4\ C_{10}H_{19}$; D_0 —initial 1,2-dialin concentration.

comparison was made at 350°C and 5 min of reaction time. The analysis shows that conversion is most affected by reactions (1), (8), and the termination reactions. Increasing the rate of reaction (1) or decreasing the rate of termination increases the total free-radical concentration, thereby increasing the rate of dialin conversion. Increasing the rate of reaction (8) increases the rate of formation of dialin radicals and tetralin. The increased production of dialin radicals results in increased naphthalene formation. The selectivity of the two products is controlled by the rates of reactions (4) and (7), that is, by the rates of hydrogen addition and hydrogen abstraction from dialin. The results of the LCA will make this dependence clearer.

TABLE III. Sensitivity of full numerical integration to rate parameters.

PARAMETER	BASE VALUE	PERTURBED VALUE	% PERTURBATION	CONVERSION	SELECTIVITY (T/N)	% CHANGE IN CONVERSION	% CHANGE IN SELECTIVITY
k_1	4.64×10^{-6}	5.01×10^{-6}	10.	.3742	.8836	3.23	-0.11
k_2	1.07×10^5	1.18×10^5	10.	.3667	.8841	1.16	-0.06
k_3	8.86×10^9	9.75×10^8	10.	.3626	.8847	0.03	0.01
k_4	8.86×10^8	9.75×10^8	10.	.3634	.8769	0.25	-0.87
k_5	8.86×10^8	9.75×10^8	10.	.3626	.8838	0.03	-0.09
k_6	6.21×10^6	6.83×10^6	10.	.3628	.8847	0.08	0.01
k_7	8.86×10^9	9.75×10^9	10.	.3621	.8928	-0.11	0.93
k_8	6.98×10^3	7.68×10^3	10.	.3802	.8853	4.88	0.08
k_9	1.38×10^3	1.52×10^3	10.	.3623	.8846	-0.06	0.00
k_{19}	1.00×10^{10}	1.10×10^{10}	10.	.3521	.8844	-2.87	-0.02

DIALIN THERMOLYSIS

• Long-Chain Approximation

A second goal of this work was to explore the utility of the LCA in analyzing complex free-radical mechanisms such as the one proposed for dialin thermolysis. The LCA can be used to determine the concentrations of stable species as a function of time or, as applied in this work, to determine relative concentrations, independent of time. The application of the LCA requires two assumptions. The first is that changes in free-radical concentrations are small relative to total free-radical concentration for any given set of stable species concentrations. The second is that the rates of initiation and termination are slow relative to the rates of propagation reactions. For dialin thermolysis, the criteria established by Côme [11] for the validity of these assumptions are

$$(23) \quad k_8 \gg 1$$

$$(24) \quad k_8/(k_1 k_{19})^{1/2} \gg 1$$

These relations are both satisfied, as shown in Appendix B. The results of the numerical integration also indicated that the assumptions were valid. Therefore the LCA was applied to determine the concentration paths of the simplified reaction system consisting of reactions (2)–(11). These reactions account for all major reaction products, and lead to closed-form solutions for product concentrations. Using the LCA and the simplified reaction system gives rise to the differential equation

$$(25) \quad \frac{dD}{dT} = -\frac{2k_7 + k_4}{k_7} - \frac{(k_5 + k_6)T}{k_7 D}$$

where D is 1,2-dialin concentration and T is tetralin concentration. This may be solved analytically, yielding

$$(26) \quad \ln \left(\frac{D}{D_0} \right) = C - \ln q + \frac{u(+)\ln|u - u(+)| - u(-)\ln|u - u(-)|}{u(+) - u(-)}$$

where D_0 is initial dialin concentration, C is a constant determined by the initial conditions, and

$$u = T/D$$

$$q = k_7 + (2k_7 + k_4)u + (k_5 + k_6)u^2$$

$$u(\pm) = \frac{-(2k_7 + k_4) \pm [(2k_7 + k_4)^2 - 4k_7(k_5 + k_6)]^{1/2}}{2(k_5 + k_6)}$$

This equation describes the path of the thermolysis. It is derived in Appendix C.

Figure 3 compares the results of the LCA, eq. (26), with the results of the full numerical integration and the experimental data. The experimental results of King and Stock [8] are also included. The three lines plotted in

ALLEN AND GAVALAS

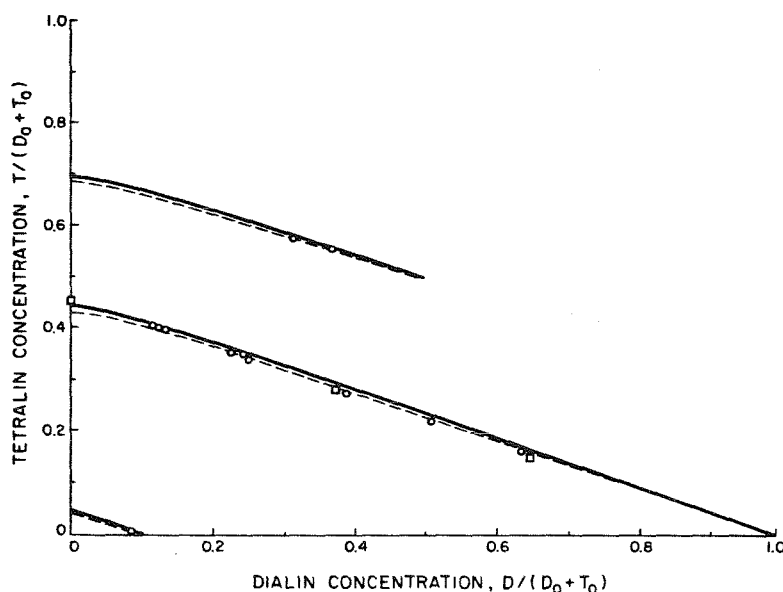


Figure 3. Concentration paths calculated by LCA. Solid lines—long-chain paths; dashed lines—full numerical integration paths; \square —data of King and Stock [8]; \circ —this work; D_0 —initial dialin concentration; T_0 —initial tetralin concentration.

Figure 3 are the concentration paths for three different starting conditions. The lowest curve is the concentration path for dialin diluted 9:1 with biphenyl. The middle curve is the path corresponding to pure dialin reactant, and the upper curve is the path for reactants consisting of equal amounts of tetralin and dialin. Examination of eq. (25) reveals that multiplying all concentrations by a constant does not change the differential equation. This means that dilution with an inert such as biphenyl has no effect on product distribution and results in the geometric similarity of the two lower curves of Figure 3. Dilution with tetralin affects the value of the second term in eq. (25); however, the first term dominates, so the upper curve is roughly similar to the lower two.

Examination of eq. (25) also reveals that the concentration paths are functions of concentration and rate constants 4, 5, 6, and 7 alone. Specifically, the ratios $(2k_7 + k_4)/k_7$ and $(k_5 + k_6)/k_7$ control product selectivity, the former ratio being larger and thus more important. The sensitivity of the results of the LCA to the values of each of the four rate constants and to temperature is given in Table IV. The most striking result is the essential temperature independence of selectivity. This independence is due to the identical activation energies of reactions (4), (5), and (7). The ratio $(2k_7 + k_4)/k_7$ is strictly independent of temperature, and the ratio $(k_5 + k_6)/k_7$ is essentially independent of temperature since $k_5 \gg k_6$.

DIALIN THERMOLYSIS

TABLE IV. Sensitivity of long-chain approximation results to rate parameters and temperature.

PARAMETER	BASE VALUE	PERTURBED VALUE	% PERTURBATION	SELECTIVITY* (T/N)	% CHANGE IN SELECTIVITY
k_4	8.86×10^8	9.75×10^8	10.	.8000	-0.77
k_5	8.86×10^8	9.75×10^8	10.	.7994	-0.85
k_6	6.21×10^6	6.83×10^6	10.	.8063	0.00
k_7	8.86×10^9	9.75×10^9	10.	.8189	1.56
TEMPERATURE	623K	685K	10.	.8060	-0.04

* Selectivity evaluated at >99.5% conversion.

Conclusion

Liquid-phase dialin thermolysis was quantitatively described by a free-radical mechanism. Values of the rate parameters derived by analogy with similar reactions in the literature and by thermochemical estimates provided an excellent fit to the data. No modifications were necessary to account for the liquid phase. Since the products of dialin thermolysis are structurally similar to coal-derived liquids, these results indicate that thermochemical methods should be useful in estimating rate parameters for coal liquids of modest molecular weight.

Application of the LCA to the complex dialin pyrolysis mechanism allowed closed-form solutions for dialin concentration as a function of tetralin concentration. This brought to light several interesting relationships. The first was that product selectivity is governed by two ratios involving only four rate constants. The selectivity is essentially determined by the ratio of hydrogen atom addition to hydrogen atom abstraction in dialin. The second result of the analysis was that dilution of the reaction mixture does not change the product distribution.

Appendix A: Selection of Rate Constants

Reaction (1): The A factor for reaction (1) was estimated using the relation $\ln(A/A_-) = \Delta S/R$ and a value of $\log A_- = 10$. A best fit to the experimental data was then given by $E = 38$ kcal/mol, a value comparable to the group additivity estimate of 35 kcal/mol.

Reactions (2), (3): Addition of hydrogen atoms to naphthalene should occur with an A factor and activation energy similar to that of reaction (7).

Thus the values chosen for reaction (3) were $\log A = 11$ and $E = 3$ kcal/mol. Group additivity estimates give $\Delta H = 24$ and $\Delta S = 25.3$. Using the relations $\Delta H = E - E_-$ and $\ln(A/A_-) = \Delta S/R$ yields $\log A = 14.5$ and $E = 27$ for reaction (2).

Reaction (4): This reaction can be considered as equivalent to an abstraction of alpha hydrogen. Gavalas [17] lists $\log A = 10$ and $E = 2.3$ kcal/mol for alpha abstraction from toluene. The reaction can also be considered as analogous to hydrogen abstraction from propylene, for which Allara and Edelson [18] report experimental values of $\log A = 11$ and $E = 3.8$ kcal/mol. Since dialin is closer to toluene than to propylene in molecular size, we have chosen $\log A = 10$. The activation energy was chosen as 3 kcal/mol.

Reaction (5): This reaction was assumed to be analogous to reaction (4).

Reaction (6): Gavalas [17] suggests $\log A = 10.3$ and $E = 9.7$ kcal/mol for abstraction of beta hydrogen. Allara and Edelson [18] recommend an activation energy of approximately 10 kcal for hydrogen abstraction from propane. Thus $\log A$ and E were chosen as 10.3 and 10.0, respectively.

Reaction (7): The best fit of the dialin pyrolysis data is given by an addition-to-abstraction ratio of 10. Benson and Shaw [16] found that the ratio of hydrogen addition to abstraction for 1,3-cyclohexadiene was 5. Hence $\log A = 11$ and $E = 3$ kcal/mol is in reasonable accord with available data.

Reactions (8)–(11): Group additivity estimates by Gavalas [17] yield $\log A = 7$ and $E = 9$ kcal/mol for these exchange reactions. Reactions (10) and (11) are considered irreversible because of the greater stability of the alpha radical. The activation energy of reaction (9) is increased by 2 kcal/mol to account for the enhanced stability of the dialin radical over the tetralyl radical.

Reactions (12), (13): Cox and Pilcher [19] list liquid-phase heats of formation of 18.0 ± 1.5 and 21.0 ± 1.5 for the 1,2- and 1,4-dialin isomers. Setting $\Delta H = 3$ kcal/mol is in agreement with these results and the experimental data. Assuming $E = 9$ for reaction (13) gives $E = 12$ for reaction (12). The frequency factor should be identical to that of reaction (8).

Reactions (14), (15): These are considered analogous to reactions (12) and (13).

Reaction (16): This reaction is similar to reaction (4). Even though the 1,4-dialin isomer has a higher heat of formation than the 1,2-isomer, the net reaction is so highly exothermic, and the transition states should be sufficiently similar that the rate parameters should be identical to those of reaction (4).

Reaction (17): This reaction is analogous to reaction (7), but will probably have an activation energy closer to 10 kcal/mol since a beta radical is being formed.

Reaction (18): This pericyclic reaction is symmetry allowed according

DIALIN THERMOLYSIS

to the rules established by Woodward and Hoffman [20]. The rate was assumed to be similar to the dehydrogenation of 1,4-cyclohexadiene to benzene. Benson and Shaw [21] report this rate as $\log A = 12.36$ and $E = 43.8$ kcal/mol.

Reaction (19): Termination reactions were assumed to be diffusion limited.

Note: Values of thermodynamic variables of stable species were taken from [22].

Appendix B: Criteria for Applying the Long-Chain Approximation

Using reaction (8) as a typical propagation reaction, the ratio of propagation-to-initiation rates must be at least

$$R = \frac{k_8[T_1\cdot][D]}{k_1[D]^2}$$

where $[T_1\cdot]$ is 1-tetralyl radical concentration and $[D]$ is 1,2-dialin concentration. The numerical integrations showed that 1-tetralyl was the dominant radical, so the balance between initiation and termination gives

$$[T_1\cdot] \sim (k_1[D]^2/k_{19})^{1/2}$$

so that

$$R = k_8/(k_1k_{19})^{1/2} = 10^{-2.0} \exp(9.5 \text{ kcal}/RT)$$

The rate constant k_8 and the ratio R vary with temperature as follows:

Temperature (K)	R	k_8
623	22.	6.98×10^3
648	16.	9.21×10^3
673	12.	1.19×10^4

In all cases, $k_8 \gg 1$ and $k_8/(k_1k_{19})^{1/2} \gg 1$, validating the application of the LCA.

Appendix C: Application of the Long-Chain Approximation

The balance of propagation reactions (2)–(11) yields the following linear algebraic system:

$$(I) \quad \frac{d[D\cdot]}{dt} = 0 = -[D\cdot](k_2 + k_9[T]) + [H\cdot] \\ \times (k_4[D] + k_3[N]) + k_8[D][T_1\cdot] + k_{11}[D][T_2\cdot]$$

$$(II) \quad \frac{d[T_2^*]}{dt} = 0 = k_6[T][H\cdot] - [T_2^*](k_{10}[T] + k_{11}[D])$$

$$(III) \quad \frac{d[H\cdot]}{dt} = 0 = k_2[D\cdot] - [H\cdot](k_3[N] + (k_4 + k_7)[D] + (k_5 + k_6)[T])$$

where $[D]$, $[T]$, and $[N]$ are 1,2-dialin, tetralin, and naphthalene concentrations; $[D\cdot]$, $[T_1^*]$, and $[T_2^*]$ are dialin radical, 1-tetralyl, and 2-tetralyl radical concentrations. The differential equations governing dialin and tetralin concentration are

$$(IV) \quad \frac{d[D]}{dt} = -[D](k_4[H\cdot] + k_7[H\cdot] + k_8[T_1^*] + k_{11}[T_2^*]) + k_9[T][D\cdot]$$

$$(V) \quad \frac{d[T]}{dt} = -[T](k_5[H\cdot] + k_6[H\cdot] + k_9[D\cdot]) + k_8[D][T_1^*] + k_{11}[D][T_2^*]$$

Dividing eq. (IV) by eq. (V) and simplifying using eqs. (I)–(III) yields

$$(VI) \quad \frac{d[D]}{d[T]} = -\frac{2k_7 + k_4}{k_7} - \frac{(k_5 + k_6)[T]}{k_7[D]}$$

Defining the variable $u = [T]/[D]$ and differentiating with respect to $[D]$ yields

$$(VII) \quad \frac{du}{d[D]} = -\frac{[T]}{[D]^2} + \frac{1}{[D]} \left(\frac{d[T]}{d[D]} \right)$$

Substituting eq. (VI) into eq. (VII) and integrating gives

$$\ln \left(\frac{[D]}{[D_0]} \right) = C - \ln q + \frac{u(+) \ln|u - u(+)| - u(-) \ln|u - u(-)|}{u(+) - u(-)}$$

where

$$q = k_7 + (2k_7 + k_4)u + (k_5 + k_6)u^2$$

$$u(\pm) = \frac{-(2k_7 + k_4) \pm [(2k_7 + k_4)^2 - 4k_7(k_5 + k_6)]^{1/2}}{2(k_5 + k_6)}$$

and C is found from the initial conditions. For pure dialin as the reactant,

$$C = \ln k_7 - \frac{u(+) \ln|u(+)| - u(-) \ln|u(-)|}{u(+) - u(-)}$$

Bibliography

- [1] B. M. Benjamin, V. F. Raaen, P. H. Maupin, L. L. Brown, and C. J. Collins, *Fuel*, **57**, 269 (1978).
- [2] D. C. Cronauer, D. M. Jewell, Y. T. Shah, and K. A. Kueser, *Ind. Eng. Chem. Fund.*, **17**, 291 (1978).

DIALIN THERMOLYSIS

- [3] D. C. Cronauer, D. M. Jewell, Y. T. Shah, and R. J. Modi, *Ind. Eng. Chem. Fund.*, **18**, 153 (1979).
- [4] D. C. Cronauer, D. M. Jewell, R. J. Modi, and K. S. Seshadri, *Ind. Eng. Chem. Fund.*, **18**, 368 (1979).
- [5] T. Yao and Y. Kamiya, *Bull. Chem. Soc. Jpn.*, **52**, 492 (1979).
- [6] R. E. Miller and S. E. Stein, *J. Phys. Chem.*, **85**, 580 (1981).
- [7] P. Bredael and T. H. Vinh, *Fuel*, **58**, 211 (1979).
- [8] H. H. King and L. M. Stock, *Fuel*, **60**, 748 (1981).
- [9] P. S. Virk, D. H. Bass, C. P. Eppig, and D. J. Ekpenyong, *Am. Chem. Soc., Div. Fuel Chem. Preprints*, **24**, 144 (1979).
- [10] S. W. Benson, "Thermochemical Kinetics," 2nd ed., Wiley, New York, 1976.
- [11] G. M. Côme, *J. Phys. Chem.*, **81**, 2560 (1977).
- [12] K. U. Ingold, "Free Radicals," vol. 1, J. K. Kochi, Ed., Wiley, New York, 1973.
- [13] R. C. Reid, J. M. Prausnitz, and T. K. Sherwood, "The Properties of Gases and Liquids," 3rd ed., McGraw-Hill, New York, 1977, pp. 455-457.
- [14] R. N. Stabler and J. P. Chesick, *Int. J. Chem. Kinet.*, **10**, 461 (1978).
- [15] R. C. Reid, J. M. Prausnitz, and T. K. Sherwood, "The Properties of Gases and Liquids," 3rd ed., McGraw-Hill, New York, 1977, pp. 60-61.
- [16] S. W. Benson and R. Shaw, *J. Am. Chem. Soc.*, **89**, 5351 (1967).
- [17] G. R. Gavalas, "Coal Pyrolysis," Elsevier Scientific, New York, 1982.
- [18] D. L. Allara and D. Edelson, *Int. J. Chem. Kinet.*, **7**, 479 (1975).
- [19] J. D. Cox and G. Pilcher, "Thermochemistry of Organic and Organometallic Compounds," Academic, New York, 1970.
- [20] For example, see T. H. Lowry and K. S. Richardson, "Mechanism and Theory in Organic Chemistry," Harper and Row, New York, 1976.
- [21] S. W. Benson and R. Shaw, *Trans. Faraday Soc.*, **63**, 985 (1967).
- [22] R. Shaw, D. M. Golden, and S. W. Benson, *J. Phys. Chem.*, **81**, 1716 (1977).

Received May 12, 1982

Accepted August 30, 1982

Chapter 9

REACTIONS OF METHYLENE AND ETHER BRIDGES

David T. Allen and George R. Gavalas

Department of Chemical Engineering
California Institute of Technology
Pasadena, California 91125

This chapter was submitted as a manuscript to the journal *Fuel*

ABSTRACT

The reactions of model compounds containing methylene and ether bridges were examined in the temperature range 350-400 °C. Aromatic substitution reactions and homolysis via a keto-enol intermediate were the dominant modes of bridge decomposition. The aromatic substitution reactions of methylene bridge compounds occurred with activation energies of approximately 10 kcal/mol and with A factors of $10^{10.5-12}$ l sec⁻¹m⁻¹. The A factors vary with the size of the rings and the substituents on the rings connected by the methylene bridges. The activation energy is relatively independent of these effects. When phenolic substituents are present, methylene bridges can unimolecularly decompose via a keto-enol tautomerism, and the rate of product formation is solvent dependent. Reactions for ether bridge reactions were much more complex and the rate parameters encompassed a much larger range of values.

Principal new conclusions and results

The rates of methylene and ether bridge cleavage were examined using model compound systems. The dominant decomposition pathways involved aromatic substitution reactions. Rates of reactions in the proposed free radical mechanisms were estimated from experimental data and group additivity methods. The results demonstrate that the reactions of multicomponent mixtures such as coal liquids are much more complex than the sum of the reactions of the components.

Methods and observations from which deduced

Batch thermolysis experiments were performed in a stainless steel tubing bomb reactor at several temperatures and reaction times for each of the model compound mixtures. Product distributions were determined by gas chromatography.

Special limitations and assumptions



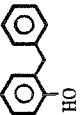
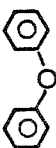



The proposed mechanisms were assumed to be free radical in nature and since stainless steel did not catalyze bridge decomposition, the reactions were assumed to be non-catalytic.

INTRODUCTION

The thermal reactions of compounds containing functional groups known to exist in coal and coal-derived liquids have been the subject of many studies.¹⁻⁶ The emphasis in most of these studies has been on measuring product distributions and elucidating reaction mechanisms for pure compounds and compounds mixed with 1,2,3,4-tetrahydronaphthalene (tetralin). Few attempts have been made at either analyzing mechanisms quantitatively or investigating the interactions between functional groups. One class of reactions where the interaction between functional groups is particularly important is the dissociation of methylene and ether bridges. On the basis of model compound studies performed on mixtures of bridged compounds and tetralin,¹ these bridges are generally considered to be inert under liquefaction conditions. However, if molecules are present in the mixture which generate atomic hydrogen during thermolysis (e.g., 1,2 dihydronaphthalene or 9,10 dihydrophenanthrene) these bridges can be broken via an aromatic substitution reaction under fairly mild conditions.

The purpose of this paper is to examine the reactions of methylene and ether bridges under conditions where atomic hydrogen is present. Specifically, the mixtures listed in Table 1 were thermolyzed in the temperature range 350-400 °C. In this temperature range, the 1,2 dihydronaphthalene (dialin) contained in the mixtures decomposes via a free radical mechanism,⁷ releasing atomic hydrogen. The hydrogen can displace the methylene and ether bridges from the aromatic rings. In modeling the reactions of these mixtures, standard free radical mechanisms will be employed and rate parameters will be estimated by thermochemical methods.⁸

Table 1
REACTION CONDITIONS

Reactants (wt %)						Reaction Temperatures (°C)	Reaction Times (min)	
								
50	0	0	0	50	0	0	350, 375, 400	5, 15, 30
0	25	0	0	75	0	0	350, 375, 400	5, 15, 30, 60
0	0	50	0	50	0	0	350, 375, 400	5, 15, 30
0	0	20	0	0	80	0	350, 375, 400	60
0	0	20	0	0	40	40	400	60
0	0	20	0	80	0	0	400	60
0	0	0	50	50	0	0	400	30

EXPERIMENTAL

All reactants except dihydronaphthalene and dinaphthylmethane were obtained from Aldrich Chemical Co. and were used as received. The dihydronaphthalene was obtained from K and K Chemicals and the 1,1-dinaphthylmethane was synthesized in our laboratory.

The thermolysis experiments were carried out in a stainless steel tubing bomb reactor. One half gram of reactants was charged to the reactor for each run. The reactants were degassed under vacuum then placed under a nitrogen atmosphere. The reactor was then inserted into a molten lead bath. Bath temperature was controlled to within 2°C of the set point in all runs. The time required for the reactants to be heated to within 2°C of reaction temperature was measured by a thermocouple sealed inside a second tubing bomb reactor. Heat-up time in all runs was under 45 seconds. The reactors were kept in the lead bath for the specified time, then were cooled with an air jet and immersion in a water bath. The reactors were cooled 100°C within 30 seconds of removal from the lead bath.

After cooling, product gases were metered and analyzed by gas chromatography. Hydrogen was the only gas product detected. Liquid and solid products were washed from the reactor with methylene chloride and analyzed on a gas chromatograph equipped with either a 30 meter Carbowax or a 30 meter DB-1 capillary column. The chromatograms were temperature programmed from 60°C to 200°C. Product peaks were identified and calibrated by comparison with pure compounds.

Table 1 lists the thermolysis experiments that were performed. Conver-

sions, as determined by gas chromatography, are given in Tables 2 and 3.

RESULTS AND DISCUSSION

The experimental results, in terms of product yields for various reaction conditions, are listed in Tables 2 and 3. Table 2 lists product yields for mixtures of dialin with various compounds carrying a methylene bridge. Table 3 lists the product yields for mixtures of o-hydroxydiphenylmethane (oHDPM) with dialin or tetralin.

The experimental results were modeled with free radical mechanisms such as the one listed in Table 4. Thermochemical estimates⁶⁻⁹ and previous experimental results⁷ were used to estimate all rate parameters except those for aromatic substitution reactions, which were estimated from the data of Table 2. Reaction 2 of Table 4 is typical of this class of reactions. The kinetic analysis for each mixture is discussed in the following sections.

Dialin and Dinaphthylmethane Mixture

The free radical mechanism shown in Table 4 was used to model the thermolysis data of a 3:1 (wt.) mixture of dialin and dinaphthylmethane (DNM). Three features of the proposed mechanism should be noted. First, the demethylation and hydrogen donation reactions of 1-methylnaphthalene were neglected because of the low concentration of 1-methylnaphthalene in the mixture and the slow rates of the demethylation reactions. The second point to be noted is the activation energy of reaction 9. The DNM radical was assigned a resonance stabilization energy (RSE) 6 kcal/mol greater than that for the tetralyl radical. The enhanced stabilization is due to both the larger size of the aromatic rings in DNM and the fact that the radical is delocalized over two ring systems in

Table 2

METHYLENE BRIDGE THERMOLYSIS DATA

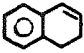
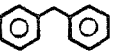

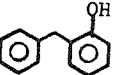
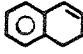
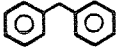
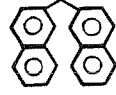
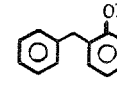
Reactants				Reaction Conditions		Conversion (%)			
				Temp (°C)	Time (Min)				
(wt%)	(wt%)	(wt%)	(wt%)						
50	50	0	0	350	5	39.	.04	-	-
50	50	0	0	350	15	50.	.06	-	-
50	50	0	0	350	30	65.	.10	-	-
50	50	0	0	375	5	52.	.10	-	-
50	50	0	0	375	15	71.	.17	-	-
50	50	0	0	375	30	80.	.58	-	-
50	50	0	0	400	5	70.	.29	-	-
50	50	0	0	400	15	89.	.49	-	-
50	50	0	0	400	30	96.	.75	-	-
75	0	25	0	350	5	30.	-	0.6	-
75	0	25	0	350	15	51.	-	0.9	-
75	0	25	0	350	30	68.	-	1.5	-
75	0	25	0	350	60	80.	-	2.4	-
75	0	25	0	375	5	51.	-	0.8	-
75	0	25	0	375	15	73.	-	2.3	-
75	0	25	0	375	30	83.	-	3.2	-
75	0	25	0	375	60	91.	-	4.0	-
75	0	25	0	400	5	64.	-	2.8	-
75	0	25	0	400	15	84.	-	4.4	-
75	0	25	0	400	30	91.	-	4.7	-
75	0	25	0	400	60	93.	-	5.0	-
50	0	0	50	350	5	47.	-	-	0.36
50	0	0	50	350	15	67.	-	-	0.47
50	0	0	50	350	30	81.	-	-	1.89
50	0	0	50	375	5	66.	-	-	0.42
50	0	0	50	375	15	74.	-	-	0.85
50	0	0	50	375	30	84.	-	-	1.91
50	0	0	50	400	5	65.	-	-	1.25
50	0	0	50	400	15	73.	-	-	1.81
50	0	0	50	400	30	97.	-	-	3.11

Table 3

•HDPM THERMOLYSIS DATA


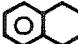
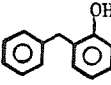


 (wt%)	 (wt%)	Reactants		 (wt%)	Reaction Conditions		Toluene Yield (%)	Cresol Yield (%)
		 (wt%)	 (wt%)		Temp (°C)	Time (Min)		
50	0	0	0	50	350	5	0.20	0.16
50	0	0	0	50	350	15	0.28	0.19
50	0	0	0	50	350	30	1.3	0.59
50	0	0	0	50	375	5	0.22	0.20
50	0	0	0	50	375	15	0.52	0.33
50	0	0	0	50	375	30	1.2	0.74
50	0	0	0	50	400	5	0.76	0.49
50	0	0	0	50	400	15	1.2	0.57
50	0	0	0	50	400	30	2.1	1.2
0	80	0	0	20	350	60	0.5	-
0	80	0	0	20	375	60	4.2	-
0	80	0	0	20	400	60	11.0	-
0	40	40	0	20	400	60	3.8	-
80	0	0	0	20	400	60	4.8	1.6

TABLE 4
THERMOLYSIS MECHANISM

NO.	REACTION	$\log_{10} A^a$	E^b
1	INITIATION: $1,2 \text{ C}_{10}\text{H}_{10} + 1,2 \text{ C}_{10}\text{H}_{10} \rightarrow \text{C}_{10}\text{H}_9\cdot + 1\text{-C}_{10}\text{H}_{11}\cdot$	8.0	37.0
2	PROPAGATION REACTIONS INVOLVING DNM AND 1-MN $\text{DNM} + \text{H}\cdot \rightarrow 1\text{-MN}\cdot + \text{C}_{10}\text{H}_8$	11.7	9.0
3	$1\text{-MN}\cdot + \text{DNM} \rightarrow \text{DNM}\cdot + 1\text{-MN}$	7.0	9.0
4	$1\text{-MN}\cdot + 1,2 \text{ C}_{10}\text{H}_{10} \rightarrow \text{C}_{10}\text{H}_9\cdot + 1\text{-MN}$	7.0	9.0
5	$1\text{-MN}\cdot + \text{C}_{10}\text{H}_{12} \rightarrow 1\text{-C}_{10}\text{H}_{11}\cdot + 1\text{-MN}$	7.0	9.0
6	$1\text{-MN}\cdot + 1,4 \text{ C}_{10}\text{H}_{10} \rightarrow \text{C}_{10}\text{H}_9\cdot + 1\text{-MN}$	7.0	9.0
7	$\text{DNM} + \text{H}\cdot \rightarrow \text{DNM}\cdot + \text{H}_2$	10.0	3.0
8	$1\text{-C}_{10}\text{H}_{11}\cdot + \text{DNM} \rightarrow \text{DNM}\cdot + \text{C}_{10}\text{H}_{12}$	7.0	9.0
9	$\text{DNM}\cdot + \text{C}_{10}\text{H}_{12} \rightarrow 1\text{-C}_{10}\text{H}_{11}\cdot + \text{DNM}$	7.0	15.0
10	$2\text{-C}_{10}\text{H}_{11}\cdot + \text{DNM} \rightarrow \text{DNM}\cdot + \text{C}_{10}\text{H}_{12}$	7.0	9.0
11	$\text{C}_{10}\text{H}_9\cdot + \text{DNM} \rightarrow \text{DNM}\cdot + 1,2 \text{ C}_{10}\text{H}_{10}$	7.0	9.0
12	$\text{DNM}\cdot + 1,2 \text{ C}_{10}\text{H}_{10} \rightarrow \text{C}_{10}\text{H}_9\cdot + \text{DNM}$	7.0	13.0
13	$\text{C}_{10}\text{H}_9\cdot + \text{DNM} \rightarrow \text{DNM}\cdot + 1,4 \text{ C}_{10}\text{H}_{10}$	7.0	10.0
14	$\text{DNM}\cdot + 1,4 \text{ C}_{10}\text{H}_{10} \rightarrow \text{C}_{10}\text{H}_9\cdot + \text{DNM}$	7.0	9.0

^aUnits of sec^{-1} for unimolecular reactions; $1 \text{ mol}^{-1} \text{sec}^{-1}$ for bimolecular rxns.

^bActivation energy in kcal/mol

DNM = 1,1-Dinaphthylmethane

1-MN = 1-Methylnaphthalene

TABLE 4 (CONT.)

NO.	REACTION	$\log_{10} A$	E
REMAINING PROPAGATION REACTIONS			
15	$C_{10}H_9 \cdot \rightarrow C_{10}H_8 + H \cdot$	14.0	26.0
16	$C_{10}H_8 + H \cdot \rightarrow C_{10}H_9 \cdot$	10.5	3.0
17	$H \cdot + 1,2 C_{10}H_{10} \rightarrow C_{10}H_9 \cdot + H_2$	10.0	3.0
18	$H \cdot + C_{10}H_{12} \rightarrow 1-C_{10}H_{11} \cdot + H_2$	10.0	3.0
19	$H \cdot + C_{10}H_{12} \rightarrow 2-C_{10}H_{11} \cdot + H_2$	10.3	10.0
20	$H \cdot + 1,2 C_{10}H_{10} \rightarrow 1-C_{10}H_{11} \cdot$	11.0	3.0
21	$1,2 C_{10}H_{10} + 1-C_{10}H_{11} \cdot \rightarrow C_{10}H_9 \cdot + C_{10}H_{12}$	7.0	9.0
22	$C_{10}H_9 \cdot + C_{10}H_{12} \rightarrow 1,2 C_{10}H_{10} + 1-C_{10}H_{11} \cdot$	7.0	11.0
23	$2-C_{10}H_{11} \cdot + C_{10}H_{12} \rightarrow 1-C_{10}H_{11} \cdot + C_{10}H_{12}$	7.0	9.0
24	$1,2 C_{10}H_{10} + 2-C_{10}H_{11} \cdot \rightarrow C_{10}H_9 \cdot + C_{10}H_{12}$	7.0	9.0
25	$C_{10}H_9 \cdot + 1,2 C_{10}H_{10} \rightarrow 1,4 C_{10}H_{10} + C_{10}H_9 \cdot$	7.0	12.0
26	$C_{10}H_9 \cdot + 1,4 C_{10}H_{10} \rightarrow 1,2 C_{10}H_{10} + C_{10}H_9 \cdot$	7.0	9.0
27	$C_{10}H_9 \cdot + C_{10}H_{12} \rightarrow 1-C_{10}H_{11} \cdot + 1,4 C_{10}H_{10}$	7.0	14.0
28	$1-C_{10}H_{11} \cdot + 1,4 C_{10}H_{10} \rightarrow C_{10}H_9 \cdot + C_{10}H_{12}$	7.0	9.0
29	$H \cdot + 1,4 C_{10}H_{10} \rightarrow C_{10}H_9 \cdot + H_2$	10.0	3.0
30	$H \cdot + 1,4 C_{10}H_{10} \rightarrow 2-C_{10}H_{11} \cdot$	11.0	10.0
31	$1,4 C_{10}H_{10} \rightarrow C_{10}H_8 + H_2$	12.0	45.0

TABLE 4 (CONT.)

NO.	REACTION TERMINATION:	$\log_{10} A$	E
32	$\text{DNM}\cdot + \text{R}\cdot \rightarrow \text{PRODUCTS}$	10.0	3.0 (reverse A=15 E=53)
33	$\text{DNM}\cdot + \text{DNM}\cdot \xrightleftharpoons{\quad} \text{PRODUCTS}$	9.7	5.0 (reverse A=15 E=47)
34	$\text{R}\cdot + \text{R}\cdot \rightarrow \text{PRODUCTS}$	10.0	0.0

DNM rather than over one ring as in the tetralyl radical. The value of 6 kcal was based on experimental results of Stein¹⁰ and Stein and Golden.¹¹ The third feature to be noted is the activation energy for the termination reactions involving the DNM radical. Normally, free radical recombinations are assigned an activation energy of zero, however, reactions involving the recombination of a DNM radical with any other radical were assigned an activation energy of 3 kcal/mol. The recombination of two DNM radicals was assigned an activation energy of 5 kcal/mol. The activation energies account for the steric hindrance to recombination created by the two naphthalene groups of DNM. The assigned values were based on a value of 7 kcal/mol for the recombination of two triphenylmethyl radicals.¹²

Termination reactions were assumed to be diffusion limited and reversible. Rates of diffusion limited reactions were estimated from the viscosity of the mixture using the Stokes Einstein equation.¹³ For the dialin/DNM mixture, the viscosity at reaction temperatures was estimated as .12+.02 cP using the correlation of Letsou and Stiel,¹⁴ giving $\log A = 9.5 \text{ l sec}^{-1} \text{m}^{-1}$.

The differential equations for radical and stable species concentration were integrated numerically using the Gear algorithm for stiff systems.¹⁵ The dialin and DNM concentrations used in the calculations were estimated from the critical properties of the mixture, using the method of Gunn and Yamada.¹⁶ Calculated and experimental concentrations of dialin, and 1-methylnaphthalene (DNM conversion) are shown in Figures 1 and 2. The agreement between the model's predictions and the experimental values is very good considering that almost all of the rate parameters were estimated a priori by thermochemical techniques or by analogy with similar reactions.

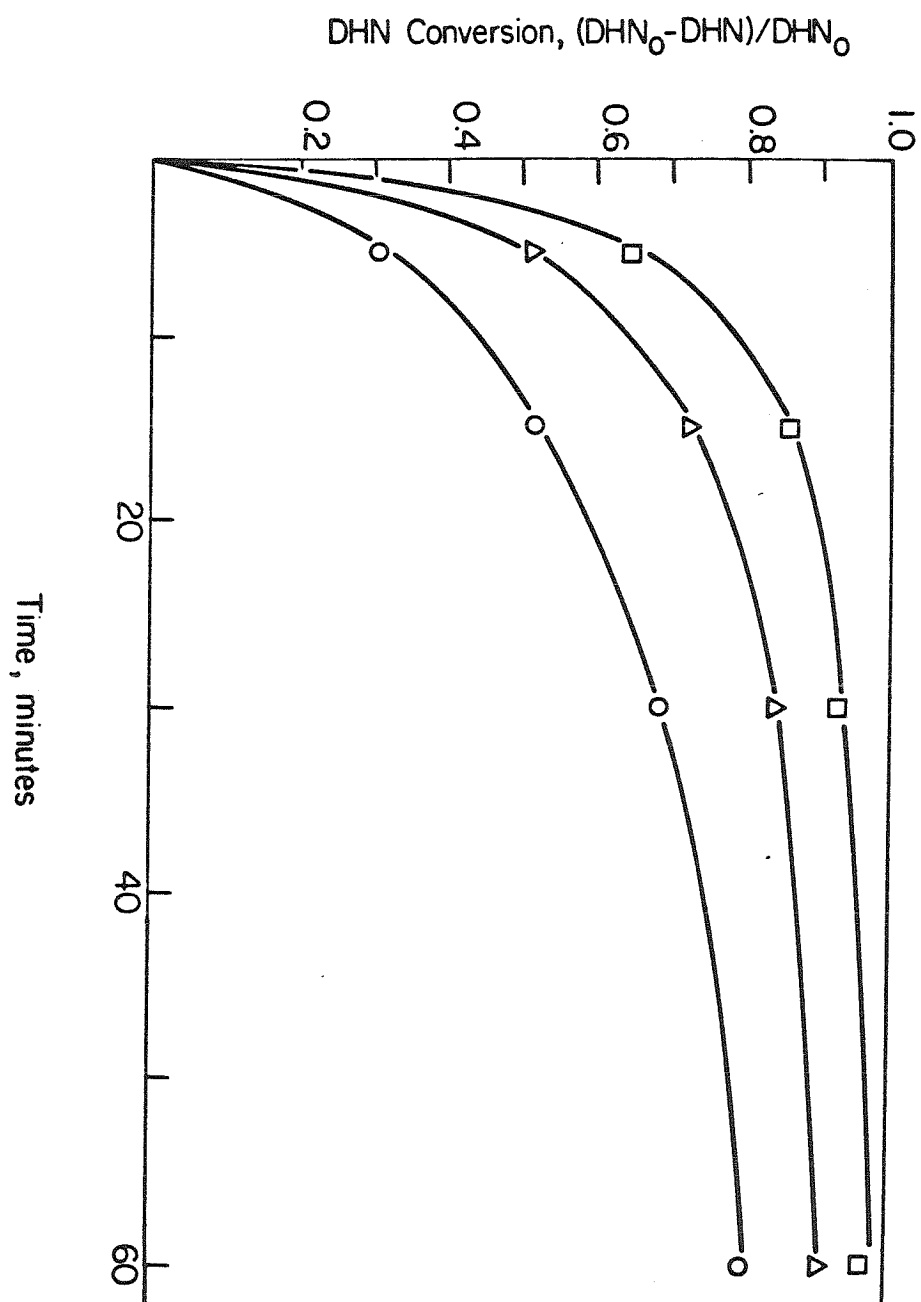
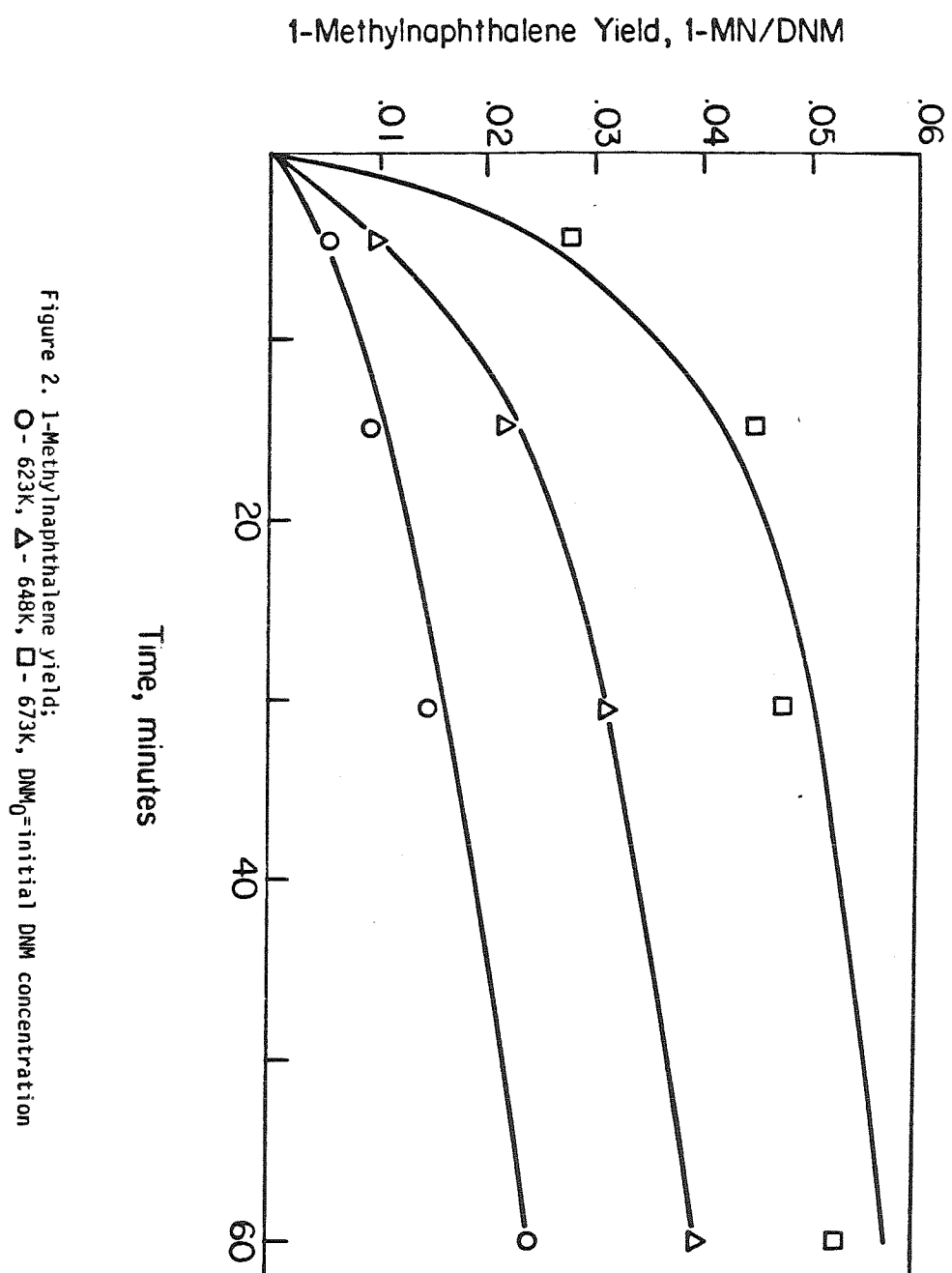


Figure 1. Dihydronaphthalene conversion;
O - 623K, Δ - 648K, □ - 673K, DHN_0 = initial dialin concentration



In order to determine the sensitivity of calculated concentrations to the estimated rate parameters, each of the rate constants was varied individually and the kinetic differential equations were integrated as before. The results of the integrations are shown in Table 5. The sensitivity of the model to reactions 15-31 has been described elsewhere.⁷ The model is most sensitive to changes in initiation and termination rates and to the rate of attack of hydrogen atoms on the methylene bridge of DNM. The relatively large dependence of conversion on reactions 11 and 12 is somewhat surprising, but it can be understood by applying the steady state approximation to the thermolysis mechanism. At the low conversions observed in this work, the rate of 1-methylnaphthalene production is directly proportional to hydrogen atom concentration. Application of the steady state approximation to hydrogen atom concentration yields equation 1.

$$\frac{d[1-C_{11}H_{10}]}{dt} = \frac{k_2 k_{15} [DNM] [C_{10}H_9]}{((k_5 + k_{13}) [DNM] + (k_{17} + k_{20}) [DHN] + (k_{18} + k_{19}) [C_{10}H_{12}])} \quad (1)$$

The rate of 1-methylnaphthalene production is linearly dependent on dialin radical concentration, whence the model's sensitivity to the rates of reactions 11 and 12.

Dialin and Diphenylmethane Mixture

A mechanism analogous to the one proposed for the dialin/dinaphthylmethane mixture was used for this mixture. The only differences between the two mechanisms are the values of the rate parameters for the addition displacement reaction, the viscosity of the mixture, and the RSE for the diphenylmethane radical. The rate parameters for the aromatic substitution reaction analogous to reaction 2 are $\log A = 11.3 \text{ l sec}^{-1} \text{m}^{-1}$ and $E = 11 \text{ kcal/mol}$. The value of the activation energy is only slightly higher than

TABLE 5
SENSITIVITY OF NUMERICAL INTEGRATION TO RATE PARAMETERS

PARAMETER	BASE VALUE	PERTURBED VALUE	% PERTURBATION	% CONVERSION OF DNM TO 1-MN	% CHANGE IN CONVERSION
k_1	4.64×10^{-6}	5.10×10^{-6}	10.	0.4459	4.4
k_2	3.33×10^8	3.66×10^8	10.	0.4711	10.3
k_3	6.97×10^3	7.66×10^3	10.	0.4274	0.1
k_4	6.97×10^3	7.66×10^3	10.	0.4283	0.3
k_5	6.97×10^3	7.66×10^3	10.	0.4273	0.0
k_6	6.97×10^3	7.66×10^3	10.	0.4271	0.0
k_7	8.86×10^8	9.74×10^8	10.	0.4260	-0.3
k_8	6.97×10^3	7.66×10^3	10.	0.4238	-0.8
k_9	5.46×10^1	6.01×10^1	10.	0.4273	0.0
k_{10}	6.97×10^3	7.66×10^3	10.	0.4271	0.0
k_{11}	6.97×10^3	7.66×10^3	10.	0.4225	-1.1
k_{12}	2.75×10^2	3.02×10^2	10.	0.4379	2.5
k_{13}	3.10×10^3	3.41×10^3	10.	0.4256	-0.4
k_{14}	6.97×10^3	7.66×10^3	10.	0.4282	0.3
$k_{32}-k_{34}$	8.86×10^8 8.84×10^7 5.00×10^9	9.74×10^8 9.72×10^8 5.50×10^9	10.	0.4092	-4.2

the value of 9 kcal/mol found for the dinaphthylmethane mixture. The lower frequency factor may imply a tighter transition state for the diphenylmethane reaction.

The RSE used for the diphenylmethane radical was 3 kcal/mol greater than for the tetralyl radical and 3 kcal/mol less than for the dinaphthylmethane radical. This assignment was again based on the results of Stein.¹⁰

The agreement between the model's predictions and the experimental values is reasonably good, as shown in Figure 3. The more pronounced scatter in the data for this mixture is due to the difficulty in measuring the lower absolute conversions.

The potential catalytic effect of the stainless steel reactor walls was examined with this mixture. Stainless steel shavings were added to the reaction mixture, increasing the surface area available to the reactants. No changes in product concentration were observed, so the reactions were assumed to be predominantly thermal.

Dialin and o-Hydroxydiphenylmethane Mixture

The reactions of a mixture of dialin and o-hydroxydiphenylmethane (oHDPM) are considerably more complicated than the previous systems examined. Additional reactions which can occur include hydrogen abstraction from phenolic groups, recombination reactions involving oxygen radicals, which are not diffusion limited,^{17,18} and methylene bridge homolysis via a keto-enol intermediate.

These various complications make the development of a quantitative model of the reactions of this mixture very difficult. However, several significant

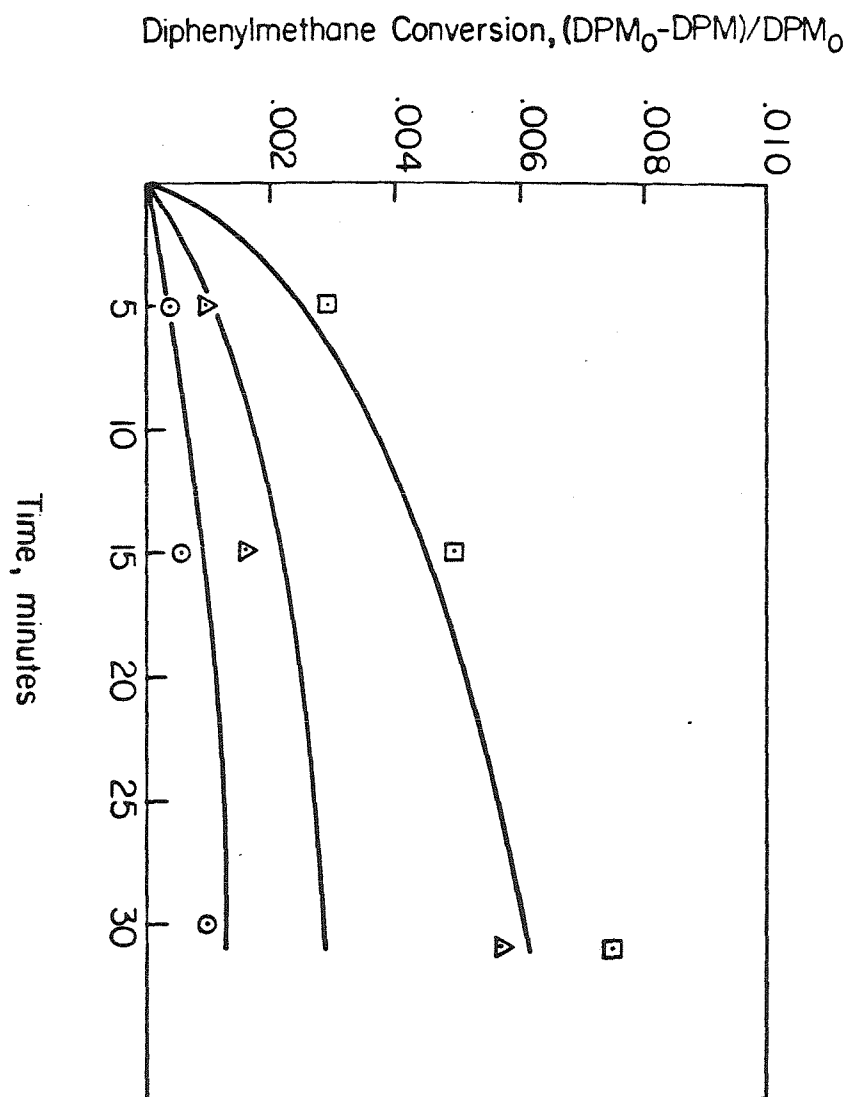


Figure 3. Diphenylmethane conversion;
O - 623K, Δ - 648K, □ - 673K, DPM_0 = initial diphenylmethane concentration

questions can be examined without a detailed model. The thermolysis experiments will indicate whether the rates of aromatic substitution reactions are effected by the substituents present on the rings and whether the keto-enol homolysis reaction proceeds through a free radical intermediate.

We begin by examining the homolysis of oHDPM via the keto-enol homolysis mechanism. The results of Table 3 show an unusual feature. The rate of bond scission was found to be higher in a 4:1 (wt.) mixture of tetralin and oHDPM than in the 4:1 mixture of dialin and oHDPM. This was unexpected since the oHDPM in tetralin undergoes homolysis whereas in dialin it can undergo homolysis as well as dissociation by aromatic substitution. It was expected that the two parallel reaction pathways in the mixture with dialin would result in higher oHDPM conversions. A possible explanation for the greater rate of bond scission in tetralin is that homolysis involves the dissociation of a keto-enol intermediate into two free radicals, as suggested by McMillen et al.¹⁹ The two free radicals can either recombine, reducing the observed rate of bond scission, or abstract hydrogen from a hydrogen donor such as tetralin, to form stable products. In the 4:1 dialin/oHDPM mixture, much of the dialin is rapidly converted to naphthalene, so that less hydrogen donor molecules are available than in the 4:1 tetralin/oHDPM mixture. The observed rate of bond scission is therefore lower in the dialin/oHDPM mixture. To test this hypothesis, a 2:2:1 mixture of tetralin, naphthalene and oHDPM was reacted. This mixture simulates the reactions of a 4:1 mixture of dialin and oHDPM in which all of the dialin has reacted, and therefore should have a lower observed rate of bond scission than both the 4:1 mixture of tetralin/oHDPM and the 4:1 mixture of dialin/oHDPM. As shown in Table 3, a lower rate was observed, so the reaction

scheme shown in Figure 4 is in agreement with all of the available data.

A second piece of information to be gained from the data of Table 3 concerns the effect of phenolic substituents on the rate of the aromatic substitution reactions. Phenolic substituents could influence the selectivity and the rate of aromatic substitution reactions. If the phenolic group has no effect on the selectivity of the reaction, then the yields of toluene and cresol should be equal. After accounting for the toluene produced in the tautomeric homolysis, roughly equal yields are observed. Comparing the rate of aromatic substitution reactions in diphenylmethane and oHDPM indicates that the phenolic group enhances the rate only slightly. In summary, it appears that reactions A and B of Figure 5 proceed at approximately the same rate, which is marginally higher than that of reaction C.

Ether Bridge Reactions

The results described above document the reactions of several methylene bridge compounds. Similar experiments have been performed with compounds containing ether bridges. Experiments performed in our laboratory indicate that the rate of cleavage of the ether bridge in diphenylether via an aromatic substitution reaction is at least one order of magnitude slower than the rate for breaking the methylene bridge in diphenylmethane. Under certain conditions, however, ether bridge compounds can be far more reactive than the corresponding methylene bridge compounds. For example, the presence of tetrahydroquinoline (THQ) enhances the rate of ether bridge dissociation via a tautomeric homolysis reaction by a factor of 200 while the homolysis of methylene bridges is enhanced by only about 20%.²⁰ In addition, it has been

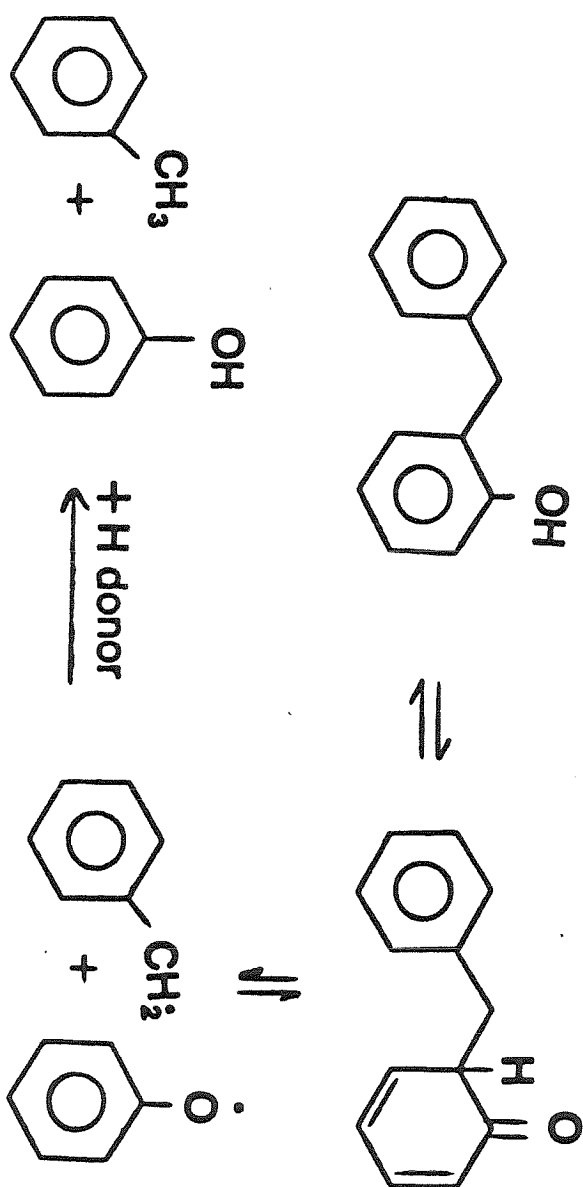


Figure 4. Keto-enol tautomerism

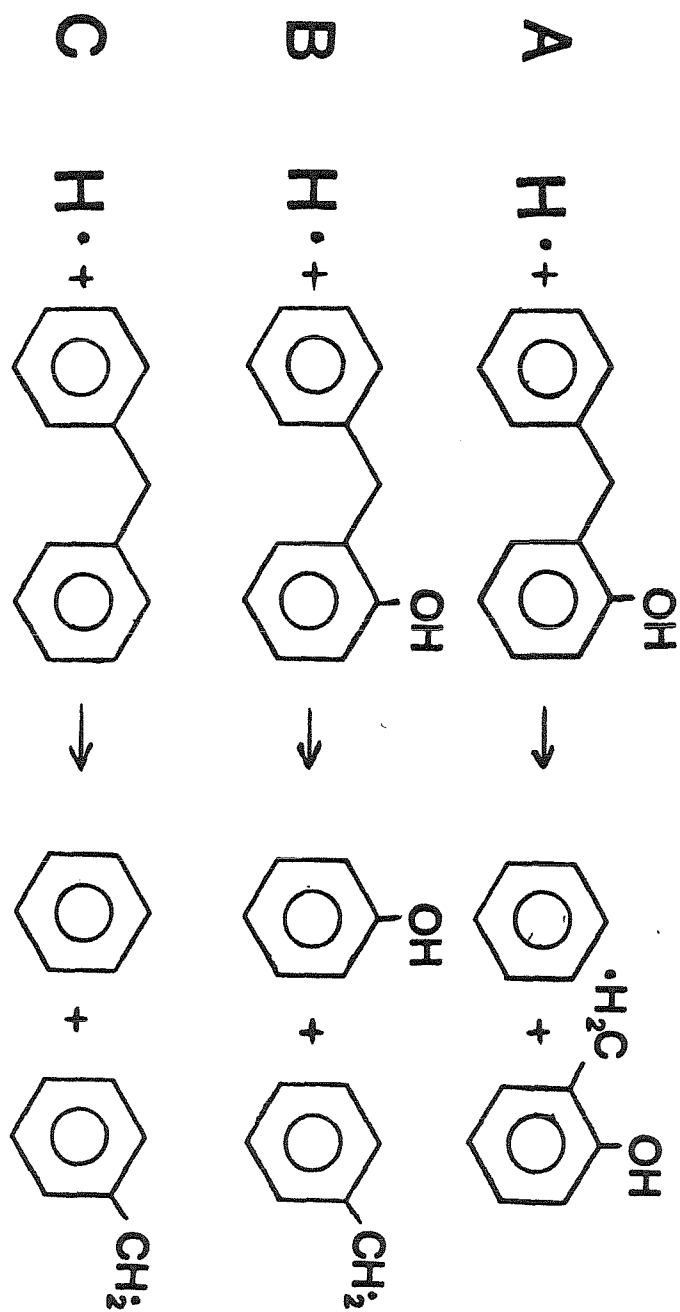


Figure 5. Aromatic substitution reactions

observed that phenols accelerate the decomposition of certain ethers but not the analogous hydrocarbons.²¹ Finally, the reactions of ether bridges appear to depend more strongly on the size of the aromatic rings than the reactions of methylene bridges.²¹ These results have an important bearing on the reactions of coal. They indicate that slight changes in the structure of ethers or the presence of additives in coal liquefaction solvents can profoundly change the reactivity of coal mixtures. A more detailed understanding of these complex reactions is necessary.

CONCLUSIONS

The rates of methylene and ether bridge cleavage have been examined using a number of model compound systems. The results indicate that these bridges can decompose under moderate conditions via an aromatic substitution reaction with atomic hydrogen. This class of reactions is important in coal liquefaction processes since hydrogen donating structures such as tetralin release atomic hydrogen as they dehydrogenate. With A-factors of $10^{10.5-12}$ l $m^{-1}s^{-1}$ and activation energies of 10 kcal/mol, the reactions are rapid. Additionally, the results demonstrate that mixtures of model compounds can have complex kinetic behaviour and that interactions between functionalities can significantly effect conversions. This implies that the reactions of multi-component mixtures such as coal liquids are much more complex than the sum of the reactions of the components.

ACKNOWLEDGEMENT

The authors thank T.A. Weston for synthesizing the 1,1-dinaphthylmethane.

REFERENCES

- [1] B.M. Benjamin, V.F. Raaen, P.H. Maupin, L.L. Brown and C.J. Collins, *Fuel*, **57**, 269 (1978).
- [2] D.C. Cronauer, D.M. Jewell, Y.T. Shah and K.A. Kueser, *Ind. Eng. Chem. Fund.*, **17**, 291 (1978).
- [3] D.C. Cronauer, D.M. Jewell, Y.T. Shah and R.J. Modi, *Ind. Eng. Chem. Fund.*, **18**, 153 (1979).
- [4] D.C. Cronauer, D.M. Jewell, R.J. Modi and K.S. Seshadri, *Ind. Eng. Chem. Fund.*, **18**, 368 (1979).
- [5] T. Yao and Y. Kamiya, *Bull. Chem. Soc. Japan*, **52**, 492 (1979).
- [6] R.E. Miller and S.E. Stein, *J. Phys. Chem.*, **85**, 580 (1981).
- [7] D.T. Allen and G.R. Gavalas, *Int. J. Chem. Kin.*, **15**, 219 (1983).
- [8] S.W. Benson, *Thermochemical Kinetics*, 2nd ed., Wiley, New York, 1976.
- [9] G.R. Gavalas, *Coal Pyrolysis*, Elsevier Scientific, New York, 1982.
- [10] S.E. Stein, *New Approaches in Coal Chemistry*, ACS Symposium Series #169, 1981, pp. 97-130.
- [11] S.E. Stein and D.M. Golden, *J. Org. Chem.*, **42**, 839 (1977).
- [12] K.U. Ingold, *Free Radicals*, Vol. 1, J.K. Kochi, Ed., Wiley, New York, 1973, pg. 52.
- [13] K.U. Ingold, *Free Radicals*, Vol. 1, J.K. Kochi, Ed., Wiley, New York, 1973, pp. 39-40.

- [14] R.C. Reid, J.M. Prausnitz and T.K. Sherwood, *The Properties of Gases and Liquids, 3rd ed.*, McGraw Hill, New York, 1977, pp. 455-457.
- [15] R.N. Stabler and J.P. Chesick, *Int. J. Chem. Kinet.*, **10** , 461 (1978).
- [16] R.C. Reid, J.M. Prausnitz and T.K. Sherwood, *The Properties of Gases and Liquids, 3rd ed.*, McGraw Hill, New York, 1977, pp. 60-61.
- [17] L.R. Mahoney and S.A. Weiner, *J. Amer. Chem. Soc.*, **94** , 585 (1972).
- [18] L.R. Mahoney and M.A. DaRooge, *J. Amer. Chem. Soc.*, **97** , 4722 (1975).
- [19] D.F. McMillen, W.C. Ogier and D.S. Ross, *ACS Div. Fuel Chem. Prepr.* **26** (2), 181 (1981).
- [20] L.F. Atherton and C.J. Kulik, presented to A.I.Ch.E. Meeting, Los Angeles, 1982.
- [21] Y. Kamiya, T. Yao and S. Oikawa, *ACS Div. Fuel Chem. Prepr.* **24** (2), 116 (1979).

Chapter 10

Model Compound Studies: Conclusions and Recommendations for Future Work

The three most significant conclusions to be drawn from the model compound studies of Chapters 8 and 9 are listed below.

- [1] Transition state theory and group additivity estimates of thermodynamic functions (1) were combined to yield order of magnitude estimates of rate parameters for liquid phase reactions. The applicability of transition state theory to condensed phase reactions of model compounds could not have been assumed a priori since the theory was developed for gas phase reactions. These theoretical estimates may not be valid in either very viscous fluids, or solvents which impart stability to transition states, but they provide reasonable results for the systems studied. Further, since the model compound systems examined are similar in structure to coal-derived products, theoretical estimates of rate parameters should be valid (within an order of magnitude) for coal-derived products of modest molecular weight. Thus, the importance of various proposed reaction pathways in coal-related processes can be evaluated quickly using estimates from transition state theory.
- [2] The dissociation of methylene bridges via an aromatic substitution reaction, reported in Chapter 9, emphasizes the fact that many reaction pathways are possible in the reactions of coal-derived materials. The commonly held view is that most of the chemical changes occurring dur-

ing coal liquefaction can be explained by unimolecular bond dissociations (2). While these pathways are undoubtedly important, other routes are also significant.

- [3] The thermal reactions of coal-related materials are believed to primarily follow free radical paths (2). The results of Chapters 8 and 9 show that free radical exchange reactions are very fast relative to initiation steps. Therefore, the steady state approximation is generally applicable and the long chain approximation is sometimes valid in the kinetic analysis of coal liquid reactions. These approximations may prove useful in developing models of the reactions of complex mixtures.

A large number of unanswered questions related to the kinetics of coal liquids still remain and could be examined effectively with model compound experiments. Several of the most significant questions are outlined below.

- [1] Thermal reactions of coal are predominantly free radical in nature, but little is known concerning the ratio of heteroatomic to hydrocarbon free radicals. Some experimental evidence indicates that heteroatomic species may be chain carriers in thermal reactions (3), but little is known of the liquid phase free radical reactions of heteroatoms. These reactions deserve further study.
- [2] The general goal of coal liquefaction is to break large coal molecules into lighter fragments. The reactions are mostly free radical. The recombination reactions of the free radicals are essentially the reverse of the

desired liquefaction reactions. The rates of these reactions should therefore be minimized, possibly by promoting free radical termination via disproportionation reactions. Work is necessary to determine how to inhibit recombination reactions or how to promote disproportionation reactions in coal systems. Model compound systems could provide useful information.

- [3] During coal liquefaction, there is a significant concentration of free radical sites on the solid coal (4). This is believed to cause hydrogen donor solvent and liquefaction product molecules to attach themselves chemically to the solid coal, reducing the yield of liquefaction products. The chemical attachment may occur via free radical recombination reactions, by substitution reactions or by other pathways. The extent and mechanism of these solvent and product adduction reactions need to be better understood. Isotopically tagged model compounds could be used to follow the course of these reactions.

Despite the general significance of the results that can be drawn from Chapters 8 and 9 and the experiments proposed above, only a limited amount of information can be generated by model compound experiments. A comprehensive model of the reactions of coal liquids would require a staggering number of studies of model compound systems. Two classes of simplifications are possible to make the problem more reasonable, however. The first is to consider only thermal reactions of coal liquids and to utilize

theoretical estimates of the necessary rate parameters. Selected model compound experiments could be performed to investigate possibilities of homogeneous catalysis (e.g., the basic nitrogen catalyzed decomposition of ether bridges). A second type of simplification would be to consider only broad classes of reactions (e.g., hydrogen abstraction, bond dissociation, etc.) in the kinetic modeling. Product formation and changes in concentration of functional groups would be estimated in a probabilistic manner. This approach has been used to model coal pyrolysis reactions (5,6) and could be used to model catalytic reactions of coal liquids.

References

- [1] S.W. Benson, *Thermochemical Kinetics, 2nd ed.*, John Wiley and Sons, New York, 1976.
- [2] D.D. Whitehurst, T.O. Mitchell and M. Farcasiu, *Coal Liquefaction*, Academic Press, New York, 1976.
- [3] L.R. Mahoney and M.A. DaRooge, *J.A.C.S.*, **97**, 4722 (1975).
- [4] L. Petrakis and D.W. Grandy, *Anal. Chem.*, **50**, 303 (1978).
- [5] G.R. Gavalas, P.H. Cheong and R. Jain, *I.&E.C. Fund.*, **20**, 113 (1981).
- [6] G.R. Gavalas, R. Jain and P.H. Cheong, *I.&E.C. Fund.*, **20**, 122 (1981).